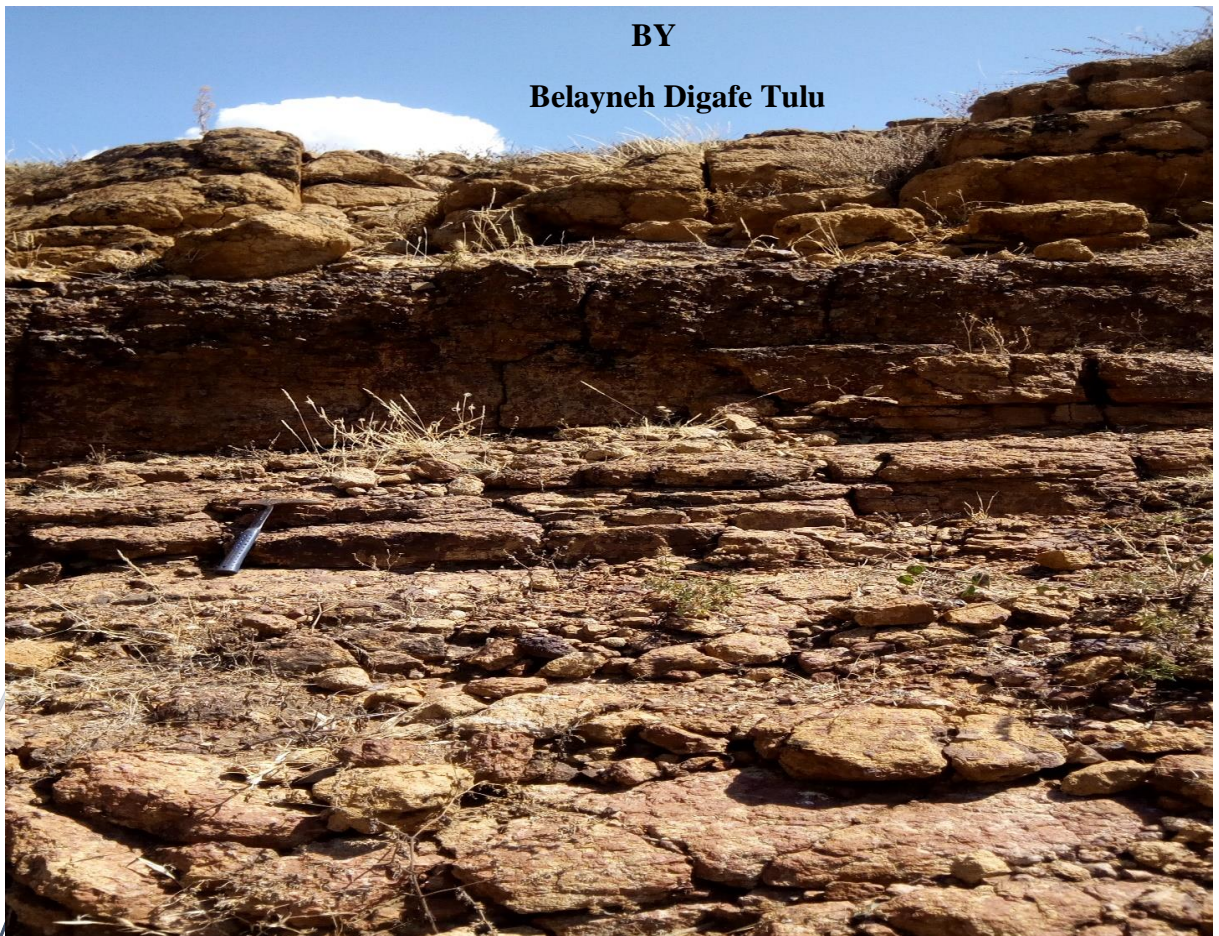




ADDIS ABABA UNIVERSITY
SCHOOL OF EARTH SCIENCES
MINERALOGY, GEOCHEMISTRY AND GENESIS OF MEKANE SELAM IRON
OCCURRENCE IN TEWA AREA, NORTHERN ETHIOPIA.

BY
Belayneh Digafe Tulu



A thesis submitted to the School of Earth Sciences, Addis Ababa University in partial fulfillment of the requirements for the degree of Master of Sciences in Resource Geology (Mineral Deposits).

ADDIS ABABA UNIVERSITY
SCHOOL OF EARTH SCIENCES
MINERALOGY, GEOCHEMISTRY AND GENESIS OF MEKANE
SELAM IRON OCCURRENCE IN TEWA AREA, NORTHERN
ETHIOPIA.

By
Belayneh Digafe

Advisor: Dr. Worash Getaneh

Co-Advisor: Dr. Balemuwal Atnafu

A thesis submitted to the School of Earth Sciences, Addis Ababa University in partial fulfillment of the requirements for the degree of Master of Sciences in Resource Geology (Mineral Deposits).

October, 2 / 2020

Addis Ababa, Ethiopia.

**ADDIS ABABA UNIVERSITY
SCHOOL OF EARTH SCIENCES**

**MINERALOGY, GEOCHEMISTRY AND GENESIS OF MEKANE
SELAM IRON OCCURRENCE IN TEWA AREA, NORTHERN
ETHIOPIA.**

By

Belayneh Digafe

Approved by the examining committee

Dr. Balemual Atnafu	_____	_____
Head, School of Earth Science	Signature	Date
Dr. Worash Getaneh	_____	_____
Advisor	Signature	Date
Dr. Balemual Atnafu	_____	_____
Co- Advisor	Signature	Date
Prof. Gezahegn Yirgu	_____	_____
Examiner	Signature	Date
Prof. Solomon Tadesse	_____	_____
Examiner	Signature	Date

October, 2 / 2020

Addis Ababa, Ethiopia.

Declaration of Originality

This thesis work is about the geologic setting and genesis of the Mekane Selam iron occurrence which is my original master's degree under the supervision of Dr. Worash Getaneh and Dr. Balemuwal Atnafu School of Earth Sciences Addis Ababa University. I want to declare that this research work has not been presented or submitted for any degree or diploma at any University (institutions). All relevant source materials used for this thesis work has been respectfully acknowledged.

Belayneh Digafe

October, 2 / 2020

Signature

Date

To the best of knowledge the above research work declaration by the candidate is correct and it has been submitted for examination with our approval as advisors of the school in the University.

Dr. Worash Getaneh (Advisor)

Signature

Date

Dr. Balemuwal Atnafu (Co-advisor)

Signature

Date

Abstract

Iron is the fourth abundant metal in Earth's crust and its ore minerals are concentrated as hematite, goethite, magnetite, siderite, illmenite and other sulfides. The Mekane Selam iron mineralization is part of the Northwestern plateau that bounded by Axum–Adigrat and Ambo lineaments of the N and SW. Mineralogy, geochemistry and genesis studies are main objective of this work. Geologic field work and mapping, X-ray diffraction, ore petrographic study of ore, geochemical analysis of host rock were applied methodologies. XRD and ore microscopic study reveals hematite, goethite, magnetite, kaolinite anatase and quartz are the principal ore minerals and associated gangue phases of ore while quartz and feldspars are petrographic composition of the host. Chemical analysis of major constituent show significant enrichment of SiO_2 , Al_2O_3 in the host and Fe_2O_3 in the ore with strong depletion of K_2O , Na_2O , MnO , MgO , CaO and P_2O_5 . High value of CIA (88.46-99.44) with depleted content of K_2O and Na_2O suggests the area is subjected to intensive weathering process. Chondurite-normalized REE pattern show enrichment in LREE and relatively smooth pattern of HREE. The pattern is consistent with the characteristics of upper continental crust, protholith of sediments and weathered terrestrial iron source. Positive Ce and negative Eu anomalies of analyzed samples suggest iron reprecipitation is occurring in weathered (supergene) oxidation leaching of REE. It indicates diagenetic alteration and the absence of hydrothermal fluid inputs during mineralization. Concentrated detrital derived elements of Zr, Al and Nb with the oolitic textures of ore samples are the characteristic of diagenetic modification in iron formation. The XRD results of goethite, hematite and kaolinites minerals indicate the genesis of Mekane Selam iron occurrence is laterite. SiO_2 - Fe_2O_3 - Al_2O_3 ternary plot of ore and host rock samples show the ore is altered to hematite due to low–strong degree of lateritization while the host rock is as a result of kaolinization to kaolinite. Field observation and exposure measurement, mineralogical and geochemical data analysis suggests the iron occurrence of the area is classified as an indicated resource. Surface weathering, REE leaching, transportation and other physico-chemical conditions enrich iron. The diagenesis and sediment recrystallization are significant iron ore formation and modification of the area.

Key words: Iron ore Genesis Geologic setting Laterite
Continental crust Geochemical Mineralogy

Acknowledgment

First of all, I would like to thank for Geological Survey of Ethiopia who facilitates the opportunity to attend my master's degree at Addis Ababa University. I have a great feeling of gratitude to my advisor Dr. Worash Getaneh for his guidance, encouragement help and constructive suggestions with comments and advices. I am on acknowledging to Dr. Balemual Atnafu head of the School of Earth Science and co- advisor of this work.

I want to express my deepest gratitude to Mr. Amdemichael Zafu for his helpful work of whole rock geochemical analysis at Belgium University of Libre de Bruxelles laboratoire G-Time Department Geosciences, Environnement et Societe.

I am gratefully thanks to Dr. David Burianek a Geologist who made the XRD mineralogical analysis of iron ore and associated rock at Czech Republic Geological Survey XRD laboratory center which is inaccessible in Ethiopia by the time.

I am also, convey my acknowledgement to my friends of Mr. Getnet Gezahegn and Abate Asen those who guided and encourageous help through their important comments and reviewing this work. My thanks would have been goes to Mr. Abisa Dugassa director of mineral exploration and evaluation directorate for his advice and facilitating suitable conditions for the field work activity.

Finally I would like to continue my grateful thanks to Abate Amsalu, Tewodrose Tilahun and Wubante Fekadu those play a great role during the field work conducted for geological mapping and sample collection by taking the possible field risks.

Lastly my glory is to the Mekane Selam administration office and all my friends and families those directly or indirectly pay necessary sacrifice for this research work next to "*Almighty of God*".

Dedication

This research work is dedicating to my beloved friends and family.

Table of Contents

Abstract	I
Acknowledgment	II
Table of Contents	IV
List of figures	VII
List of Tables	IX
CHAPTER ONE	1
1. Introduction	1
1.1 General back ground	1
1.1.1 Location and accessibility	2
1.1.2 Physiography and drainage	3
1.1.3 Climate and vegetation	5
1.1.4 Population and settlement	6
1.2 Statement of the problem	7
1.3 Research Objective	8
1.3.1 General Objective	8
1.3.2 Specific Objective	8
1.4 Methodology	8
1.4.1 Field work and Geological Mapping	8
1.4.2 Laboratory test and chemical analysis	10
1.4.3. Petrographic study	12
1.5 Significance of the research	13
1.6 Research overview	13
CHAPTER TWO	14
2 Literature review	14
2.1 Pervious work	15
2.1.1 Previous study on iron occurrence of Ethiopia	16

2.2 Process of iron ore formation.....	18
2.3 Exploration	18
2.4 Processing	19
2.5 Mining.....	21
CHAPTER THREE.....	21
3 Regional geology and tectonic setting	21
3.1 Introduction.....	21
3.2 Regional geology.....	22
3.3 Tectonic setting.....	27
CHAPTER FOUR	28
4 Local geology.....	28
Introduction	29
4.1 Geology of the study area.....	29
4.2 Limestone.....	30
4.2.1 Petrography of limestone.....	31
4.3 Mudstone–shale.....	33
4.3.1 Petrography of mudstone	33
4.4 Sandstone.....	34
4.4.1 Thin section descriptions	37
4.5 Volcanic lava flow	42
4.5.1 Petrography of basalt.....	43
CHAPTER FIVE	45
5 The Mekane Selam iron occurrence.....	45
5.1 Nature of mineralization and the ore bodies	47
5.2 Host rock	50
5.3 Ore and gangue mineralogy.....	50
5.4 Geologic history.....	59

CHAPTER SIX	61
6 Geochemistry of the sedimentary rocks	61
Introductions	61
6.1 Geochemistry of the host rock	62
6.2 Geochemistry of the iron ore	68
Introduction	68
CHAPTER SEVENE	71
7 Discussions	71
7.1 Geologic setting	77
7.2 Interpretation	79
7.3 Genesis of iron	81
7.4 Recourse of the area	84
CHAPTER EIGHT	86
8 Conclusion and recommendation	86
8.1 Conclusion	86
8.2 Recommendation	88
References	89

List of figures

Figure 1. <i>Location and accessibility map of the area.</i>	3
Figure 2. <i>DEM physiographic map of the study and surrounding area.</i>	4
Figure 3. <i>Drainage pattern of the study and surroundings.</i>	5
Figure 4. <i>Weather and climate conditions of Mekane Selam area.</i>	6
Figure 5. <i>Distribution of iron occurrence in Ethiopia.</i>	17
Figure 6. <i>Basic iron ore interrelated operational stapes according to (Upadhyay et al., 2009 and Nomura et al., 2015).</i>	20
Figure 7. <i>Flow sheet for iron and steel extraction process according to (Kumar, 2003 and Spoerl, 2016).</i>	20
Figure 8. <i>Regional stratigraphy modified from (Getaneh Assefa, 1991).</i>	26
Figure 9. <i>Regional geological map modified from (GSE, 2015).</i>	27
Figure 10. <i>Lithological map of the study area (A) and geologic cross section along A-B (B).</i>	30
Figure 11. <i>Field photographs of fossiliferous (A) and non - fossiliferous (B) limestone.</i>	31
Figure 12. <i>photomicrograph of MSL4 (A) PPL, (B) XPL and MSL6 (C) PPL, (D) XPL for limestone with 10X magnification power.</i>	33
Figure 13. <i>MSh1 (A) XPL, (B) PPL and MSh2 (C) XPL, (D) PPL observation for mudstone with 10X magnification.</i>	34
Figure 14. <i>Field photographs of top and lower sandstone section and the ore body.</i>	36
Figure 15. <i>Section log taken from the sandstone unit exposed below the basalt and near the road cut.</i>	37
Figure 16. <i>MSd5Alteration at the boundary (A) and filled space by secondary minerals (B) in XPL observation and 10X magnification.</i>	40
Figure 17. <i>MSd3 angular – sub angular and sorted arkose sandstone under XPL (A) and PPL (B).</i>	40
Figure 18. <i>MSd6 sorted arkose type sandstone in XPL (A) and PPL (B) observation 10X magnification.</i>	41
Figure 19. <i>MSd8 poorly sorted arkose sandstone under XPL (A) and PPL (B) observation with 10X magnification.</i>	41
Figure 20. <i>MSd10 moderately sorted arkose type sand under XPL (A) and PPL (B) observation.</i>	42
Figure 21. <i>Massive to Layered volcanic lavas flows (A) and stratified pyroclastic tuff (B).</i>	43
Figure 22. <i>XPL (A) and PPL (B) observation of MSa1 and XPL (C) and PPL (D) observation of MSa5 basalts by 10X magnification power.</i>	44
Figure 23. <i>General local stratigraphy of the study area.</i>	45

Figure 24. Field photographs of laterite (A), massive – oolitic (B) and inter bedded (C) iron ore of the study area.	49
Figure 25. Sketched diagram of MSB13 (A) and MSB16 (B) showing mutual grain boundary and replacement relationship of goethite with hematite and the gangue.	53
Figure 26. Photomicrographs of platy-hematite crystals MSB2 (A) and MSB13 (B) oolith and botryoidal feature of Goethite and interlayered hematite ore.	53
Figure 27. MSB8 (A) and MSB9 (B), Redish – grey brown weathered Goethite replacing the hematite and anhedral dumpy crystal developed in association to hematite.	54
Figure 28. MSB13 (A) specularite - interlayered hematite (bright) and MSB14 (B) oolith – botriodal of goethite red, brownish- grey with disseminated magnetite.	54
Figure 29. MSB16 Ooid specularite-pisolitic fabric (A) and acicular or laths crystals fill voids or fractures regular reflections of hematite and bluish tint of Goethite iron oxides (B).	55
Figure 30. XDR diffraction of sample MSB-1 layered – massive iron ore middle part –layered rim.	56
Figure 31. XRD diffraction of sample MSB-10 iron ore strata bound with hosted sandstone.	57
Figure 32. XRD diffractions of sample MSB-5 interlayered needle silica with massive iron ore.	57
Figure 33. XRD diffraction value for the sample MS-DB3 weathered iron ore.	57
Figure 34. XRD diffraction value of the sample MS-LW massive - oolitic iron ore.	58
Figure 35. Hypothetically sketched for geologic history and model of the ore deposit.	61
Figure 36. REE pattern for the iron ore, the host rock and surrounding fine sediments.	67
Figure 37. Multi element distribution for both iron ore and host rock samples.	67
Figure 38. Liner plots of geochemical data for major oxides of both iron ore and host rock.	74
Figure 39. Ternary Al_2O_3 - SiO_2 - Fe_2O_3 plot showing different degree of laterization for iron bearing rock after (Shellmann, 1986).	76
Figure 40. Plot of Th vs U to show the source of sediments after (McLennan et al., 1993).	79
Figure 41. Correlated plot for Si- Qtz and Al- Kaolinite.	80
Figure 42. Ternary plot of SiO_2 - Al_2O_3 - Fe_2O_3 showing iron enrichment by laterite after (Gardner and Walsh, 1996).	83
Figure 43. Ternary diagram of SiO_2 - Al_2O_3 - Fe_2O_3 showing the genetic relationship after (Dury, 1969; Bassam and Tamar, 1998).	84

List of Tables

Table 1. <i>Recalculated modal compositions of arkose sandstone.</i>	38
Table 2. <i>XRD mineralogical analysis of iron ore samples.</i>	58
Table 3. <i>Chemistry of iron ore samples analyzed for XRD study.</i>	58
Table 4. <i>Major element chemistry of host and associated rock.</i>	64
Table 5. <i>Trace element chemistry of the host and surrounding rock.</i>	64
Table 6. <i>Major element geochemistry of the iron ore sample.</i>	69
Table 7. <i>Trace element analysis of iron ore samples.</i>	70
Table 8. <i>Estimated resource of Mekane Selam iron occurrence.</i>	85

List of acronyms

AAU	Addis Ababa University
AD	Afar depression
AISIC	American Iron and Steel Institute Company
BIF	Banded Iron Formation
BNB	Blue Nile Basin
BNG	Blue Nile Gorge
BNR	Blue Nile River
CIA	Chemical Index Alteration
DEM	Digital Elevation Model
DGES	Department of Geosciences Environment et Societe
DLS	Debre Libanose Sandstone
EIGS	Ethiopian Institute of Geological Survey
FV	Field of Observation
GIS	Geographic Information System
GPS	Geographic positing system
GSCR	Geological Survey of Czech Republic
GSE	Geological Survey of Ethiopia
Gt	Goethite
Hm	Hematite
HREE	Heavy Rare Earth Element
ICP-AES	Induced coupled plasma – emission atomic spectroscopy
ICP-MS	Induced coupled plasma -mass spectrometry
ICV	Index of Compositional Variation
LILE	Large ion Lithophile Elements
LOI	Loss on Ignition
LREE	Light Rare Earth Element
MER	Main Ethiopian Rift
MG	Magnetite
NE- SW	North East – South West
NW	North West
PPL	Plain Polarizing Light
REE	Rare Earth Elements
SE- NW	South East – North West

UCC	Upper Continental Crust
ULB	University of Liber de Bruxelles
UTM	Universal Transverse Mercator
XPL	Cross Polariz Light
XRD	X-ray Diffraction

CHAPTER ONE

1. Introduction

1.1 General back ground

The Blue Nile basin is one of the main East African sedimentary basins found in Ethiopia in addition to Mekele, Ogaden, Gambela and Rift basins (Getaneh Assefa, 1991). The formations filling the basin are unconformable overlain by the volcanics of Northwestern plateau. The basin is tectonically bounded from the East and South East by escarpments of the Main Ethiopian Rift and from N and S by Axum-Adigrat and Ambo lineaments respectively (Gani et al., 2008). The withdrawal of the Mesozoic sea water from the northern and central parts of Ethiopia started to deposit meandering and braided type of sediments within Blue Nile Basin. The basin is known by its industrial and energy resources (Welela Ahmed, 2002). Economic minerals of the basin are cropping out due to erosion and cross cuttings by rift system together with plateaus of Ethiopia (Mogessi et al., 2002). The current research work is conducted in the northwestern sub-basin of Blue Nile Basin. Since, the sub basin and surrounding volcanic traps are less investigated for their metallic resource, this study will shade light on this gapes. Mekane Selam area is part of Blue Nile Basin. It is covered by Mesozoic sedimentary and Cenozoic volcanic rocks of sandstone, limestone, basalt and pyroclastic tuff. Preliminary reports indicate that there is occurrences of iron mineralization in the vicinity of Mekane Selam (GSE, 2018). However, there is no detail exploration work yet. Since iron is the most abundant element with more application in current industry, studies on such vital element is crucial for economic development of Ethiopian. Iron has variety of ionic charges and ore minerals. Mainly it occurs in the form of magnetite (Fe_3O_4), hematite (Fe_2O_3), siderite (FeCO_3), illmenite (FeTiO_3), goethite ($\text{FeO}(\text{OH})$) or limonite ($\text{FeO}(\text{OH}) \cdot \text{H}_2\text{O}$) and sulfides (James, 1966). It is concentrated in many other sedimentary and magmatic fractionations of mafic rock. Iron has both chalcophile and lithophile or oxide and sulfide properties (affiliations) so that it can be concentrated in mafic and felsic varieties (Roob, 2013). Sedimentary rocks can reserve 15% of total iron formations of economic resources (Bogges, 2006). Their formation is linking with the Precambrian sedimentary succession and exact source is not yet determined (Bekker et al., 2010). The Earth's dynamic environmental, evolutionary and geochemical change affects the style of deposition and mechanisms of iron formation. However, the endogenic, exogenic and physico-chemical conditions of the environment played vital role

for the formation and corresponding iron deposition. An economic iron ore deposit is concentrated best within igneous and sedimentary terrains. Precambrian and Mesozoic sedimentary rocks of Ethiopia are considerable hosts for present metallic and industrial minerals and also have potentials of oil and gas deposit (Kazmine, 1972 and Tadesse Alemu, 2012). The resource and mineralization is associated with fracturing, quartz veins – reefs, weakly folded and stratified traps (Kazmine, 1972). For the current and future rapid increase of construction industry of Ethiopia, iron is the most possible and available mineral resources. The developed and civilized world industry use iron ore mineral as a leading raw material. This very fast growing and expensive industry can be solved through systematic exploration and production of small and large iron occurrences or resources rather than importing from abroad. The genesis of Ethiopian iron is viewed as Precambrian basic intrusion hosted, banded type associated with Precambrian ferruginous quartzite, and secondary laterite or gossan related (Solomon Tadesse, 2009). From economic point of view banded or stratified type and late injections of iron dominated basic magma mineralization process can form an economic concentration of big iron ore deposit (Solomon Tadesse, 2009; Solomon Tadesse & Worash Getaneh, 2015).

1.1.1 Location and accessibility

The study area is located in the northwestern part of Ethiopia and occupies the northeastern part of Blue Nile Basin. It is the southwest continuation of Wollo and is part of the south Wollo zone Borena Woreda, specifically in Tewa locality. It is bounded by geographic coordinate of 1181000 – 1190000 Northing and 448000 – 458000 Easting in UTM (Universal transverse Mercator). The area covers a total of 90 (km²) coverage to investigate iron occurrence. It can be accessed through 490km main asphalt road from Addis Ababa – Dejen – Mertule Mariam - Mekane Selam and 60km distance of dry weathered gravel road to arrive the target area. The second possible access road of the area is 161 km asphalt road from Addis Ababa – Gebre Guracha and dry weathered (288km) gravel road of Gundo Meskele - Mekane Selam. The accessibility and location of the study area for iron occurrence in relation to the surrounding area is illustrated in (Fig.1) below.

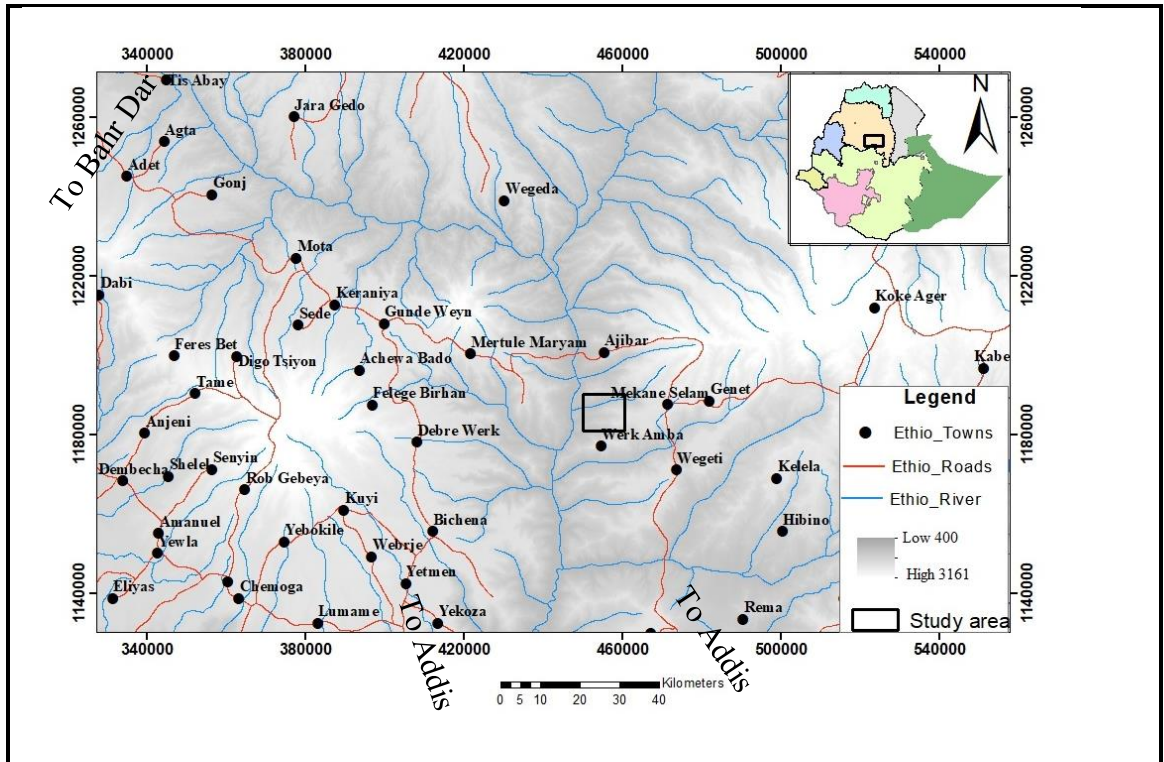


Figure 1. Location and accessibility map of the area.

1.1.2 Physiography and drainage

As indicated in the location map of (Fig.1), the study area is part of the central highlands that is characterized by deep gorges and cuts by south to southwest flowing streams. The sharp cross cut of stream channels and gully erosional surfaces are the main features of the plateaus and volcanic escarpment. Its physiographic condition can be divided in to different topographic features of continental plateaus of flood lava flows, mountainous shield volcanoes, deep gorge and the escarpment of the steep cliffs. The plateau is the main feature of north Ethiopia that is formed by lava flows. The hills, ridges and deep gorges are also common topographic features of the area. These geographically important physiographic features of the area are the outcomes of continuous and deep cutting of Mesozoic sedimentary carbonate successions and siliclastic sediments. The central shield volcanoes are parts of Cenozoic volcanics that created the mountainous feature, whereas the cliff forming escarpment is the outcome of erosion and tectonic faulting. These features are in association with different Tertiary lava flows of ridges and northern highlands. The plateaus and highlands occupy the northeastern to east and south east side of the study area. The main physiographic conditions of the study and surrounding areas are illustrated from the Digital Elevation Model (DEM) physiographic map below (Fig. 2). The major continuation

of rift escarpment and emplacements of the outpouring basic lava flows with pyroclastic bimodal compositions of the plateau has determined the landscapes of the region. Vertical gully and east west riverine erosion is the most characterized features of the mountainous basaltic and pyroclastic topography of the study and surrounding areas.

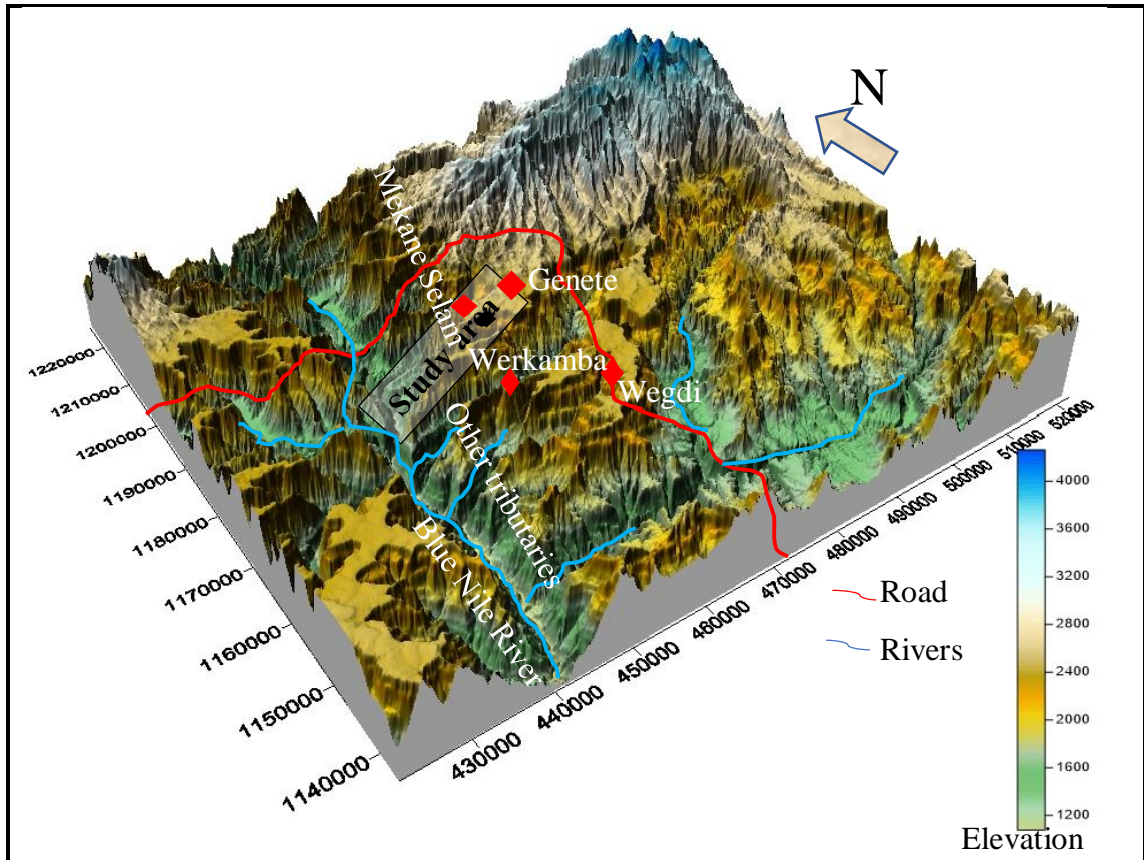


Figure 2. DEM physiographic map of the study and surrounding area.

The drainage pattern of Mekane Selam and surrounding areas shows southward flow of main Abay River. Following that a numbers of west ward and east ward flowing rivers join the Abay River. Besides that there are networks of streams which flow northwest to southwest towards those tributary rivers. The tributaries of the main rivers are able to enhance its volume seasonally. The east west flow of local streams and rivers are sourced from the raged elevated topography of Ethiopian highlands and plateau. Drainage systems is characterized by parallel to sub parallel and sub rectangular pattern. Dendritic and radial distribution of drainage pattern of the basin and central shield volcanos are the most characteristics of the drainage pattern as shown from the drainage map of the area below (Fig.3). The structures and topographic landscapes of the area control the flow direction

and distribution of the drainage pattern. Volcanic traps and shields develop dendritic and concentric to radial drainage system. Parallel to sub- parallel drainage and radial pattern is the common features of the basin following fractures and weak zones of the sequence.

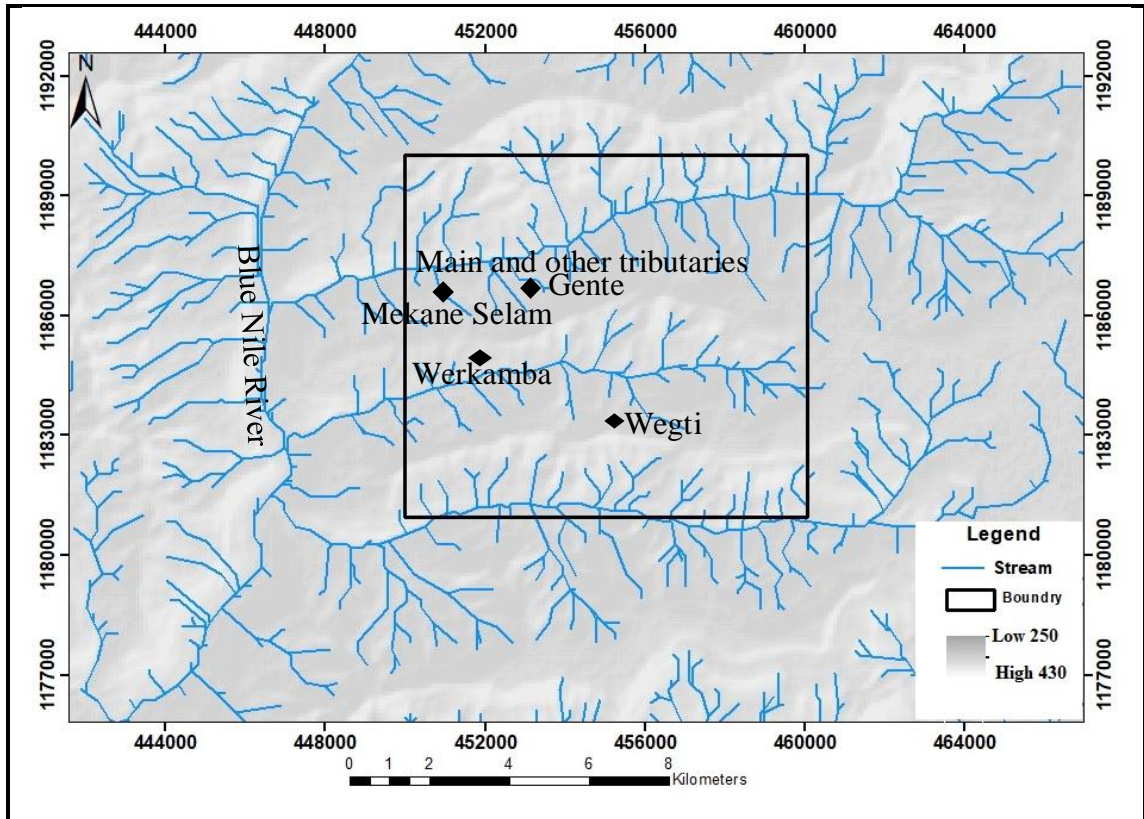


Figure 3. Drainage pattern of the study and surroundings.

1.1.3 Climate and vegetation

The study area is known by its tropical to sub-tropical weather conditions and has the highest precipitation during June to the end of September. Climatic conditions of the area are inferred from the climatic graph (Fig.4) and indicated that mid of June to end of September are the most critical months of rainy time. It is mainly warm to subtropical which is described by high precipitation with limited infiltration. The area obtains high rain fall twice per year, in most cases during the end of May to mid of September. It is characterized by low rain fall from October to end of April and mid of May. The considerable dry time of the area is interpreted rain fall while the averagely hot temperature condition remains consistent. The annual maximum rain fall of the area is ranging from 300- 350mm to 1000-1500mm from the main Ethiopian highlands to the basin and low land areas.

(<https://en.climate-data.org/africa/ethiopia/amhara/Mekane-Selam-928333/>).

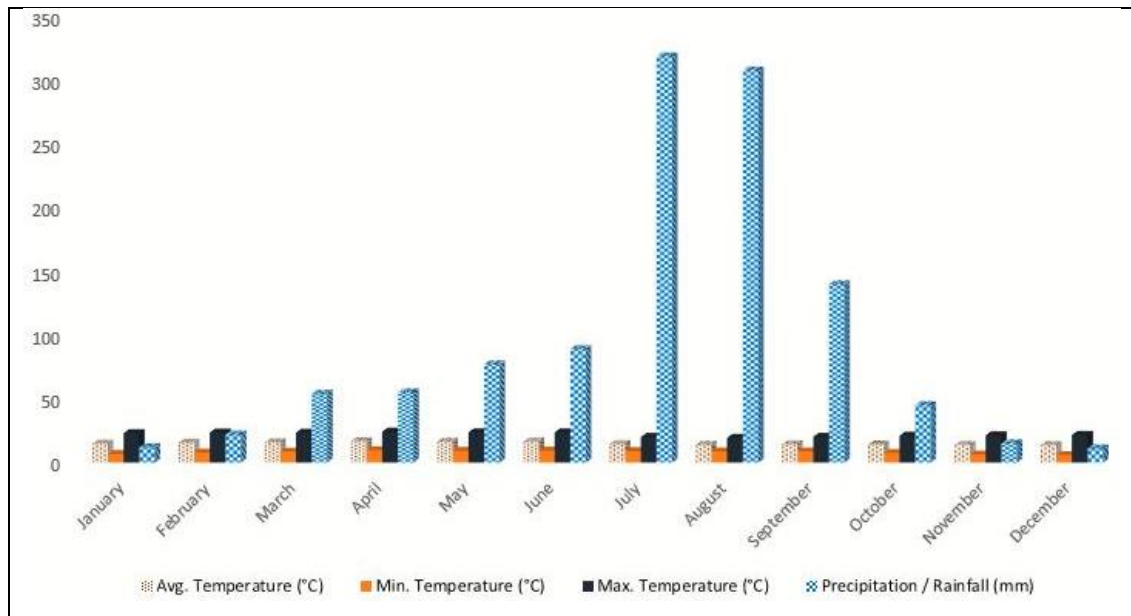


Figure 4. *Weather and climate conditions of Mekane Selam area.*

1.1.4 Population and settlement

The study area is covered by sparsely distributed and short plants. The rocks of study area are well exposed due to the sparsely vegetation cover. The common vegetation of the area include bushes, acacia, trees and other desert resistance short plants. The high lands of the surrounding area are covered by the long trees and some rarely distributed of vegetation of desert area like acacias and short bushes. The trees of plateau are used for house construction and for making of ladder and fire woods especially in rural areas of the study area. The farmers use the highland tree plants for the different agriculture tools and other purposes. The desert plant of acacia is very good agriculture tool in farming.

The population density of the area is widely dispersed most dominant population of the area can be considered as the main ethnic groups of Amhara who speak Amharic as their mother tongue language. The distribution of the population is well planned for house construction and farmland usability. The people of study area also adopted the cattle raring in addition to the different production of agricultural products of fruits and food cereals. The dominant agricultural products adopted and produced by the people are Teff, Wheat, and Maize etc. Tomato, Potato, Cabbages, onions and others fruits are also cultivated. The religion followed by the population is mainly the Orthodox Christianity and Muslim with

few protestant followers. Population growth of the northern plateau, is especially the highland area fast and is rapidly changing the land use and land cover from forest to agriculture. The sociability, well coming of guests and respectful attitude is the common life style of highland people.

The population of the area is widely dispersed throughout the study area and surrounding towns of Mekane Selam. The small houses of the people are mostly built at the hill of the basin and highlands of the area while reserving the low lands and flat areas for the agricultural and small seasonal irrigation purpose. Settlements of the area is sparse in the desert environment and densely populated on the highlands. Following the topography which is suitable for land use and possibility of town in future the population settlement is dense enough.

1.2 Statement of the problem

The Blue Nile basin is one of the known sedimentary basins in Ethiopia. It is well stratified and exposed basin. The resource potential of industrials and energy minerals with geological environmental conditions makes the basin to be attractive and drew the attentions of many researchers in the past. Large potentials of iron ore related with magmatic and sedimentary origin of Bikilal (magmatic), Bale, Sekota, Kefa, Harer and different parts of Tigray (sedimentary) area are resources of iron (Solomon Tadesse, 2009 and Ethio- korian, 1986). A detailed geological investigation including drilling, geochemical, geophysical and other physical studies were conducted on Bikilal iron ore deposit (Ethio-Korian, 1986). Geological, geophysical, geochemical investigations were done by researcher from Geological Survey of Ethiopia and other companies on other iron potentials of the country which are found in southern and northern parts of Ethiopia (Solomon Tadeses, 2009). However, the iron potentials of Mekane Selam area is not known and not well studied so far. This makes loose comparison the iron occurrence of the area with other resources of the country. There is a clear indication of the occurrences of metallic mineral resource potential of Mekane Selam and surrounding area especially for iron mineralization. The genesis, geochemistry, geologic environment and others are not studied. The metallic mineral resource potential of the northern Ethiopia especially Mekane Selame iron occurrence is unrecognized resource and not considered as iron potential area. There is limited geological, geochemical and other resource investigation by Geological Survey of Ethiopia. However, the work conducted in the area is not enough to assess the mode of formation and geologic setting of the area. Generally the current research project is mainly focused on the iron potential of the Blue Nile basin more specifically Mekane

Selam. Preliminary report by GSE (2018) indicated iron occurrences in Mekane Selam and surrounding. But, this work doesn't include the genesis and mode of iron occurrence.

1.3 Research Objective

1.3.1 General Objective

The main objective of this research work is to describe the geologic setting and determine the possible genesis of Mekane Selam Tewa area iron occurrence.

1.3.2 Specific Objective

The specific objectives of the current research includes:

- Identify and describe the lithologic units or host rocks.
- Produce lithological map of the area and mineralized zone at scale of 1: 25,000.
- Characterize the petrography of ores and host rocks.
- Explain the geologic history and genesis of the mineralized area.
- Preliminary investigation to determine the quantity of the iron occurrence.

1.4 Methodology

In order to accomplish the above objectives of this research, different types of technical works were conducted. It includes the following outdoor observation and indoor analytical investigation activities. Geological, mineralogical and geochemical laboratory and petrographic analysis are the principal research methods applied for the current work. The chemical, mineralogical and petrographic data were analyzed, synthesized, presented and finally interpreted.

1.4.1 Field work and Geological Mapping

The research work is done mainly by practical field work and laboratory examinations. It is the principal methodology applied for this work to do practically through actual observation to the ground and performing sample testing. Primary data like lithological units, representative samples of the iron and rocks were has been collected for further laboratory analysis under this activity. Geological field work is important to know the distribution of ore body and lithology of the area. The field work activity has been divided in to three main phases of work. Pre field activities, field work activities and post field activities until the compilation of the research work.

1.4.1.1 Pre field work

Literature reviews and collecting any secondary data relevant for the current study from previous works. Surveying of secondary data insights about the general frame work of the regional geology, geologic history, tectonic setting and structural condition with deformational history of the study area were collected and analyzed. Satellite image interpretation, remote sensing and google Earth software analysis and interpretation were the most important tools for understanding the geology and structural conditions of the area.

The accessibility, lateral extent, physiographic and weather conditions of the area and population settlement and behavior as well as means of communications were gathered from people who know the area. Determination and decision on the total project area in square km from DEM map study, traverse line orientation and line spacing between the traverse as well as number of samples to be collected were conducted. Synthesis, Analysis and interpretation previous works conducted on the area have been done during the pre-field phase of the research.

1.4.1.2 Field work

Field observations on mineralized zone, documenting of geologic structures and lithologic variations were conducted. The best and suitable traversing lines were selected and used to describe the lithologic units as well as iron ore of study area. Field measurements of the exposed ore body and lithology with descriptions were conducted. The ore body horizontal continuity and vertical variation were investigated from field observation. Geologic mapping at a scale of 1:25,000 is completed. The different geological units and ore mineralization has been mapped and described prior to the use of arc map (GIS) software to digitize the field map. Where the lithological boundaries, ore body variations and positions of samples were documented using geographic position system (GPS). Collecting representative samples of iron ore and associated rocks were used as a primary data for the study.

1.4.1.3 Post field work

Preparation of ore and rock samples for geochemical analysis and petrographic description are the primary activities in this phase of the research. Collecting, interpreting and presenting the laboratory geochemical results followed the sample preparation phase. Polished section of iron ore were prepared for microscopic study and characterization of ore samples. Under this study the mineralogical content, textural pattern, grain size

distributions, microstructures of the ore minerals were described and characterized with respect to other ore minerals. Thin section description of rock samples with their interpretation and presentation were also the tasks of this research work under post field phase. Final report writing from analysis and interpretation of the chemical, mineralogical and petrographic results followed the laboratory works.

1.4.2 Laboratory test and chemical analysis

1.4.2.1 Mineralogy (XRD)

Mineralogical (quantitatively and qualitatively) and geochemical analysis are the most vital laboratory tests which have been done for the current research work. Powder X-ray diffraction belongs among standard methods of solid matters analysis. It provides information about phase composition of sample (qualitative and quantitative phase analysis), and crystal structure of matters (crystal structural analysis). Application is also used at textural research (texture analysis).

Portable X-ray Fluorescence (PXRF) is a technique for chemical compositional measurement in which X-rays of a known energy are directed towards a target or sample, causing the atoms within the material to emit "fluorescent" X-rays at energies characteristic of its elemental composition.

Five iron ore samples were sent to laboratory for mineralogical and other analysis using X-ray diffraction (XRD). The economically valuable and non-valuable mineralogical contents of the ore is identified after mineralogical differentiation. The mineral identification and characterization of the iron ore is done by using X-ray diffraction method. The ore minerals are ground in to fine powdered for mineral analysis. The iron ore samples collected from Mekane Selam area for mineralogical identification and analysis were labeled considering the name of the area and corresponding block numbers. Then prepared at Geological Survey of Ethiopia (GSE) for mineralogical laboratory work. Five (5) varieties of iron ore samples (MS-B1, MS-DB3, MS-B5, MS-B10 and MS-LW) were prepared in powdered form at mineralogical laboratory center of Geological Survey of Ethiopia. The powdered ore samples were sent to the laboratory of the Geological Survey of Czech Republic. Qualitative mineralogical content, chemistry and interpretation were done in the XRD laboratory analysis found in the same laboratory. The powdered samples preparation was done in the Geological Survey of Ethiopia using jaw crusher and grinding mill. The rock crushers minimizes the large size rock samples to 10 – 5 mm gravel size and the jaw crusher crashes the 10-5 mm sized sample in to 5-1mm size. The crashed samples by jaw crusher

to 5-1mm was again powdered by grinding mill to 0.063 mm very fine powder of iron. Finally the powdered iron ore samples were sent to the Geological Survey of Czech Republic (GSCR) laboratory center for mineralogical identification and analysis.

1.4.2.2 Geochemistry (ICP-MS and ICP-AES)

Geochemical analysis were done using chemical element detection instruments. The detection limited and accuracy of ICP-MS and ICP-AES is important first criterion. Inductively coupled plasma mass spectroscopy (ICP –MS) and inductively coupled plasma atomic emission spectroscopy (ICP–AES) were applied to detect the chemical elements and elemental composition of the rocks of the study area. The major and trace element concentration of the collected representative ore and host rock samples were analyzed by ICP-AES and ICP-MS respectively. Those analysis of major and trace element geochemistry are useful to study the rock classifications, to determine the degree and intensity of weathering and to understand the genesis of ore deposit. Major elements are mainly useful for rock classification and quality of iron determination. Whereas the trace and Rare Earth Element (REE) analysis is used to determine the genesis of the deposit. Geochemical analysis of mineralized and non- mineralized rock of study area were conducted for trace and major element content study. Using ICP-MS (inductively coupled plasma mass spectroscopy) and (ICP-AES) Inductively Coupled Plasma Atomic Emission Spectroscopy) the trace and major element geochemistry of iron host rock and ore will be analyzed. This method is important to know the chemical composition and classification of rocks and to understand the origin of iron mineralization. For the current research work a total of sixteen (16) representative rock and iron ore samples were sent to the chemical laboratory analysis in Belgium. Those selected samples for geochemical analysis were prepared at Addis Ababa University, School of Earth Science. The samples were milled using ceramic and tungsten carbide miller. The Geochemical analyses were done in Belgium University of Libre de Bruxelles (ULB), Department of Geosciences, Environment et Societe (DGES) chemical laboratory of G- Time. Six sandstones labeled as (MSd1, MSd2, MSd3, MSd4, MSd8 and MSd11), seven (7) iron ore (MSB3, MSB4, MSB6, MSB7, MSB11, MSB12 and MSB15) and three (MSH1, MSH2 and MSH3 mud - shale samples were analyzed for major and trace element analysis in Belgium.

1.4.3. Petrographic study

The rock samples that were collected from the study area were prepared in thin slab section based on their lithological variability. This is important for the petrographic mineral identification, modal composition and description, structural, textural and other relevant data collection. Also used to understand the rock variability and mineralogical change as well as analysis with interpretation purpose of current study from petrographic analysis. The petrographic description and analysis were applied for the iron host rocks and the ore itself. Host rocks of the ore is studied and analyzed using thin section of rocks where the iron ore is done by polished section of the roe. Light transparent petrography and reflected microscope were the selected instruments for this rock and ore study respectively.

1.4.3.1 Thin section

The study of thin section is very important task for rocks to understand the history of the sediment were pass through. The description and analysis was done with the help of polarizing microscope development. Through this instrument the rock fabrics, mineral composition, grain size, grain shape, roundness and origin of the rock was interpreted from results. The sandstone, mudstone or shale, limestone and basalt samples were gathered from the area during field season. Those are ready for thin section preparation, descriptions and possible interpretation. A total of 11 rock samples were collected from the study area depending on the rock variability and degree of weathering. Five sandstone (MSd3, MSd5, MSd6, MSd8, and MSd10), two mud or shale (MSh1 and MSh2), two limestone (MSL4 and MSL6) and two basalt (MSa1 and MSa5) representative samples were collected and prepared for thin section study. From field observation the most favorable rock that host the iron ore is sandstone. The thin section samples were analyzed to determine their, modal composition, texture, cementing materials and geological setting of the area. The thin section study also important for the appropriate rock naming and determine the possible origin of the sediment source. Those collected rock types are prepared for thin section rock samples at Geological Survey of Ethiopia central laboratory. However, descriptions of thin sections were done at Addis Ababa University (AAU) petrographic laboratory section School of Earth Science.

1.4.3.2 Polished section

Iron ore samples were studied from the laboratory polished section of ore samples. A total of six (6) iron ore (MSB2, MSB8, MSB9, MSB13, MSB14 and MSB16) samples were collected for polish section analysis. Those samples collected from the field based on their distribution, weathered conditions, ore variability and types of host rock. Polished section of the ores were prepared in the Ethiopian Geological Survey laboratory. The collected representative samples were prepared for polish section texture, color, and reflectance characterization, mineralogical assemblage discrimination and mineral paragenesis purpose. Light reflected ore microscopy were the most suitable and selected instrument for this analysis. All descriptions and characterization study was done at ore microscopy laboratory section in Addis Ababa University School of Earth Science. The study of ore samples from prepared polished section is helpful to identify constituent ore minerals and the associated gangues. Thus may give clue for the iron ore depositional mechanism and environmental conditions. In addition to this critical information were obtained for the practical iron ore processing and mining activity from their associated gangues and hosts. Important to choice the best processing methods that environmentally friend to enhance the use of resources.

1.5 Significance of the research

The iron resource potential of the research area is poorly explored and delineated as it compared with North and South part of the country. This thesis work is important to consider Mekane Selam and surrounding area is one of the iron mineral resource area and for indication of the iron ore potentiality of northwestern of Blue Nile basin. And it may be a reference or used as a secondary source materials for any researchers to searching and detail investigation or study of other metallic and non metallic mineral resources to the feature exploration. This study provides an opportunity to understand the origin of sandstone hosted iron ore mineralization. To comprehend the genetic model for the iron ore occurrence in the study area that can be utilized to understand the genetic process of iron ore of similar deposits.

1.6 Research overview

Generally the research project of current study is organized and structured in to different main chapters and significant sub chapters. The first chapter can give general frame work and information about the background, location and accessibility, physiographic, climate conditions of the area. Main and specific objectives, applied methodology and problem of

the research statement and importance of the research are included within this part of the work. Secondary data collections (literature reviews), information on iron ore formations, explorations, mining, processing and productions of the iron resource and overview of the iron resource of Ethiopia are mentioned in chapter two of this work. The regional geology and tectonics of the general sedimentary basins as well as volcanic trap of Ethiopia were highlighted in the third chapter. The geological units characterize the research work area with petrographic results were discussed and illustrated under chapter four. Within the fifth chapter the iron occurrence of Mekane Selam and surrounding, with XRD and ore petrography mineralogical constituent, nature of the iron mineralization, geological history and host rock of the area were covered and described. Geochemistry of iron, host rock, country rocks and laboratory results are mentioned and discussed in chapter six of this thesis. The discussion part, geologic setting of the area, origin (genesis) of iron is and the final conclusions with possible recommendation were discussed and included within chapter seven and eight of the current research work respectively.

CHAPTER TWO

2 Literature review

Iron is the fourth abundant element of Earth's crust element with a total 95% metal grade (Goldschmidt, 1888-1947 and Solomon Tadesse, 2009). The 5% of our earth's crust is occupied by ferrous group elements (Gross, 1996). Its geochemical property makes iron to occur in oxides and sulfide ore minerals with rare native formation. It is the most common metal that oxidized in surface environment to convert from ferrous (Fe^{2+}) to ferric (Fe^{3+}) valance state (Robb, 2005). Iron is economically important element that occupies 15% of sedimentary rock (Bekker et al., 2010; James, 1966). Iron is characterized by strong behavior for oxygen affinity and its oxide comprises varying quantities of silicon, sulfur, manganese and phosphorus elements (Spoerl, 2016). Iron is the dominant constituent of majority of rock types chemically known by its Fe^{2+} (ferrous) and Fe^{3+} (ferric) states. Therefore, its ore mineral formation is a factor of oxidation to reducing state. The oxidation condition of the environment favors precipitation of different iron oxides (Lewis, 1976; Bekker et al., 2010). It is oxidized to ferric iron and reduced to ferrous in the free oxygen (oxygenated) and deficient oxygen (anoxic) environment respectively (Taylor and Macquaker, 2011). Iron is deposited in both sea floors as primary precipitation and solutions of non - associating with volcanic or hot brines circulations (Moscow and Ussr, 1973). Genetically banded iron formation is chemically positive enrichment by Eu and

negatively depleted in Ce as well as LREE relative to HREE indicates hydrothermal mineralization process (Eugene et al 2014). The geologic environment of iron deposition is viewed as a wide range of crystallization of heavy mineral settling, metamorphic alterations, sedimentary precipitation and secondary lateritic weathering (AISI, 1999; Solomon Tadesse, 2009). Iron is the world leading metal of the current industry. Its supply is significant to substitute the large import and export expenditures of any country (Jonsson et al., 2013). Hematite content of iron ore hosted in Precambrian to sedimentary formation is the most world's economical source of iron (Beukes et al., 2003; Solomon and Worash, 2015). The requirement for this element is the back bone for the developments of today's industry (Sahoo et al., 2018). The availability, strength in different applications and its economic cost makes iron useable of all metals (Solomon Tadesse. 2009). According to American iron and steel institute company (AISIC, 1999) the mineralogical contents of iron ore is grouped as oxides, carbonates, sulfides, and silicate minerals. Hematite, magnetite goethite, taconite and others are the most known iron ore minerals (Divkota and Paudel, 2012; Asume et al., 2019).

2.1 Pervious work

The study area of this research work is not studied previously from the economic point of view except few studies on oil and gas potentials of neighboring localities. However, previous studies and delineation of iron ore mineralization potential in Ethiopia is taken as a guide for the investigation of Mekane Selam area iron occurrence. The iron ore mineralization potential in the southern and northern parts of Ethiopia is used as a reference (Solomon Tadesse, 2009).

The northwestern plateau where the present study area is found previously studied with respect to different geological and resource aspects (Getaneh Assefa, 1991 and Welela Ahemed, 2002; 2009) conducted a detailed descriptions for the sandstone unit as Debre Libanos Sandstone (DLS) and Muger mudstone. This unit of the area is the main host rock for iron ore mineralization observed today. Another resource of the region is oil seep near Wereillu area (Kazmin, 1975, Serawit Amene and Tamrat Mojo, 1999; Welela Ahemed, 2002; 2009). Adigrat sandstone of Blue Nile Basin and Debre Libaose sandstones are the main targeted formations for oil and gas exploration (Welela Ahemed, 2002).

Muger mudstone and DLS were deposited under Semi-arid to humid to tropical climate in association with rapid fluctuation discharge (Welela, 2002). Continentally originated Mesozoic sediments of northern Ethiopia are less favorable formation for oil and gas and metallic mineral resource exploration but are suitable for non- metallic mineral resources

occurrence (Kazmin, 1975 and Kiffer et al., 2004). According to Danile Meshesha and Shino (2007, as cited in GSE, 2015) the plateaus flood basalt is distinctly separated and also dated. The Ethiopian plateau including the northwestern one is the result of several distinct volcanic centers and magmas erupted at different times (Kieffer et al., 2003). Northern Ethiopian plateaus petrographic and geochemical integration with emplacement age study and volcanic section near Blue Nile overlay on Mesozoic sediment was conducted by Beccualuva et al. (2009).

2.1.1 Previous study on iron occurrence of Ethiopia

Iron mineralization history and application concept in Ethiopia is begins from the early uncivilized mankind's. The resource of iron in Ethiopia is observed from the small indication and occurrence to the level of ore deposit. The mineralization of this resource is difficult to say there is enough ore deposit in the country. Some of the iron ores were known in different parts of Ethiopia from occurrence to deposit level. Concerning iron ore potential most parts of Ethiopia were reconnaissancely prospected and explored by Ethio – Korean (1988), Solomon Tadesse (2009) and Geological Survey of Ethiopia (2017 - 2019). In different parts of the country. However, the economic and more detail works were restricted in a few areas. The iron ore mineralization of Ethiopia is formed due to intense weathering of volcanic rocks and attract the economic interest (Kazmin, 1975). Generally in Ethiopia two main iron ore mineralization areas like Bikilal and Melka Arba are known. A detailed geophysical, geochemical and geological prospection were done by Ethio- Korean project on Bikilal and Melka Arba iron ore (Masresha Gebreselase, 2000 and GSE, 2002). An exploration program for uneconomical iron ore deposit would have been conducted in Ethiopia since from Italian occupation (Hmrla, 1966). Geological and geophysical prospecting work indicates a total of 800,000 tons of iron ore reserve. The estimation of this amount contains 65% average grade of Fe in Wollega (Gulliso-Yubdo-Koree and Billa areas), (Rudis, 1964). Iron exploration project conducted in Ethiopia bales to estimate 58 million ton reserve at Bikilal and genetically magmatic origin of iron. Out of this 23.3% is magnetic and 41% total Fe were documented from the geological works of drilling and trenching (Ethio-Korean 1988). The Bikilal iron ore deposit of Ethiopia was the well-known in Wollega and recently discovered deposit of the country have the same genesis to world iron (Solomon Tadesse, 2009). The iron ore resource of Ethiopia is explored using geophysical and geological as a prospection works in Melka Arba area (Masresh G/ Selasse, 2002 and Solomon Tadesse, 2009). This iron ore is commonly hosted in gabbroic massive rock and disseminated within Syn – Tectonic to magmatic model of emplacement

(Masresha G/ Selasse, 2002). Hematite mineralogical content found in the Blue Nile sedimentary Basin rocks as cementation is an indication of secondary iron resource in the country (Getaneh Assefa, 1991 and Welela Ahmed, 2002). It is a clear cementing raw material for the lower formation of (Adigrat sandstone deposit). Iron potentials of Ethiopia is discovered in its deposit and occurrence level in northern, western and south western of the country (Solomon Tadesse, 2009). Fracture filling, late magmatic hydrothermal type of iron ore body that is non promising in economic aspect is reported around Kunni, Deder and Galleti area in Harerge (EIGS, 1990). Banded ironstone type small extent in Tsole, Faduni Boya, Belgagu areas has been investigated in iron concurrence exploration project (GSE, 1986). Laterite iron was identified within Tertiary volcanic rocks of basalt, rhyolite, trachyte and tuffs around Dim, Arbaminch and Gamo Gofa area (GSE, 1975). This iron ore mineralization of the area is hosted within Mesozoic sediment and Cenozoic to Tertiary volcanic. In addition there are many areas were known by iron occurrences in Ethiopia like Gordma, Chago, Dimma, Mai Gudo, Melka Sedi, Adua and Entcho (Solomon Tadesse, 2009). Yubdo, Nejo, Kata, Sirba, Korkandi, Kiltukara and Wobera Kiltu are some areas of iron occurrence in Ethiopia identified by (GSE, 2000). Iron ore mineralization of Ethiopia prospected and discovered in different areas are mineralogically dominated by magnetite, hematite and limonite (Solomon Tadesse, 2009). Iron ore resource potentials of the country are distributed at different regions and localities few of them are shown in (Fig.5).

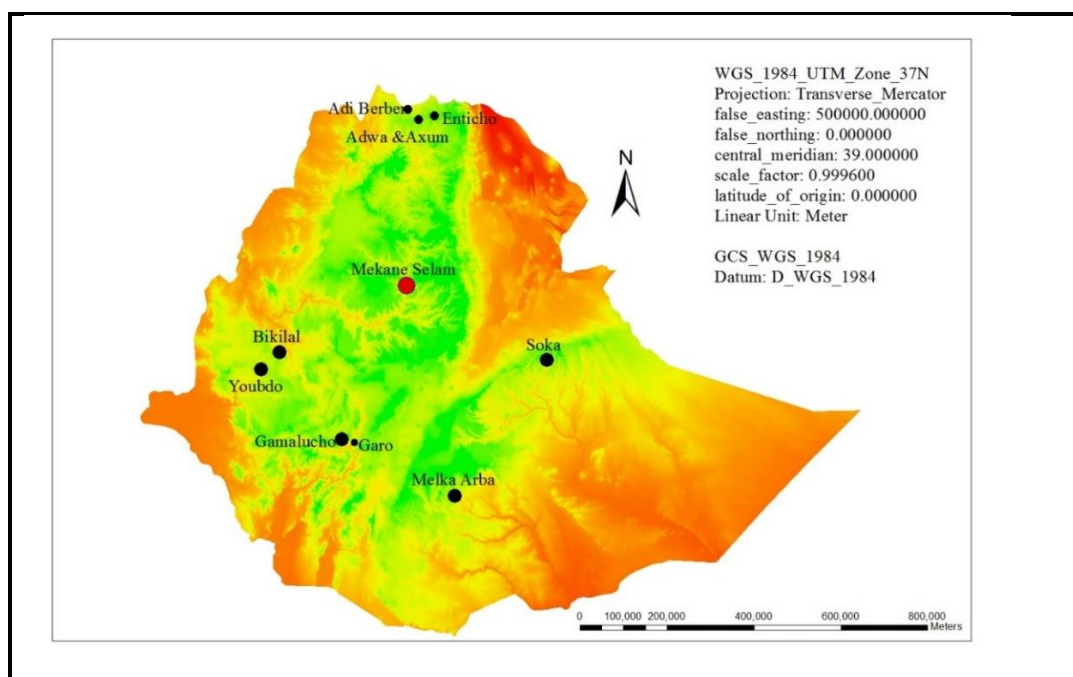


Figure 5. *Distribution of iron occurrence in Ethiopia.*

2.2 Process of iron ore formation

The wide range of industrial applications throughout the world of iron take attentions of users to know its process of formation and quantity. However, the beneficiation, economic technology and quality of the ore minerals are the most critical factors of iron application. The formation of iron ore takes place in wide range of geologic time within volcanic to sedimentary geologic environment and have different distribution. Now adays different geologic settings and processes are suitable areas for iron formation as well as deposition. Concerning the iron ore distributions, it is differently formed and also differently distributed in various regions with variable concentrations. The magmatic to exhalative and sedimentary precipitation is the common modes of iron formation and deposition. Magma related hydrothermal solutions alters sedimentary carbonates mineralogy to skarn type iron (Solomon Tadesse, 2009). Among them the sedimentary and magmatic iron ore mineralization is some of the occurrences in Ethiopia. Magmatic iron is concentrated due to heavy iron mineral crystallization settling processes from liquid magma. The deposition and concentration of iron ore is mainly due to iron rich chemical precipitation in oceans (banded iron is the largest sedimentary iron concentration), surface rock weathering (residual laterite iron) and direct crystallizations of Fe from magma (Solomon and Worash, 2015) gives economic iron deposit. Geochemical inheritance of source magma, hot fluids and parent rock enriched in iron is important for magmatic, hydrothermal exhalative and sedimentary iron formation respectively (Roob, 2013). The early precipitated banded iron rich sediment is laterally modified and enhance its Fe content by hydrothermal process (Bhattacharya and Ghosh, 2012).

2.3 Exploration

Exploration of a mineral deposit is an activity performed to assessing the resource potential of particular mineral. Rapid increase of iron demand in the home land country and through abroad facilitate the exploration as well as beneficiation of iron ores. The earth's iron ore deposit was exploited and consumed by early humans. In order to create constant demand and consumption of iron resource very sophisticated exploration task is needed. Searching the previously existing iron ore resources for their mining operation may be the simplest activity. However, in iron exploration program discovering new ore deposit, determining the areal extent and Fe grade is the difficult task. Iron Exploration consists of discovering the ore, quantify the resource through applying geological mapping with logging, geophysical surveying, geochemical analysis and magnetic techniques are the most

employed for the exploration activity. The iron ore reserve can be estimated with the help of gravity, magnetic and self-potential different geophysical exploration techniques (Christiansen et al., 2018). To conduct iron ore deposit exploration ground magnetic and electrical surveying techniques are used from the susceptibility and resistivity data interpretation respectively (Bayowa et al., 2016).

2.4 Processing

Beneficiation and the end product of the iron ore in relation to their gangue impurities were the most critical factors of iron processing and extraction. The commerciality iron ore is influenced by the mineralogical content and particular oxidation state of iron oxides (Kanorr and Bornefeld, 2012). Iron ore with high Fe, low Aluminum and phosphorous content requires simple technology of beneficiation. However, ores characterized by high aluminum and phosphorous and lateritic–goethitic ore with low Fe needs specific technique (Upadhyay et al., 2010). The XRD and microscopic mineralogical quantification of the constituent phases of iron ore is optimizes the metallurgical processing and mining operations (Villiers and Lu, 2015). Blast furnace, routes (pig iron) and direct reductions are the most common processes of iron production methods (Asuke et al., 2019; Muanguiz et al., 2012). Iron ore passes through different processing paths since its discovery until the production of steel. In blast furnaces iron is processed through mining, crushing, separating, concentrating, mixing, pelletizing and shipping. Metallic iron is economically extracted from the iron ore rich in iron oxides. To extract the metal grade of iron from hematite, magnetite, goethite and other sulfides mineral processing is needed. The iron ore processing and extraction produces iron metal and steel. Iron ore mineralization is occur with different gangue minerals or impurities. The mineralogical content, type of gangue minerals associated within the iron ore controls the choice of technological beneficiation treatment. The mineralogical characterization of an ore deposit from ore petrography and XRD study are of major importance for mineral processing. This mineralogical study plays a vital role in selections of the appropriate processing method. In the processing of iron ore for better beneficiation there must be an increase in the content of Fe and decreasing the proportions of impurity or gangue. This very critical condition is met through washing, jaggging, gravity separation, magnetic separation and using advanced technology of grinding, crashing, roasting and screening are also seriously applied for the better treatment and beneficiation of iron from its impurities. The iron ore processing and steel production method with major operations is illustrated in following diagram.

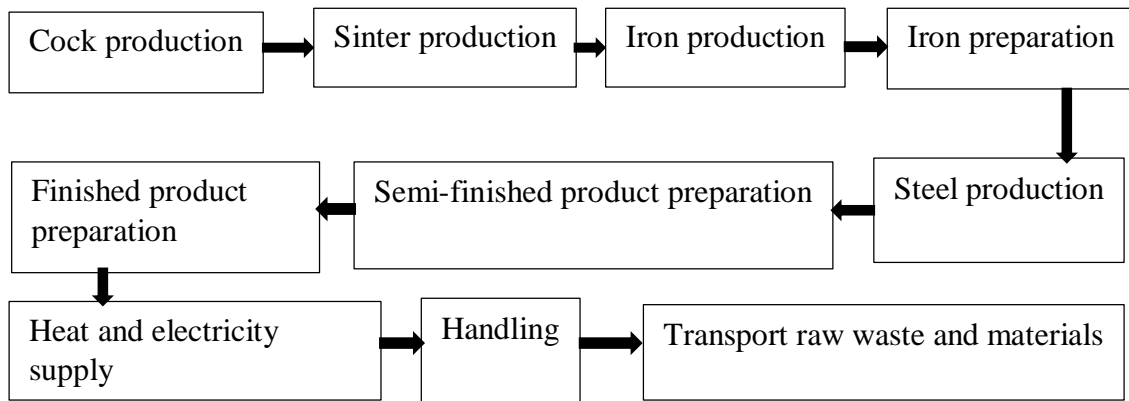


Figure 6. Basic iron ore interrelated operational stages according to (Upadhyay et al., 2009 and Nomura et al., 2015).

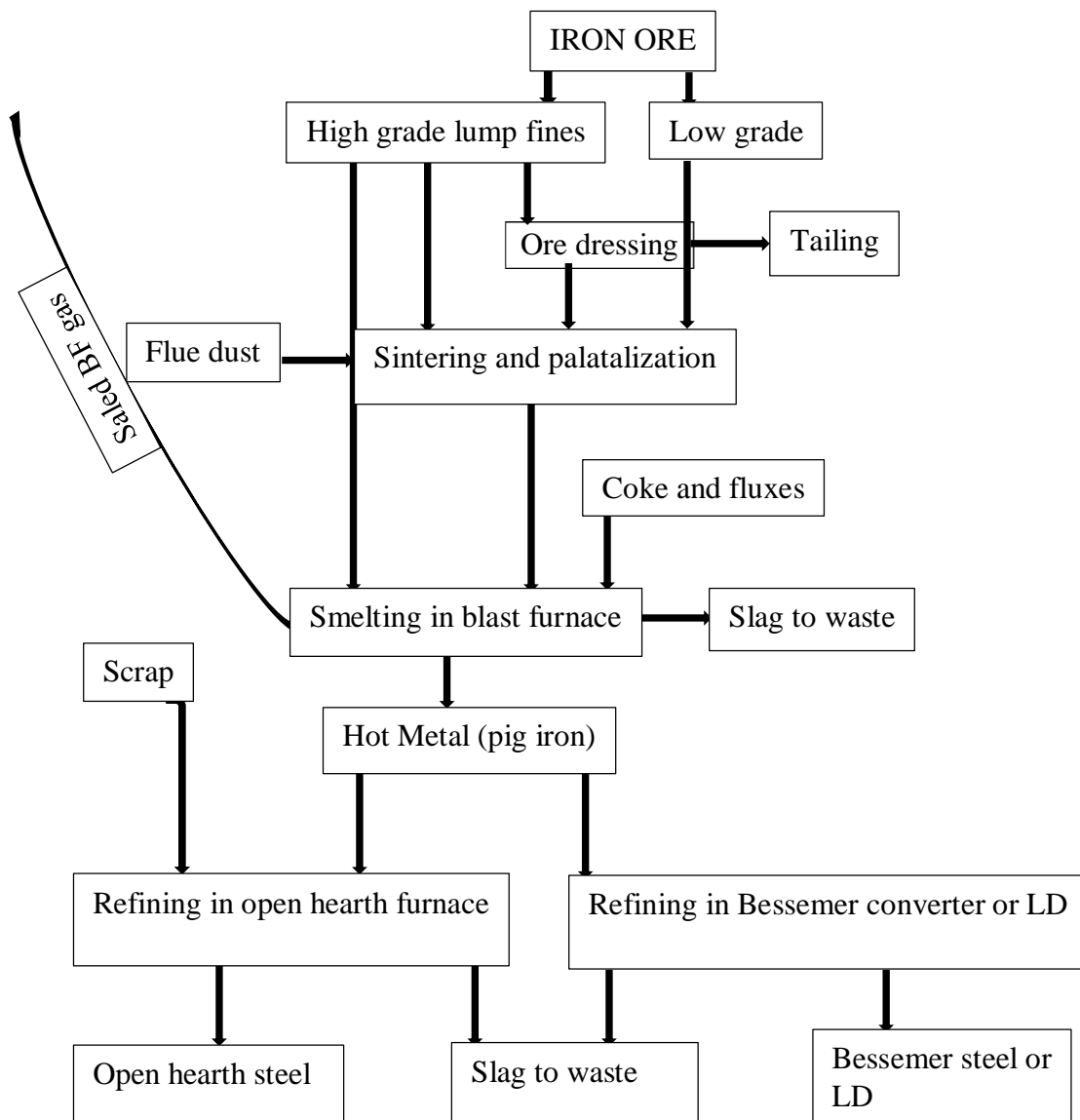


Figure 7. Flow sheet for iron and steel extraction process according to (Kumar, 2003 and Spoerl, 2016).

2.5 Mining

The iron ore is mined from all igneous, sedimentary and metamorphic rock types that hosts enough economical concentrations of Fe. However the mining method selected for the iron ore is dependent combinations of various factors. Ore deposit type, extensions, technology applied, geologic formation of surrounding rocks, ore shape and environmental conditions are some of them. Mining of iron ore passes through exploration, mine development, underground and open pit extraction, ore beneficiation, storage with transportation and mine closure and reclamation. The mining activity of iron ore may be conducted by both surficial and underground mining method based on the ore deposit. The overburden materials of the iron ore dictates the mining activity to be applied. Bog iron ore can be mined by simple digging where, others need open cast pit and deep underground works. The most common iron ore mining activities have been conducted by large open pit excavation and removal of surface overburden. Surface mining is applied when the ore is close to the surface. In general most iron ore were mined by surface mining method (commonly open pit and open cast). But, some of the large iron deposits around the world are mined through underground mining activity. Small ore bodies are mined by manual mining techniques rather mechanized. Floated type of ore are easily dug, with picks, crow bars and spades manually. In order to mine iron from its sub surface deposit mechanized mining were chosen and well assisted by drilling as well as blasting. However, the proximity of ore body to surface determines which method is employed. Magmatic to hydrothermally related iron ore deposits are commonly extracted by underground mining method. Finally the open pit and underground mining of iron ore must consider environmental issues. The overburden, waste rocks and mine water consists of suspended dissolved metals with fluids dumped properly. Rehabilitation of the normal environment is the final considering issue of mining activity before mine closure.

CHAPTER THREE

3 Regional geology and tectonic setting

3.1 Introduction

A number of geo scientific researches were conducted in East African Rift system, and western and southern plateaus of Ethiopia. The northwestern Ethiopian plateau is part of the African rift and basin formation mainly consisting of flood basalt and older sediment sequences. Geologically the northern basins are described by different volcanic

sedimentary and underlying basement rocks. However the northern plateau and associated basins are predominantly known by Tertiary to Quaternary volcanic complexes and different sedimentary successions. The flood basalt volcanic plateau was an emplacement of Afar mantle plume that extends to the rift margin. Basins and volcanic trap of the northern plateau episodically affected by the uplifting and seasonal erosion with extended rift escarpment.

Tectonic setting of Blue Nile and Upper River basins are considered as the Horn of African Rift (HAR) sedimentary basins that are controlled by rifting and continental breakup. The tectonic forces of Earth's crust is important controls to generate sedimentary basins in the area. The basin formation and developments with its associated sediment filling of most basins are assisted by extensional rifting, uplifting–subsidence and denudations or erosional process.

3.2 Regional geology

Precambrian basements, late Paleozoic to early Tertiary sediments and Cenozoic volcanic with associated sediments are the main lithological units of Ethiopia. (Kazmin, 1975; Mengesha Tefera et al., 1996). Sedimentary and volcanic varieties are the components of the basement rocks (Serawit Amene, 1999). The physiographic features of Ethiopia is characterized by Northwestern and Southeastern extensive plateaus, Main Ethiopian Rift Valley (MER) and Afar Depression (AD) (Getaneh Assefa, 1991 and Mengesh Tefera et al., 1996). From those features the Blue Nile Basin is one of the main sedimentary basins of the country that is found in Northwestern plateau. This basin is underlain by Neoproterozoic crystalline rocks and overlain by Oligocene to Quaternary volcanic (Gani et al., 2008). It is occupied by siliclastic continental sediments which are grouped in to Mughar Mudstone and Debre Libanose Sandstone (DLS) (Getaneh Assefa, 1991). The evolutions of the basin is divided in to three dominant phases: Pre-sedimentation, sedimentation and post sedimentation phases. The pre sedimentation phase is characterized by pre rifting and crystalline basement rock denudation and peneplanation (Getaneh Assefa, 1991). Sedimentation phase is described by: Marine transgression for sandy mudstone, lower and upper limestone, gypsum unit sedimentation. Marine regression that is responsible to deposit alluvial/fluvial upper sandstone (DLS). Post sedimentation phase occurred during Oligocene period and is documented by thick volcanic eruptions and quaternary top volcanism are emplaced which are related with Mantle Plume of Afar volcanic eruptions (Getaneh Asesfa, 1991 and Gani et al., 2008). In additions, the

sedimentary evolution of the Blue Nile Gorge is outlined by (Russo et al., 1994 cited in Gani et al., 2008). According to Aubry, (1886), Stefanini, (1933), Merla et al.(1973 and 1979 cited in Getaneh Asefa, 1991) the Northwestern, Shoa and Wollo sandstone with upper gypsum sediments are characterized and conformably overlay to the lagajima limestone. Typically different sedimentary formation show various depositional mechanism at different basins. That is Karroo sediments around Ogaden basin, Adigrat Sandstone in Abay basin Denakil Alpe and Rift Valley (Senbeto Chwaka, 1981 cited in Serawit Amene, 1999) and Abbate et al., 2014). The continental clastic Paleozoic to Mesozoic sediments are cropping out in Abay River Gorge including Tigray, Harer and other areas of the Ethiopia (Kazmin, 1972, 1975 and Getaneh Asefa, 1991). Mesozoic sedimentary sequence of Abay Basin is continuously exposed within upper Abay and Jema River valley and unconformably overlaid by the tertiary volcanic. (Tamtat Mojo and Serawit Amene, 1995). In this sub basin the sediments are characterized by limited thickness of about 100 and 120m thick sections of clastic sediments near Blue Nile Gorge and Jema River respectively (Abbate et al., 2014). The sediments deposited within this basin are due to the presence of NE-SW oriented fault system in central to northeastern part of Abay (Gani et al., 2008). This structural system is the probable reason for the Blue Nile Basin is divided in to Muger Mudstone of western part and DLS of northeastern to central part of two sub basins (Welela Ahmed, 2009). Stratigraphic section of Blue Nile Basin from the base to top is described as Precambrian basement, Karroo sediments, middle and upper carbonate and sulphate Hamaneli formations, Muger mudstone, DLS and volcanic trap of the plateau (Welela Ahemed, 2002). The Lower sandstone, shale and gypsum, limestone, shaly sandstone, upper sandstone and massive flood lavas are the basin log section made by Getaneh Assefa (1991). The Limestone, gypsum and shale units are outlined by Krenkle, (1926). According to GSE (2015) Lower sandstone, gypsum unit, fossilized limestone, upper sandstone and basaltic lava flows are regional stratigraphic units of the Blue Nile Basin. The structural and stratigraphic studies used for reconstruction about the basin geological history are studied by Gani et al. (2007 cited in Gani et al., 2008). The DLS crop out regionally at different parts of the country around Lemi area, Muger and Jema Rivers (Getaneh Assefa, 1991). Similarly it is also, found in Mekeke and Ogaden basins (Byth, 1972 / 73; Worku T., 1988; Hunegnaw A., 1998 as cited in Welela, 2009). The DLS unit is regionally correlated with Nubian Sandstone, Sudan, Yemen, Kenya and Saudi Arabian Sandstone (Getaneh Assefa, 1991). This unit is also classified as the upper sandstone (Mohr, 1962; Kazmin, 1975 and Merla et al., 1973 as cited in Welela Ahmed, 2009).

According to Shumbro (1968, cited in Welela Ahmed, 2009). The (DLS) unit is described as the Ambaradom formation. Also, it is described and classified as Debre Libanose Sandstone and the Muger Mudstone by Getaneh Assefa, (1991). The weathered and fertile volcanic trap of northwestern plateau is unconformably overlain on the DLS lithologic unit (Welela Ahmed, 2002). Upper Sandstone of Blue Nile Basin is characterized by upward fining in texture with lenses of conglomerate resulted from meandering river sedimentation (Welela Ahmed, 2009). Horizontally bedded, massive beds, laminated shale, mud and siltstones and fine to medium grained sandstones are the common features of (DLS) (Welela Ahmed, 2002; 2009). The sandstone, shale, siltstone and conglomerate varieties of late Paleozoic to Mesozoic age are the main filling rocks of peripheral parts of Ethiopian sedimentary basins (Mengesha Tefera et al., 1996). Sandstone, shale and silty clastic sediments of Abay basin is unconformably overlay the lower or (Adigrat) sandstone (Jepson and Athearn, 1961 as cited in Mengesha et al., 1996). The Adigrat sandstone formation is variably overlaid unconformably on the Precambrian basements. This unit is slightly unconformably underlain by late Paleozoic to Mesozoic sedimentary rocks of Northern Ethiopia (Mengesha Tefera et al., 1996; Kazmin, 1975). The western, southeastern including northwestern Ethiopian highland plateaus cover large area. Those volcanic products consist of both the flood basalts with approximately same chemical and mineralogical composition and parts of sedimentary successions (Kieffer et al., 2004 and Mengesha Tefera, 1996). Alkaline and thioitic basalts of south and west margin of Afar depression in Northern Ethiopia have some successive interbedding with cretaceous regressive sandstone (Gouin and Mohr, 1964 cited in Mengesha Tefera et al., 1996). The Eastern to Western part of Africa and Arabia tephritic basalt was extensively exposed during the Oligocene in relation with terrestrial sediment deposition (Abbate et al., 2014). The distributions of flood basalt in the North South, West and East was genetically reconstructed as migrated from the Afar Depression center of volcanism (Kazmin, 1979). Flood basalts of the plateau is tectonically culminated due to the emplacement of alkaline shield volcanoes (Mengesha Tefera, et al., 1996). Where the volcanic emplacement of ash and coarse pyroclastic fragment products are from the trap segments composed of basalts to siliceous varieties (Kazmin, 1975). This flood basalt has 600000km² containing the youngest Quaternary sediments of conglomerate, sand and clays exposed in in Afar and northern margin of the Rift (Kazmin, 1975; Kieffer et al., 2004). The mineralogical composition of flood basalts consists of aphyric to phyric and phynocryts of plagioclase and clinopyroxene without or few olivine (Kieffer et al., 2004). The outcomes of

geochemical trace element distribution and isotopic constituent of the northern shield and flood basalt is due to complex evolution through progressive changes (Kieffer et al., 2004). The volcanic intertrapean of northern margin is characterized by common features of lignite seam and content of fossilized organism (Rodriguze, 1919 and Gtaneh Assefa and Saxena, 1984 cited in Abbate et al., 2014). According to GSE (2015) the tertiary rock units are dominated by basaltic lava flows and pyroclastic tuff underlain by Mesozoic sedimentary rocks. Those are separated into different units of alkaline and tholitics (Daniel Meshesha and Shino, 2007). The northwestern plateau is consist conglomerated to muddy sandstone, limestone and volcanic lava flows as a regional geologic units (GSE, 2015). The flood basalt of plateau is deeply weathered of alkaline with transitional basalt and intercalations of pyroclastic materials (Mengesha Tefera et al., 1996). According to Getaneh Assefa (1991) lithological stratigraphy of the northwestern part of the country were has been established.

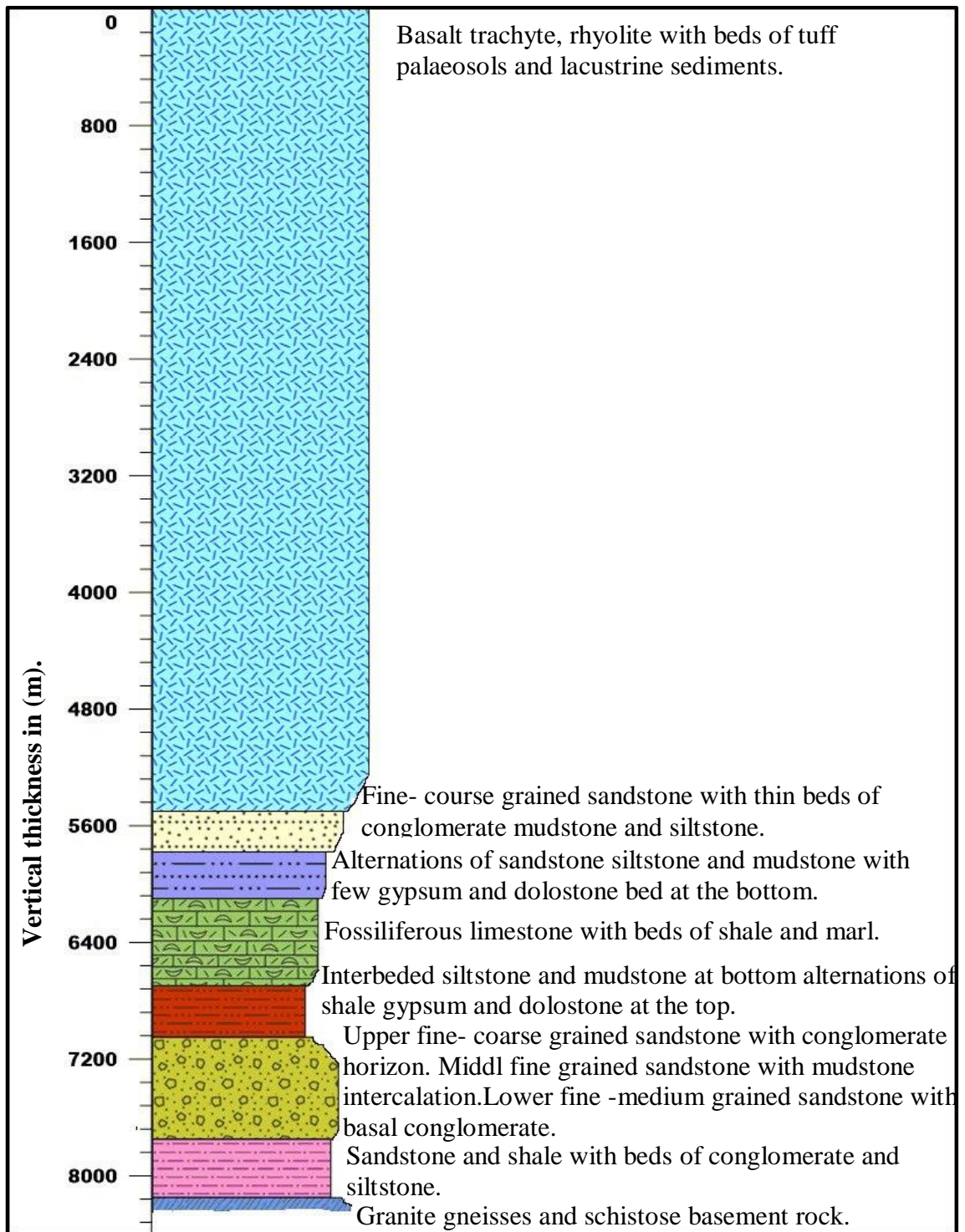


Figure 8. Regional stratigraphy modified from (Getaneh Assefa, 1991).

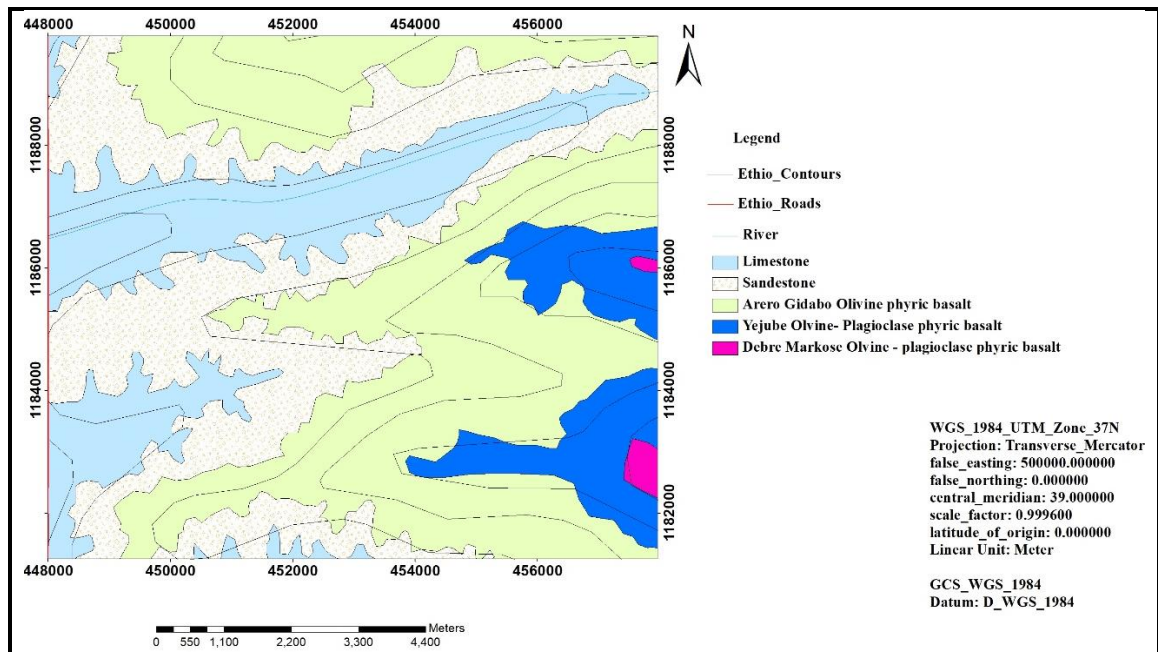


Figure 9. Regional geological map modified from (GSE, 2015).

3.3 Tectonic setting

The initiation and developments of Grate East African Rift System affects Ethiopia and crosses its plateau in to two. This was prime causative tectonic force for the formation of varieties of main and sub continental sedimentary basin that is filled by rapid erosion and volcanic products (Mengsha Tefera et al., 1996). Northern and central Africa was affected by the lithospheric extension to north of Blue Nile Basin and SE-NW oriented thinning (Fairhead, 1988; McHargue et al., 1992; Binks and Fairhead, 1992 cited in Gani et al., 2008). Blue Nile Basin is formed within NW oriented extensional rift related to the Main Ethiopian Rift (MER). The rift extension is filled by Mesozoic continental clastics, marine carbonate to sulphate and volcanic lava (Gani et al., 2008). The Karroo refitting is the second possible tectonic force to develop the basin that propagated from South Africa and end up to Ethiopia (Flores, 1973; Kamin-Kaye, 1978; Canon et al., 1981 cited in Welela, 2002). The Northwestern plateau and associated basin's Mesozoic sediments were sandwiched unconformably by basement and volcanic lava flows (Gani and Abdelsalam, 2006 cited in Gani et al., 2008). The Blue Nile Gorge (BNG) sediments are underlain by the oldest Precambrian basement rock and overlain by trap volcanic (Getaneh Assefa, 1991; Welela Ahmed, 2002). The extensional to transtensional movement and development in the African continent is important for the formation of basins followed by depositions of the karroo (formation overlain by Adigrat sandstone) sediment (Welela Ahmed, 2002). The

transgression of sea associated with thermal and continuous subsidence of Early Jurassic period were deposited the Hamanili limestone formation (Welela Ahmed, 2002). Meandering River and Braided River systems were the main depositional mechanisms of Mugher Mudstone and DLS formation. This is due to sea withdrawal from central and Northern Ethiopia in late Jurassic to Early Cretaceous (Getaneh Assefa, 1991 and Welela Ahmed, 2002). According to Getaneh Assefa (1991) Mugher Mudstone comprise gypsum dolomite shale alternation with fine to medium grain sandstone. Where the Debre Libanose Sandstone (DLS) is characterized by fine to medium grained sandstone with laminated lenses of locally distributed conglomerate. Uplifting and regression processes are responsible for this formation. (Getaneh Assefa, 1991). Regressionally formed sandstone series are conformably overlaid the limestone unit of northern Ethiopian plateaus sequence (Dainelli, 1943 cited in Getaneh Assefa, 1991). Both the Precambrian and Tertiary volcanics are the commonly associated geologic units of Blue Nile Basin in addition to the Mesozoic sedimentary succession (Welela Ahmed, 2009). The Precambrian lithologic varieties in the basin are (Alge group) consists of quartzite, granite, granodiorite, gneiss, hornblende-biotite gneiss and diorite with metasediments (Kazmin, 1975; Mengesha Tefera et al., 1996 and Welela Ahmed, 2009). The underlying high grade metamorphic rocks of western Ethiopia Geba domain is part of the basins lithology (Teklewoled Ayalew and Moore, 1989 cited in Welela Ahmed, 2002). It is overlaid by the sedimentary rocks. The Geologic formation of Blue Nile Basin including the upper sub basin is characterized by a thick depositional succession of clastics continental sediments of sandstone, siltstone, Mudstone with shale (Jepsen and Athearn, 1964 as cited in Welela, 2009). This history of deposition is supported by (Kazmin, 1975; Getaneh Assefa, 1991 and Mengesha Tefera et al., 1996). The fine to medium grained sandstone, siltstone and mudstone with large percentage of rounded to sub rounded texture poorly sorted sandstones are the sequence of sediments are found in basins of Ethiopia (Welela Ahmed, 2009). Those pre Adigerat (Karoo) clastic sediments are exposed in different parts of Ethiopia around Finchaarea Ogaden and Mekele Outliers although their distribution is not well established (Jepsen and Athearn, 1964; Worku T., 1988; Busser and Schrank, 2007 cited in Welela Ahmed, 2009).

CHAPTER FOUR

4 Local geology

Introduction

The research work area is dominated by lithologic units that are classified as Mesozoic, Tertiary and Quaternary rock varieties in geologic times. The Mekane Selam area is part of the upper sub - basin of the Blue Nile. Geologically the area consists of both the sedimentary and volcanic rock types. The current study area is located in the south west of Mekane Selam town which is built on the plateau of basaltic terrain. The northwestern plateau and corresponding basin are economically significant to the industry of the country. The industrial minerals commonly found in the area are most importantly applicable for the construction and other industrial field of application. However, metallic mineral exploration and investigation is uncommon to the northern plateau and basin. Although, at about 35km from Mekane Selam town the sedimentary terrain is considerably mineralized area. This terrain is known by its sedimentary iron mineralization which does not extend to the volcanic rock. The study area is localized in sedimentary succession specifically in the sandstone. The area is selected for this research work based on the practical exploration of hematite type iron ore mineral concentration in the environment.

4.1 Geology of the study area

The research area is part of northwestern Ethiopian plateau and sedimentary basin. It consists of the Mesozoic clastic and carbonate rocks and tertiary volcanic basalts with associated pyroclastic deposits. The lithological units of the area are exposed to the north east of the upper Blue Nile River (BNR) cuts to that of Mekane Selam. Dominantly the study area is comprising of fossiliferous limestone, thin beds of mud or shale, coarse lenses of conglomeratic sandstone, iron ore bed, weathered – fine grained sand sediment and volcanic lava flows. This stratigraphic section of study area is well exposed from the upper Blue Nile River onward to the Mekane Selam said. The general succession of rock stratification is cropped out from limestone to volcanic lavas bottom to top with an inter beading of iron ore to the sandstone. Except volcanic lavas the rock types of study were horizontally beaded to the normal sedimentary stratification. The volcanic complexes of Mekane Selam and surroundings were unconformably overlay to sedimentary rocks. The constituent geologic units of the area were mapped together with the inter beaded iron mineralization that occurs at different blocks as illustrated in (Fig. 10).

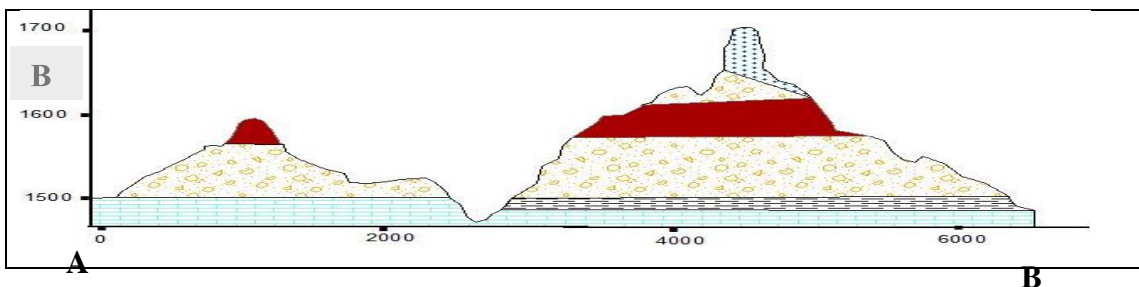
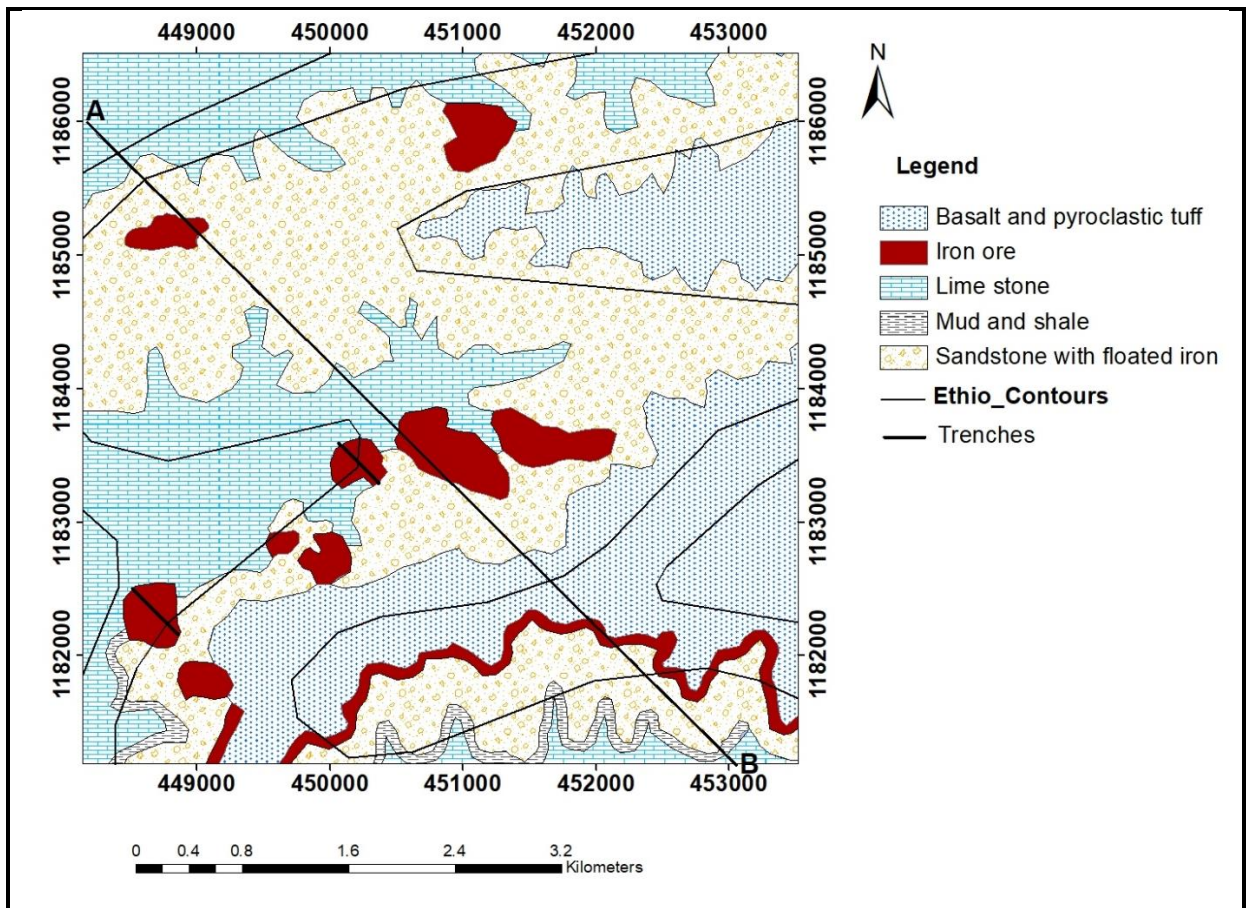


Figure 10. Lithological map of the study area (A) and geologic cross section along A-B (B).

4.2 The Limestone Unit

The Blue Nile Basin limestone is extending to the upper sub basin to the Mekane Selam and Mertule Mariam side from the Basin River gorge. Limestone is the largest lithological unit exposed in the current research area. This unit is extensively exposed from the river cut to the sandstone upper succession with approximately 2000m thickness. The limestone unit of the study area is the steep cliff former carbonate rock near to the river cut. Near the sandstone boundary, it forms moderate to gentle topography. It is characterized by light, yellowish and brownish red (Fig.11). The limestone of this area is two types distinctly different in its fossil content from lower and top parts. It is dominated by fossiliferous

carbonates and clastics of the ferruginous materials from the river cut to sandstone contact. The carbonates are characterized by their fossil content and texturally consists of the micrite and sparite grains. The limestone is inter bedded with friable yellowish marly carbonates and very fine sediments of transported from overlaid sandstone. The fossil content of the unit is not uniform throughout the entire part. The lower portion of the unit is dominantly fossiliferous and the top near to the sandstone boundary is non-fossiliferous. The Non fossiliferous limestone has shiny surface and consists of coarse calcite and silicified precipitates. Upper part of the limestone is form gentle to moderately steep topography of the area near to the sandstone boundary. The sedimentation mechanisms is vary from well compacted and lithifid to friable fine sediments of clay and carbonate materials. This unit is not considered as the host rock for the iron mineralization.



Figure 11. *Field photographs of fossiliferous (A) and non - fossiliferous (B) limestone.*

4.2.1 Petrography of limestone

The petrographic (thin section) descriptions of limestone is prepared and described using petrographic microscope. The thin section observation shows fine carbonate grains of non-translucent (micrite) and cementing of shiny (sparite) grains. Most part of thin section is occupied by micritic carbonate grains. The transparent sparite components are coarse grains and are found filling in fractured or dissolved part. The dominant components of the limestone are orthochemicals and allochems. Micrite and sparites are the main components

of orthochemical components. The bioclastic dominated fine limestone components of the thin section is the micrites and the clear white cementing and precipitated in the dissolved pores of the lime cavity are the sparites. The allochems are characterized by ooids (spherical to sub spherical) and peloids (spherical to elongated carbonate grains) and the interaclsats (elongated fragments) of the limestone components. The ooid - peloid and skeletal carbonate fragments are erratically distributed within the fine matrix (micrite) component. The skeletal carbonate grains are few in proportion and display internal structure of ooids. In terms of percentage the micrite is dominant followed by sparite and the allochems are occupies the smallest proportion. The limestone thin section of samples MSL4 and MSL6 are photographed from the microscope and illustrated in (Fig. 12).

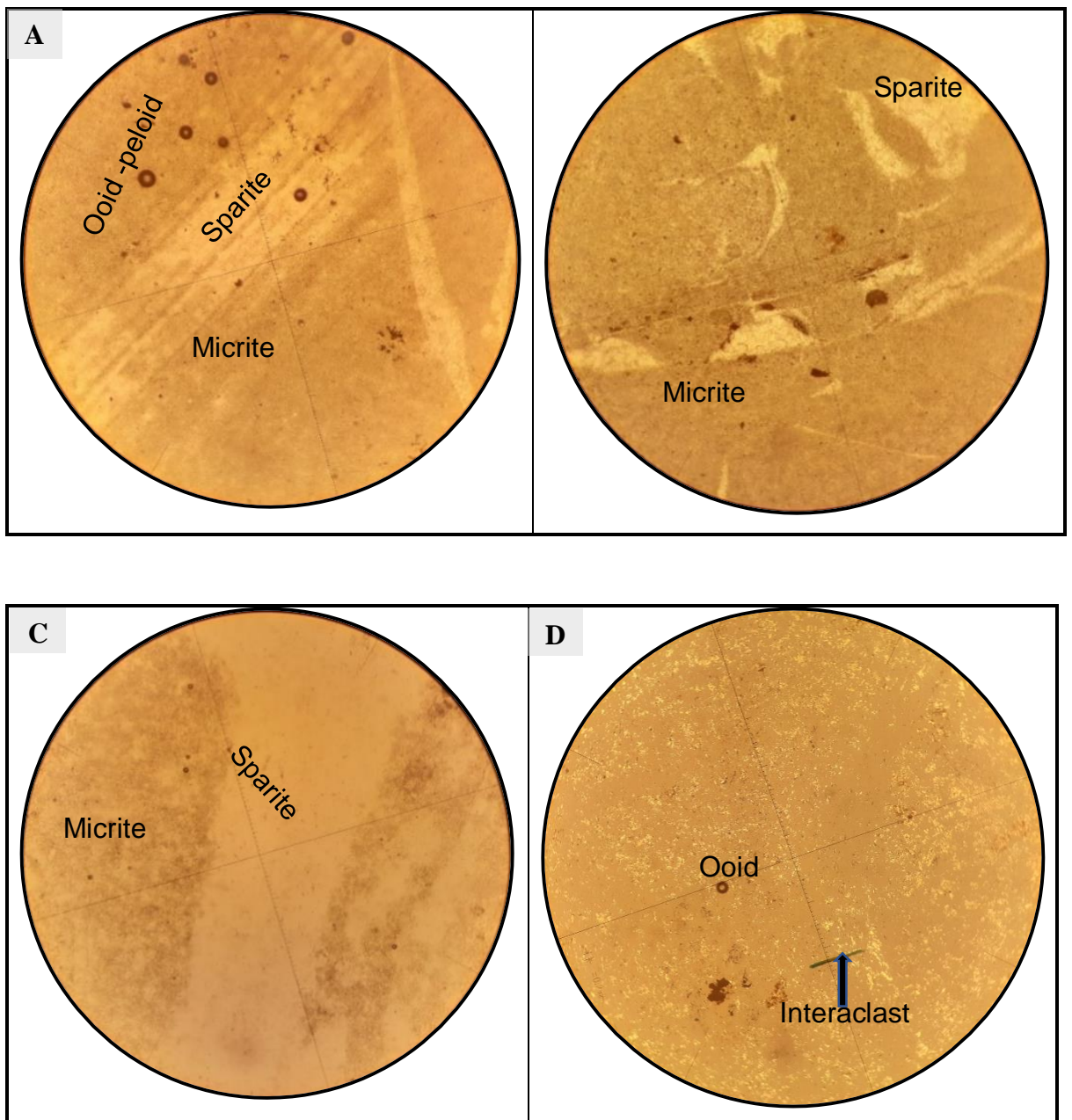


Figure 12. *photomicrograph of MSL4 (A) PPL, (B) XPL and MSL6 (C) PPL, (D) XPL for limestone with 10X magnification power.*

4.3 The Mudstone–shale Unit

The shale or mud stone is the second rock type conformably overlies the limestone unit and is very thin and undifferentiated layer of the study area. It is characterized by yellowish to light grey with partially cementation by hematite. The exposures of this thin layer of friable to slightly compacted sediment shows fissility on exposure level. The degree of weathering in this thin laminated layer is not less than the overlying sandstone. This lithology is not well exposed and cropping out in small size at the boundary of limestone and sandstone units. Due to its limited extent it is difficult to map this unit. However, the unit has been illustrated on the geological map of study area as a thin lamination with limited continuation bed (Fig. 10).

4.3.1 Petrography of mudstone

Two thin section are prepared for fine compacted to friable sediments. It is prepared from hard or compacted rock collected at the limestone and sandstone contact to describe under the microscope. The petrographic characterization of this fissile, friable and fine rock is dominated by ground mass. It is cementing for coarse grain minerals. The coarse grain minerals within this rock mainly altered plagioclase and orthoclase (due to weathering) oxide minerals, and little quartz. Quartz is light or colorless under PPL. The rock is fine grained and show stratification. (fine ground mass and coarse minerals show sorting) to the ground mass. The plagioclase of this sample is white grey to brown pleochroic in (PPL) observation. The morphology of the minerals are angular to sub angular and shows extinction to the cleavage direction. Orthoclase minerals are dark grey angular to sub angular grain and coarse texture. Rounded and angular dispersed opaque minerals are the components of this sample. The rock minerals are moderately sorted but highly oxidized to hematite. The percentage modal compositions of this thin section is determined from the five respective field of observation. From the total five observation each mineral composition is recalculated to 100%. The Quartz, plagioclase, orthoclase, opaques (iron oxide) and ground mass modal composition of MSh1 3.6%, 7.2%, 7.2%, 5.2% and 76.8% while MSh2 comprises 3%, 6.4%, 5.6%, 6.8% and 78.2% Quartz, plagioclase, orthoclase, oxides and matrix respectively. Weighted composition to 100% shows high proportions of

clay as ground mass dominated sediment and low content of quartz and feldspar are characterize the muddy shale rock. This petrographic description and approximate modal composition under microscopic observation MSh1 and MSh2 comprises 76.8% and 78.2% ground mass respectively. Sedimentary rocks with matrix (ground mass) >75% is considered as mud pitijone (1975). Therefore, those compacted fine sediment samples are classified as mudstone. The photomicrograph of thin section number MSh1 and MSh2 are illustrated from (Fig.13).

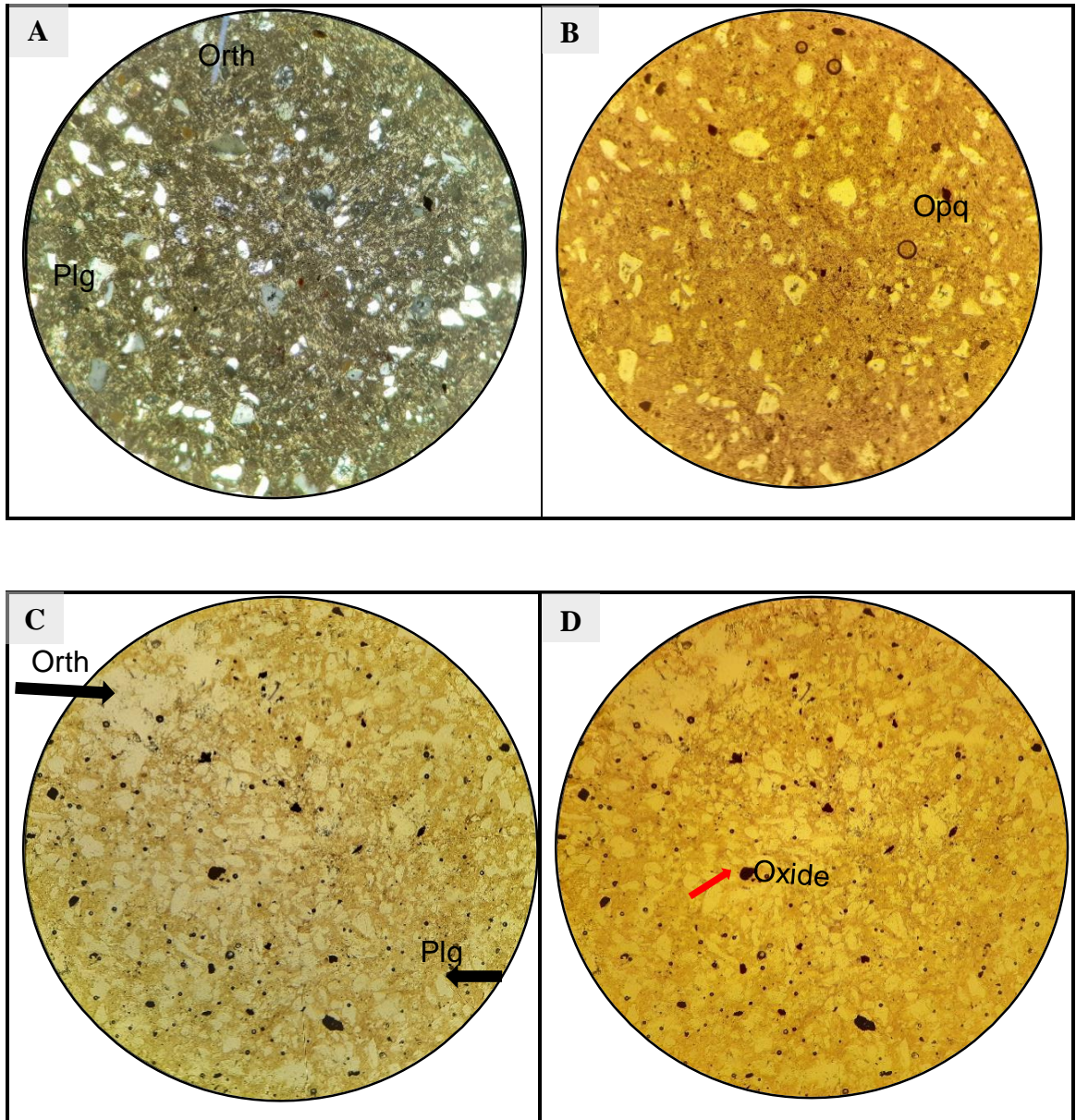


Figure 13. MSh1 (A) XPL, (B) PPL and MSh2 (C) XPL, (D) PPL observation for mudstone with 10X magnification.

4.4 Sandstone

Sandstone of the study area is the principal unit and well exposed lithology. This rock type is characterized as white to brownish grey in color and sandy to gravely in size. It is exposed on the slightly gentle topography relative to limestone and volcanic basalt. This lithologic unit of the area is the main target of this research work. The iron mineralization of the area is hosted within this unit as a continuous horizontal bed and blocks of iron. The sandstone of study area locally shows two distinct stratigraphic section. It is exposed on the top of the iron bed and below the ore body. The top section sandstone is exposed as a thin interlayer on the iron ore. This layer of sandstone is thin weathered overburden for the ore body and texturally it is fine to medium grain of compacted rock. It is light grey to white color constituted by fine lenses of quartz gravel. The thickness of overburden for this section is vary from 0-4m. It is removed completely to partially from the ore body due to erosion. The most top part of this section is covered by soils derived from weathering of overlaying basalt. The lower portion of the sandstone has gradational contact with the limestone and thin mudstone of the area. This section shows structural grading of quartz gravel and fine sediments. It is characterized by weathered to fresh and fine to coarse sand grains with lenticular conglomerated thin lamination of gravel size. However, the top section of sandstone lacks this lower conglomerated lenses. The iron bed is occurs at different blocks in the study area. The top part sandstone has variable thickness for these different iron blocks. In Agiagora and Lege worke iron ore blocks the top sandstone section is weathered and fine rock. The sandstone of these blocks have 1-6m thick. The Millo blocks have as thick as 2.5-6m and fine sandstone. The lower section sandstone weathered product is undifferentiated with the residues of iron fragment. The bedding of this sandstone is characterized by gradational structures with upward grain variations. Fine cemented silt to clay portion and medium to coarse grained sand and gravel is upward coarsening with lenses of conglomerated quartz gravel to pebbles. The conglomerated lenses of quartz ranges from rounded to sub rounded grains in morphology. This sandstone shows mineralization from the effect of the top iron bead as iron float due to iron bed fragmentation. It is highly eroded and forms steep valley and slight hills in the study area. The sandstone that forms hill are mineralized. The extreme erosion and Transportation of the sandstone from different direction exposes and cut the iron ore continuity in to resistant sandstone blocks with iron ore bodies.

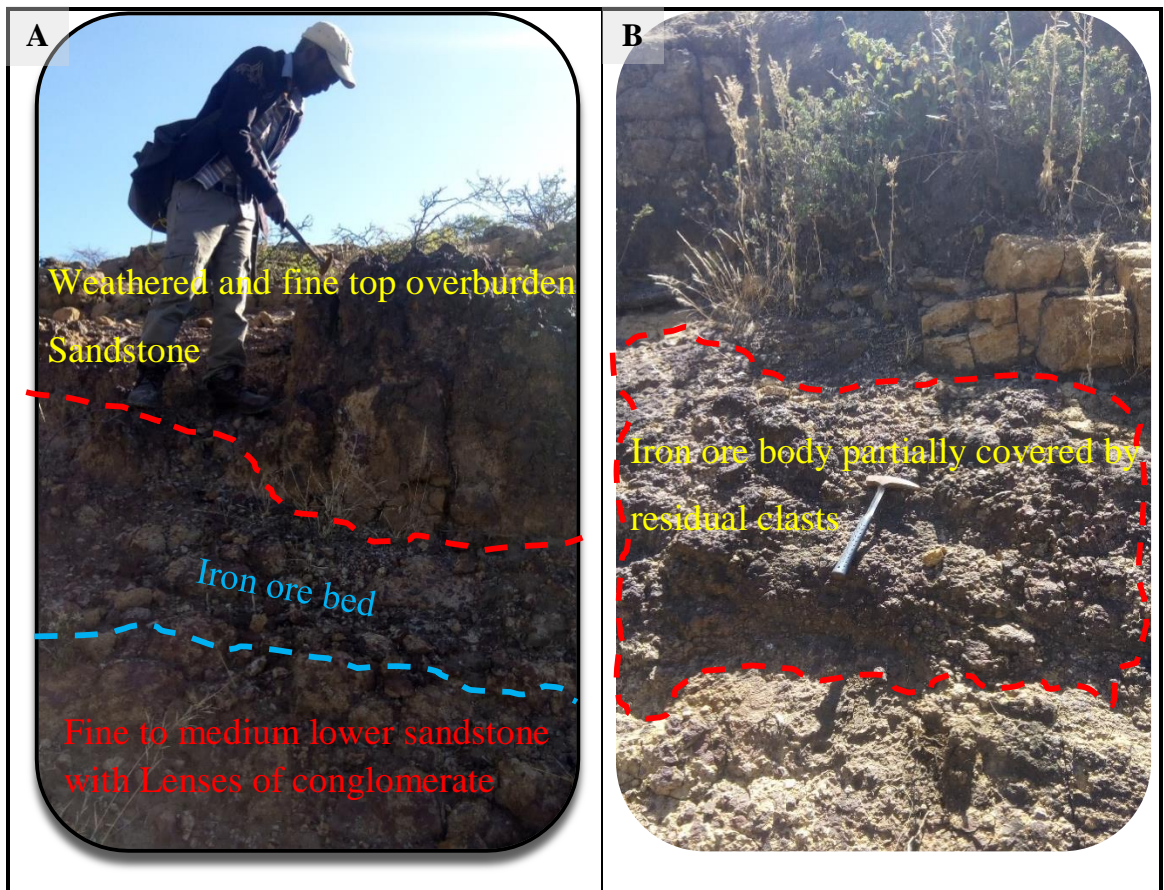


Figure 14. Field photographs of top and lower sandstone section and the ore body.

The photograph (Fig.14) shows well exposed iron ore body interlayering in the two distinct sandstone section (A) and the ore body is slightly exposing but, found in the lower section partially covered by residual host clasts and weathered laterite iron fragments (B).

The sandstone unit found in the lower section generally consists of fine to medium grained sands and thinly beaded gravel conglomerated lenses of quartz. It is texturally characterized by upward grading from fine grain unconsolidated sediments bottom followed by compacted fine sandstone, then compacted pebbles and boulders of variegated color alternation with friable clays and sands.

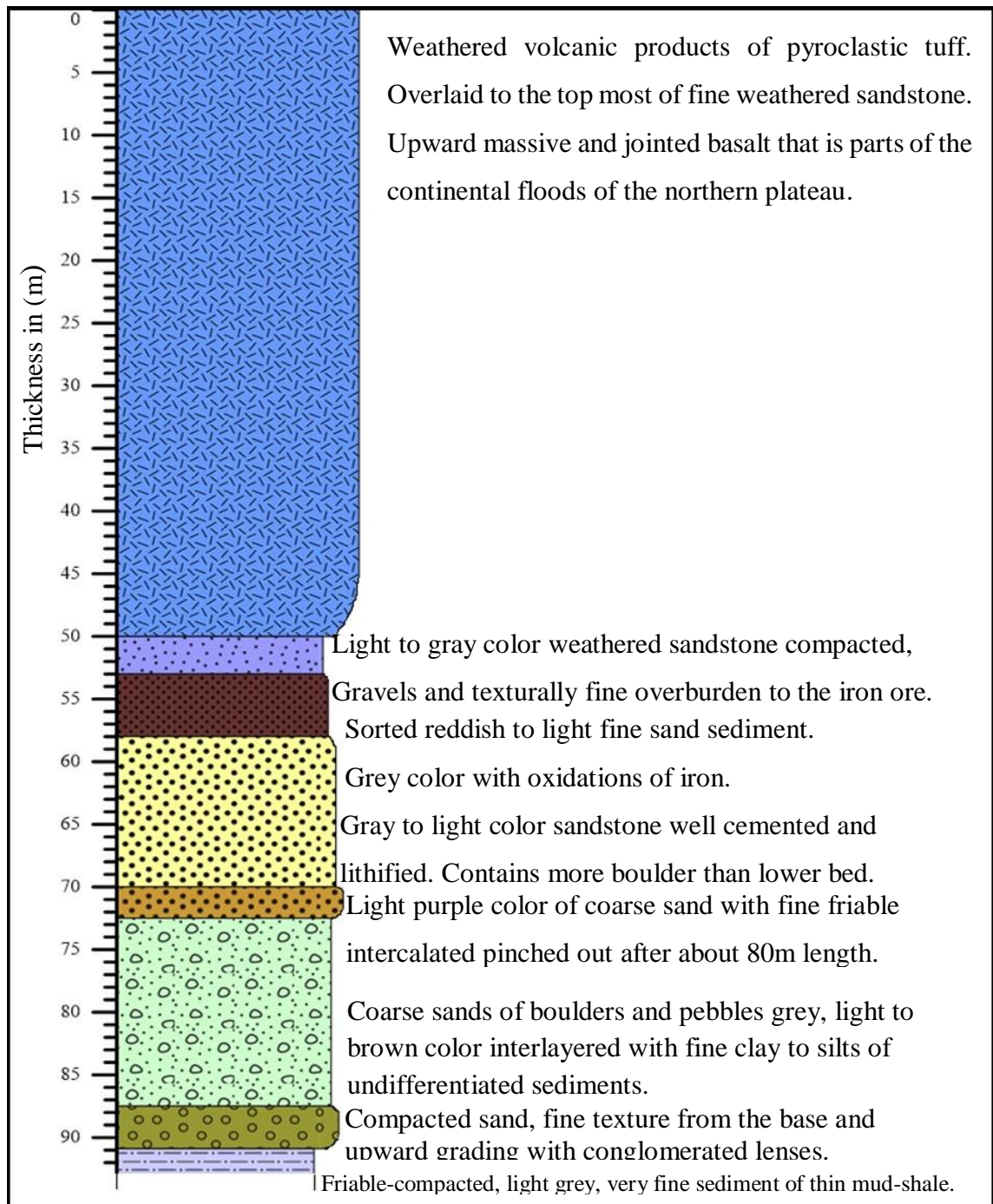


Figure 15. Section log taken from the sandstone unit exposed below the basalt and near the road cut.

4.4.1 Thin section descriptions

Study of rock thin section is vital to understand the history of sediments passed. Through the polarizing microscope rock fabrics, mineral compositions, grain size, roundness and sorting and shape were described. A total of five representative sandstone rock samples were selected based on the grain size, color, weathering degree and other geological variations for thin section description. These samples are described in petrographic study

as commonly three main framework components of quartz, feldspar, lithic (matrix) framework and other oxide minerals. The thin section samples were observed both under crossed and plane polarized light. The feldspars are distinguished as the orthoclase and plagioclase. The identified minerals include orthoclase, plagioclase, quartz, opaques and fine ground mass. The potassic feldspar is dark grey to brown and altered at the boundary of plagioclase grains. It shows pealeochroism and parallel extinction to the cleavage surfaces. The quartz is white to brighter grey shade depending on the orientation of mineral grain. However, the plagioclase is light grey to brownish grey color and altered. The angular to sub angular grains of the quartz, plagioclase and orthoclase feldspars are the characteristics of the iron hosting sandstone. The texture is poorly sorted to moderately sorted and the coarser grained minerals are cemented by fine ground mass. The analyzed sandstone is compositionally dominated by feldspar and quartz. It is texturally and compositionally immature. The angular-sub angular texture and immaturity is as a result of residual and insignificant transportation of sediment deposition. Grain to grain relationship shows mutual grain boundary and interconnected by fine matrix of binding sediments. Quartz is the most weathering resistant mineral where the feldspars are easily weathered but the remnants exist by showing surface alteration. The binding fine sediments are clay, calcite and silt size quartz. Opaque minerals observed in the thin section with black color under plane and crossed polarizers are the iron oxides. The open spaces of the sandstone are filled with secondary minerals as a result of surficial weathering and alteration. Weathering process has highly affected the orthoclase and plagioclase grain boundary. These features of the sandstone are clearly observed from the thin section examination of the rock. The mineralogical modal composition of the thin sections (MSd3, MSd5, MSd6, MSd8 and MSd10) is given in (Table 4). The modal compositions of individual constituent minerals are approximately estimated from six fields of observation (FV) and recalculated to 100%.

Table 1. *Recalculated modal compositions of arkose sandstone.*

Thin sec. No,	Minerals	Recalculated mineral composition
MSd3	Quartz	40.83%
	Plagioclase	20%

	Orthoclase	16%
	Opaque	12%
	Ground mass	11.17%
MSd5	Quartz	36%
	Plagioclase	26.5%
	Orthoclase	29.5%
	Opaque	2.33%
	Ground mass	5.67%
MSd6	Quartz	15.67%
	Plagioclase	33.67%
	Orthoclase	45.83%
	Opaque	4.5%
	Ground mass	0.33%
MSd8	Quartz	12.83%
	Plagioclase	30.67%
	Orthoclase	40.5%
	Opaque	8.5%
	Ground mass	7.5%
MSd10	Quartz	49%
	Plagioclase	15.67%
	Orthoclase	13.5%
	Opaque	7.67%
	Ground mass	14.16%

The thin section descriptions of five sandstone samples (MSd3, MSd5, MSd6, MSd8 and MSd10) under petrographic microscope have 11.17%, 5.67%, 0.33%, 7.5% and 14.16% cementing ground mass respectively. Based on the sandstone rock classification made by pitijon (1975) the ground mass is less than 15%, feldspar > 25% and low quartz with very few fragments hence, this sandstone is named as arkose. The petrographic description of the sample shows the rock is compositionally arkose. Compositional immaturity of the sandstone is due to both quartz and feldspar contents. Angular – sub angular texture is due to residually deposited that shows textural immaturity.

The sandstone thin section photomicrograph taken from the petrographic microscope are illustrated as follows.

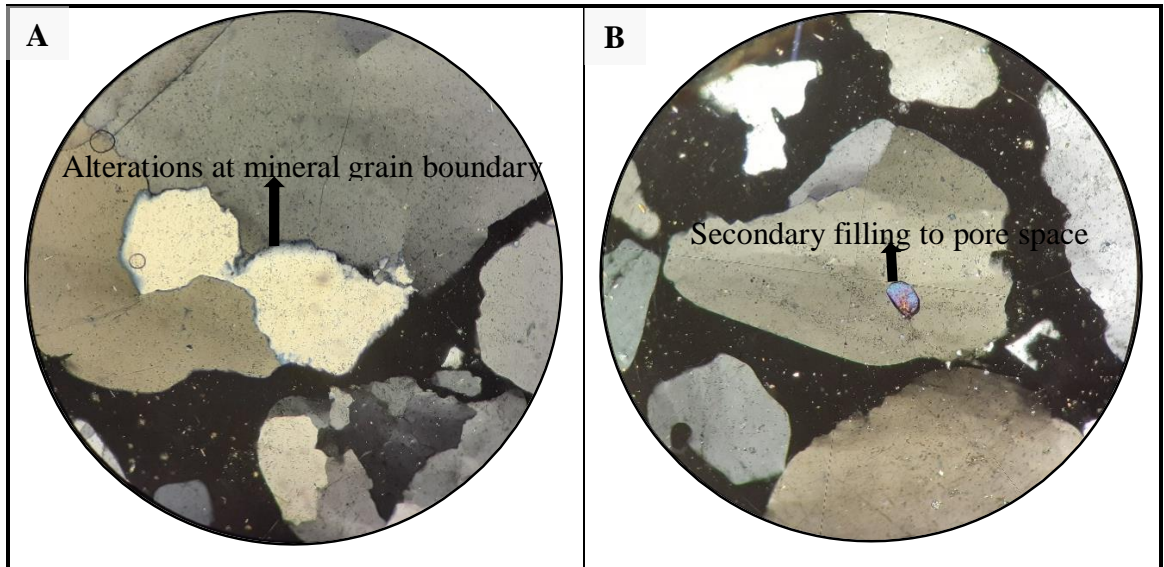


Figure 16.MSd5 Alteration at the boundary (A) and filled space by secondary minerals (B) in XPL observation and 10X magnification.

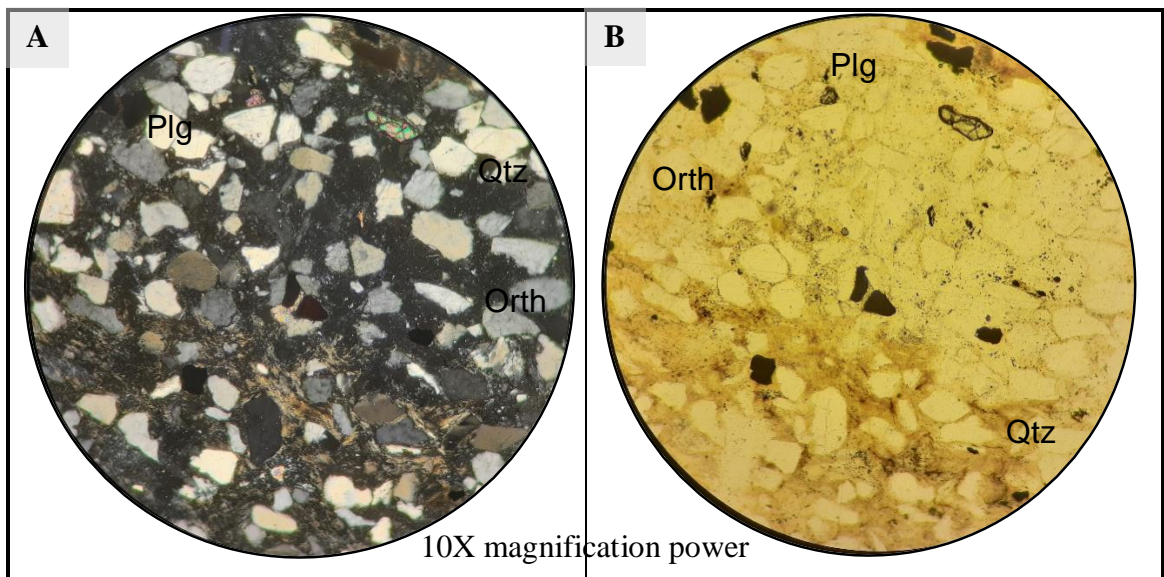


Figure 17.MSd3 angular – sub angular and sorted arkose sandstone under XPL (A) and PPL (B).

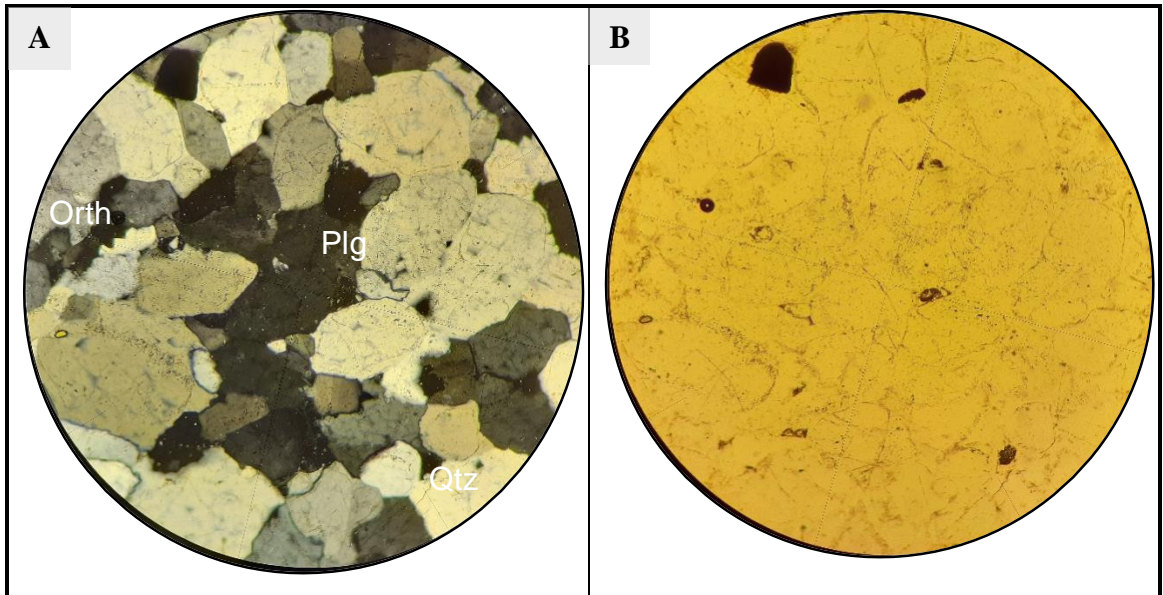


Figure 18. MSd6 sorted arkose type sandstone in XPL (A) and PPL (B) observation 10X magnification.

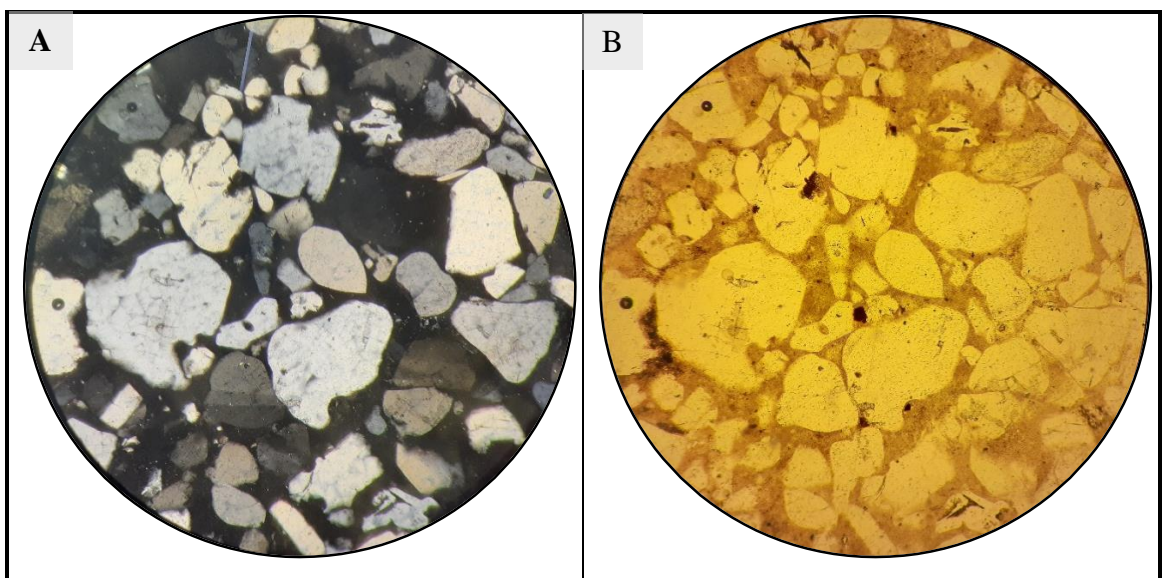


Figure 19. MSd8 poorly sorted arkose sandstone under XPL (A) and PPL (B) observation with 10X magnification.

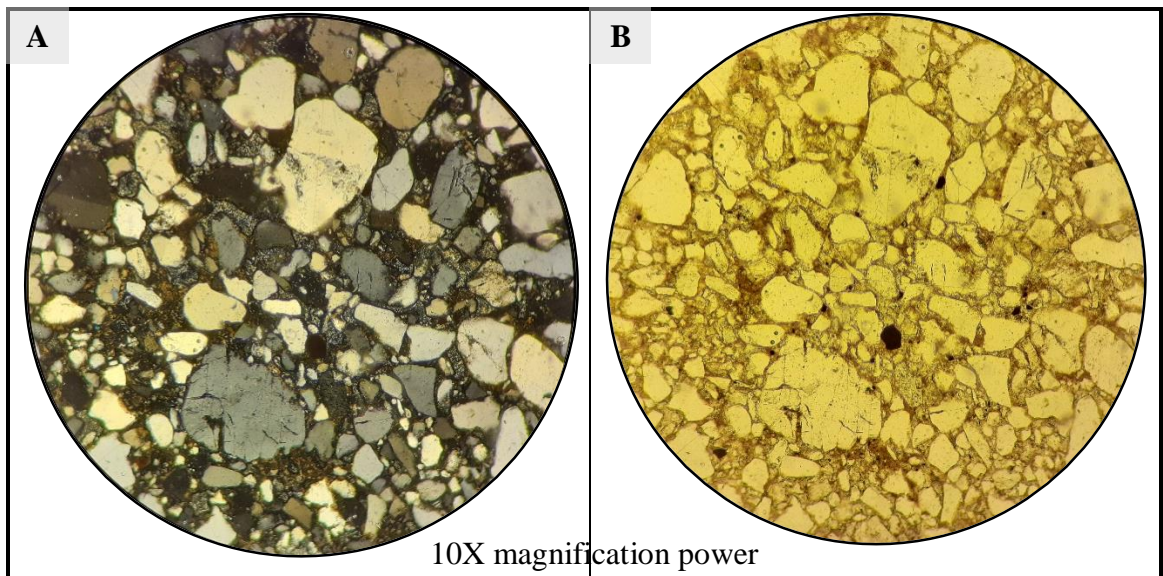


Figure 20. MSd10 moderately sorted arkose type sand under XPL (A) and PPL (B) observation.

4.5 Volcanic lava flow

The northwestern plateau is an extension of continental flood basalts in northern part of Ethiopia. This volcanic unit is overlaid to the Blue Nile sedimentary Basin. It is define the Quaternary to Tertiary varieties. The volcanic lava flows found in surrounding to Mekane Selam area is part of the plateau. It forms the rugged topography of the area. The volcanic lava flow of the area is thick sequences of about 500m plateau overlaying the iron hosting sandstone unit. The top part of the lava is extremely weathered and produced fertile soil product which is used for agriculture practice on the plateau. The main rock unit that constitutes the volcanic lava in general is basalt and pyroclastic. The basaltic lava flow is massive to columnar and forms very steep slope mountains of northern Ethiopia. The pyroclastic tuff and ash materials stratified and structural lenses to the volcanic. The ash fall deposits and pyroclastic are alternatively stratified with the agglomerated volcanic boulders. The basaltic lava flows of the area are the principal construction material for road construction and maintenance.



Figure 21. *Massive to Layered volcanic lavas flows (A) and stratified pyroclastic tuff (B).*

4.5.1 Petrography of basalt

Petrographic descriptions of the volcanic lava flow found in the Mekane Selam area were done using two thin sections (MSa1 and MSa5). The petrographic characteristics of this rock unit mainly plagioclase, biotite, pyroxene and some oxide mineral. Plagioclases of this thin section sample is light grey to dark grey color, perfectly twinned, shows cleavage, pleochroic and extinction which is parallel to the cleavage direction. The biotite of this rock is reddish to yellowish color in plane polarized light (PPL). The perfect one directional cleavage of biotite is clearly displayed under PPL of the microscope. Dark color observed in the crossed plane polarized (XPL) is the plagioclase but highly weathered part. It is bright brown-white and its perfect cleavage is displayed in the plane polarized light observation. The pyroxene mineral of this thin section is occupy some portion of the rock. It is characterized by pink red and deep green color. It is pleochroic under PPL observations but due to weathering effect the cleavage is not well distinguished. The reflectance color of pyroxene in cross polarized light become white under plane polarized light. The oxides

minerals of this rock is dark color in both plane polarized light. In sample MSa1 petrographic description plagioclase, biotite and opaques are the identified minerals with modal compositions of 74.4%, 20.4% and 5.2% respectively. However, MSa5 contains 76.6%, 9.6% and 13.8% modal compositions of plagioclase, opaques and pyroxene minerals accordingly their order.

The petrographic description and modal composition of studied samples show the rock is classified as basic volcanic (basalt). The microphotographs of MSa1 and MSa5 are shown in (Fig.22).

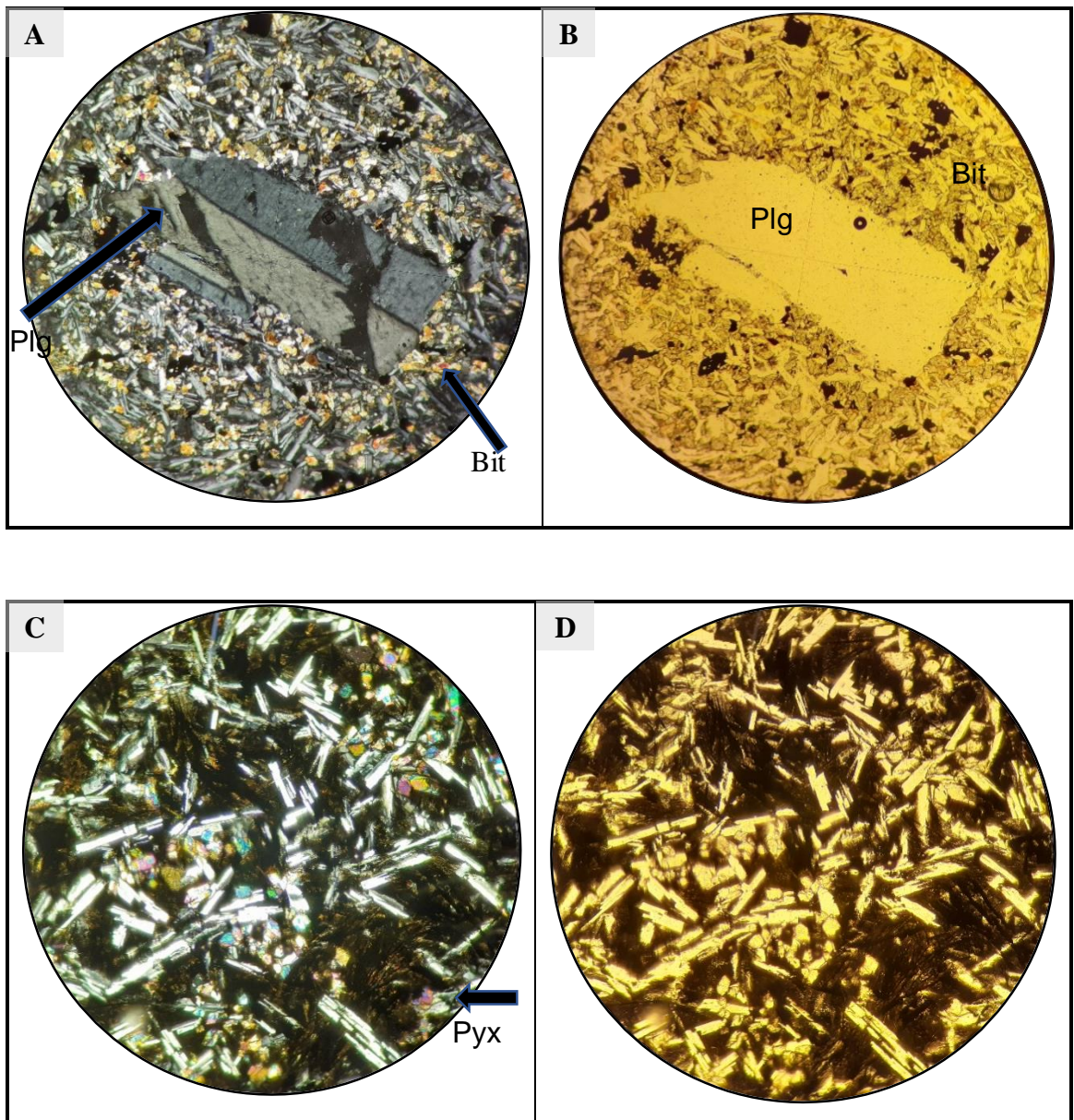


Figure 22. XPL (A) and PPL (B) observation of MSa1 and XPL (C) and PPL (D) observation of MSa5 basalts by 10X magnification power.

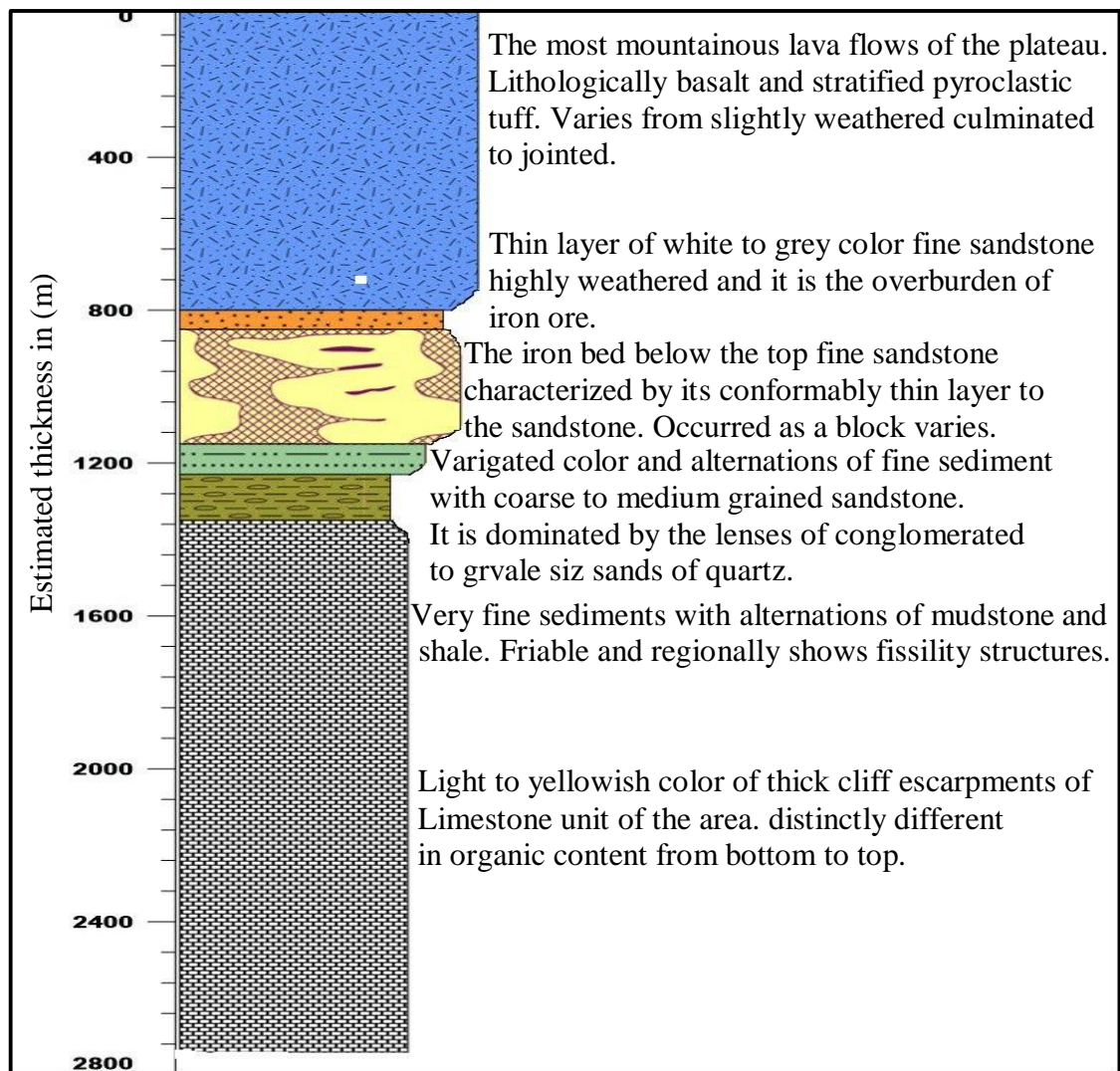


Figure 23. *General local stratigraphy of the study area.*

CHAPTER FIVE

5 The Mekane Selam iron occurrence

The iron occurrence of Mekane Selam is variably inter bedded within ferruginous fine to medium grained sandstone. The area is dominated by volcano-sedimentary cover including limestone, mud-shale, sandstone, bedded iron ore and volcanic rocks. The iron mineralization is localized within the siliclastic sedimentary formation. White, red-grey brownish sandstone variety is the main host of the iron occurrence of the area. Specifically weathered quartz and feldspar dominated fine sedimentary rock is the mineralized rock.

The iron ore is overlain by the volcanic rocks. This iron mineralization is part of the northwestern plateau and conformable to sedimentary rock. The occurrence of iron derived from residual laterite sandstone profile. The mineralized zone is localized within this lithologic unit. Iron mineralization occurs as thin bed and fragments of residual hematitic clasts. The texture of iron fragmentation is angular to sub angular and varies from cobble to gravel size. At the contact with the basalt and top most sandstone the iron ore is partially covered by weathered volcanics. The ore body is thin tabular bed in this contact zone. Mineralized and locally transported gravel size clasts are results of laterite weathering of surrounding rock. This lateritic weathering is cropped out at the most contact of the ore and top basalt cover. The iron ore of the area is one of the stratigraphic horizon of the mapped lithology (Fig. 10). The ore body is mapped mainly within the sandstone. However the iron ore is found as floats along the valleys. Mineralization zone is observed between the two distinct sections of sandstone mentioned previously and the ore is forming a bed. Erosion and gravitational collapse displaced the iron bed to the lower sandstone section. Therefore, the ore mineralization not restricted in bedded type. It was fragmented and dispersed to lower sandstone as cobbles and boulders of iron ore. These fragmented ores were mapped as sandstone with floated iron (Fig. 10).

The Mekan Selam iron mineralization basically occurs within four (4) distinct blocks. The iron ore body occupies nine (9) small areas in those blocks (see Fig. 10). Classifying the ore in to different mineralized blocks is for simplicity of mapping purpose. The mineralized zone is partitioned and identified at different sandstone blocks. Partitioning of the mineralized zone in to blocks are due to erosion and valley cuts. These mineralized zones are known by different locality names. The iron ore blocks are locally named as Dasue, Millo, Agiagora and Lege Worke. Those blocks of mineralization zones are topographically found in the hill forming sandstone and the ore intercalated within sandstone. However, the valley forming sandstone is not mineralized. These blocks of iron are remnants of erosion process and continuity of the ore is washed away from its horizontal bedding. The iron ore beds have various thickness and overburden sandstone in those different blocks. The mineralization around Lege worke block thinly bedded and continue horizontally near to the volcanic contact. The ore body of this block is laterally continuous to the Mekane Selam town (northeast) and pinched out due to the volcanic (overburden). However, the iron ore body of Agiagora, Millo and Dasu blocks are non-continuous thin bed. But, ores of those areas are recognized as hill forming blocks of iron. The ore mineralization of the area is

well exposed. The continuity and vertical thickness of the ore body estimated and measured from simple trenching and exposed ore bodies.

5.1 Nature of mineralization and the ore bodies

The iron mineralization nature of Mekane Selam area is bedded in the sandstone unit of the area. It also occurs as floats to the flat and valleys of the same unit. This floated iron ore concentration is due to erosion and residual deposition. The nature of the ore body and type show variation from hematite-goethite type, stratified-massive and oolitic-lateritic type. In addition to these nature residual iron clasts characterize the ore body. Medium and course gravel size hematite iron clasts are typical characteristics of the ore. The observed iron clasts are products of laterite weathering process. This highly weathered product of ores residually deposited at the contact of top sand and basalt. It has oolitic and sub angular-sub rounded texture of gravel size iron. The ore body at the lower contact of light grey-white and lenses of conglomerated sandstone is layered in nature. The iron mineralization of the study area is generally characterized by variable nature of deposition. The quality of iron is high in the gravel size clasts however; fine sand and precipitated silica impurities are lowering the quality of layered type iron. The iron ore body found at different blocks were well exposed and easily accessed.

The iron ore of Lege worke block is thin and laterally continue and partially covered by weathered volcanic. The thickness of iron ore body of this block is variable in different field observation and measurements. Exposed ore body measurement gives 3m, 4m, 6m, 2m thickness for the ore body at 4 measurement station. The overburden of this bed is variably as thick as 2-3m average (2.5m). The overlaid sand is weathered fine sand and become negligible to the east. This horizontally thin bedded iron ore body is extending to about 4 km from around Agiagora block. The Lege worke block ore body has dramatically changing overburden materials and vertical thickness. However, the iron mineralization of Dasu, Millo and Agiagora blocks are found as blocks on the erosion remnant sandstone hills.

The Millo block ore body is the best in quality and occupies the large thickness. This ore body has low overburden thickness. The iron ore of this blocks were highly affected by the valley cut and partitioned to five (5) areas of iron ore bodies (see Fig.10). This block contains much of iron ore concentration of the study area. The largest ore body thickness is measured within this block. The iron bed is thick up to 8m from place to place for this

specific block. The ore is covered by 3m to negligible overburden fine sandstone. However, there are field observation and exposed ore body measurements show variable thickness. Area one of this block has thickness of 2m, 3m, 4m, 5m, and 6m. Area two of the block shows 2m, 4m, 4m, 5m vertical thickness. 3m, 4m, 4m, 5m and 5m thick ore body is for area 3. 4m, 5m, 6m, 7m iron ore body thickness measured for area 4. Finally area 5 has 4m, 5m, 7m and 8m iron ore thickness. This field observation and measurement shows the Millo blocks have the highest vertical thickness and the iron quality of this block is best from other blocks. The ore body of this block is massive and laminated bed with less residual clasts. However, the mineralization of Millo block dominated by yellowish color altered hematite. This heavy and highly altered ore body is the goethite which is reporting by XRD study. The average overburden and possible depth of the ore body is inferred from 15m long and 1m deep trench taken in this block.

The third iron mineralization zone is Agiagora block. The ore body of this blocks also have a variable thickness. An overburden of this block is thin layer sand-silty size sediment. The exposed ore body is measured at different stops for the block. The field measurement gives (3m and 4m for ore body one 4m for ore body two and 3m, and 4m thickness for ore body three from different measurement station. It is very weathered, residually deposited and massive iron ore type. The ore body of this block is texturally characterized as cobble–fine sands and angular to sub angular weathered clasts. Residuals and sand grains are characterized by highly enriched hematitic iron. The ore body thickness and lateral continuity of mineralization in Agiagora block is assisted by 6m length and 1m depth manual trench.

Another iron mineralized block of study area is locally named as Dasue. This block is difficult to access. The Dasue blocks of iron ore is highly weathered. The thickness decreases towards the northwest volcanic cover. However, the thickness of the ore body varies at different sites. There are two areas of mineralized zone within this blocks. The different station exposed ore body measurement in Dasue block shows 2m, 3m and 1m, 2m vertical thickness for the two ore bodies. Laterite type iron is the characteristics of this block. The fragmentation of iron clasts in this block shows high quality red streaking hematite. Extremely weathered and leached quartz grains are in situ deposited. The clastes are angular and sub angular - sub rounded with less oolitic textures. The ore mineralization mechanism is residual to erratically disperse within horizontally deposited sandstone. This type of ore deposition is due to weathering process and surface laterite.

Generally the iron ore mineralization of Mekane Selam area observed at different blocks shows non-uniform ore deposits type. The massive and stratified iron ores are the common ore deposit type for those various blocks. The mineralized ore is exposed due to erosion and corresponding cuts. Massive–hard and friable clasts laterite iron ore is the main characteristics of Mekane Selam iron occurrence. Iron mineralization of Dasue and Agiagora blocks were characterized as lateritically weathered. However, iron mineralization of Lege Worke and Millo blocks are dominantly iron bed and oolitic which lacks lateritic clasts. Therefore, iron ore body of Mekane Selam area is vary from massive – oolitic (weathering results produce birds eye), inter bedded with the ferruginous sandstone and lateralized deposit type (Fig.24). These different ore types also have variable thickness as described above for different blocks. The massive iron ore body shows surficial tarnished due to the hematite is hydrated to goethite iron ore. The climatic data of the area is characterized by seasonally high rain fall and found in sub-tropical zone. This is important environmental condition for Laterite iron mineralization through increase rock weathering and leaching of metals from Fe source rock.

The quantitative and qualitative XRD analyzed iron ore samples of the area shows the average content of hematite and goethite (45.3 and 34.3 wt%) respectively. The chemistry result of those ore samples reports as useful iron. Those mineralogy and chemical analysis outcome indicates the Mekane Selam iron mineralization has the better quality.

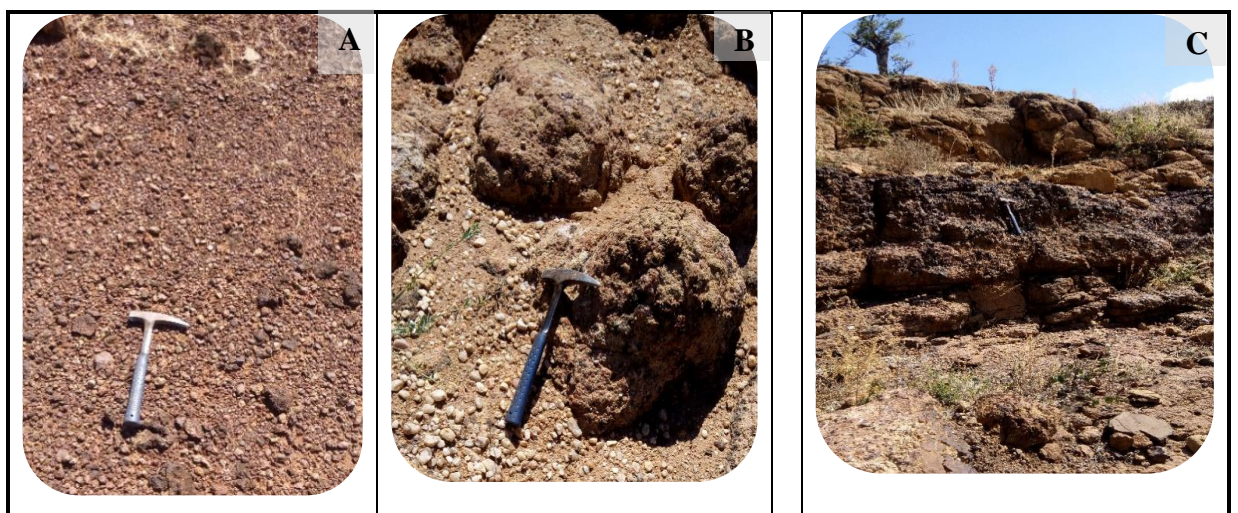


Figure 24. Field photographs of laterite (A), massive – oolitic (B) and inter bedded (C) iron ore of the study area.

5.2 Host rock

The Debre libanose sandstone (DLS) of the northwestern Ethiopian plateau is the main host rock for iron mineralization of Mekane Selam area. The iron occurrence of this area is restricted to the sandstone unit. The volcanic and other surrounding carbonate rock are not the host of iron. The sand grain fragments of the host are mineralized in hematite. Those iron mineralized fragments are sand sized grains and weathering products. The host rock is weathered and compositionally quartz and feldspar dominated. Fine and gravel size with alternation lenses of laminated conglomeratic clasts are characteristics of the host. The mineralization areas are divided to different blocks as mentioned above. The host rock of Legewerke iron block is variably thick and it is typically reddish brown fine to medium grained. Weathered, fine-coarse grained sand and silty texture with lenticular conglomerates are the common features of the host rocks of the ore body. Weathered sand is enriched by residual and oxidized iron. The lower layer of host rock is coarse and shows lenses of quartz gravel. However the top layer of the host is fine grain and non – conglomeratic sandstone. These two layered sandstones are host and sandwich the iron ore body. The top fine sandstone is partially covered by weathered volcanics. The sandstone near the shale-mud contact (Fig.10) moderately sorted, partial-well compacted with dispersed lenses of quartz gravel. The fine grained fissile shale - mud are contaminated by hematite precipitation from top iron mineralization. The host rock shows relatively uniform appearance in vertical section. It is characterized by typical zoning of grain size difference and interlayering of laterized iron bed. In addition, structurally the host is described as horizontal-sub horizontal striking with almost horizontal bedding. The 2-4 degree dipping of the bed is due to the horizontal sedimentation is modified by surface weathering process. The host rock fabrics are locally upward grading and fining for the top sediment.

5.3 Ore and gangue mineralogy

Iron ore is made from various iron bearing minerals and gangue. Iron ore mineral is the abundant earth's crust rocks from which the metallic iron is extracted. These ore minerals exist in different forms and amount in various geologic environments. The identification of mineralogy of the Mekane Selam iron occurrence is carried out by ore microscope discrimination and X-ray diffraction study of ore samples. The studied samples of the area show the ore mineralogy is dominating by hematite and goethite. The content of ore mineralogy are hematite (30-60%), goethite (8-59%) and magnetite (0.5-3%) while

kaolinite (11-23.5%), quartz (1-21%) and anatase (1%) are associated gangues of the iron ore body of study area.

Hematite, goethite and fragmented magnetite are the XRD identified iron oxides constituent minerals. However, kaolinite, quartz and others are the corresponding gangue phases. Using ore microscopy the opaque and oxides found in the host rock are identified as hematite and goethite ore minerals. Polished section petrography and XRD mineralogical study revealed hematite, goethite and magnetite are the constituent ore minerals. However, these studies also revealed kaolinite, quartz and anatase are the major constituent gangue phases of study area. The Mekane Selam iron ore is oolitic and layered bright hematite and dark grey kaolinite and Quartz gangues in polished section study.

Goethite is observed as secondary replacing hematite. At grain boundaries hematite shows replacement by goethite. Surface alteration of goethite is an indication of hematite replacement by goethite. This replacing goethite shows oolitic-botryoidal texture under ore microscopic observation (Fig.26 B). It is characterized as red - blue oxidation surface tints under polished section study (Fig.29 B). It has low reflectance and massive – ooidal with grey – brown appearance. The goethite is filling spaces between hematite and brown - dark grey gangues. It shows blurred dirty surficial expression around the bright hematite boundaries. It is randomly dispersing through hematite and gangue. The goethite is characterized by massive relief and grey bluish tint and replacing the hematite. The shape is sub hedral and highly altered or oxidized (Fig.27 A). The boundary of goethite and hematite is distinguished by blue - reddish gangue fine sediment.

Hematite appears as layered main ore and dispersed as cementing matrix between the ore and gangues. The hematite ore is characterized by bladed, specular and ooid interlayering texture (Fig.28 A). The oolitic and pisolitic texture of the ore is distorted and perfect ooids with elliptical - rounded hematite (Fig. 29 A). High reflectance, bright color observation is typical features of hematite. Horizontal stratification of sedimentary structures with fine gangues are characteristics of hematite ore under petrographic observation. In addition to interlayering lenses of hematite grains show wavy and platy appearance to the normal stratification (Fig.26 A). White to grey white with a bluish tint is typical distinguishing features of hematite ore mineral. The hematite shows moderate reflectance and bright color with interlayering features with fine gangue sediments (Fig.26 B).

The iron ore of Mekane Selam mainly characterized through its pisolitic (ring of Fe_2O_3), bands and oolitic hematite and goethite texture in microscope study. The ooid clastes of iron are mineralized and cemented by hematite. Hematite and goethite iron ore minerals are alternatively show light and dark reflectance. The textures of these ore minerals are continuous concentric–elliptical thin layers of oolitic under ore petrography. Very rare disseminated and fragmented magnetite is identified from the polished section examination as small black dots (Fig. 28 B). Circular to elongated black-grey dark color magnetite is distributed within bright hematite ore. MS-BD3, MS-B5 and MSB 13 iron ore samples show magnetite in XRD (Fig.32&33) and as weathering resistant fragmentations in polished section study respectively.

The mineral paragenesis of iron ore can be determined from the relationship of hematite and goethite ores. Mutual grain boundary is observed relationship between hematite and goethite. At the boundary and in between sedimentary interlayers the goethite is on replacing hematite and gangue minerals. The bluish - reddish alteration of iron ores with erratically dispersed magnetite through the hematite and surrounding gangue are results of secondary surface weathering. Therefore, the goethite is younger secondary ore mineral. This ore microscopic study of the iron ore samples were help to infer order of constituent ore minerals and associated gangue phases. The ore paragenesis and goethite replacement for hematite in polished iron ore is illustrated in the sketched diagram (Fig. 25 A & B).

Kumar et al (2010) describes the presence of goethite ore mineral is typical characteristic of laterite iron deposition through recrystallization of micro platy hematite during burial. Hematite iron ore is precipitated from Fe bearing solutions during continental crust weathering and input to the basin (Schwertmann, 1969; Worash and Solomon, 2015). Therefore, these previously determined facts of mineralogical study leads to understand the iron mineralization of the study area is results of laterite formation.

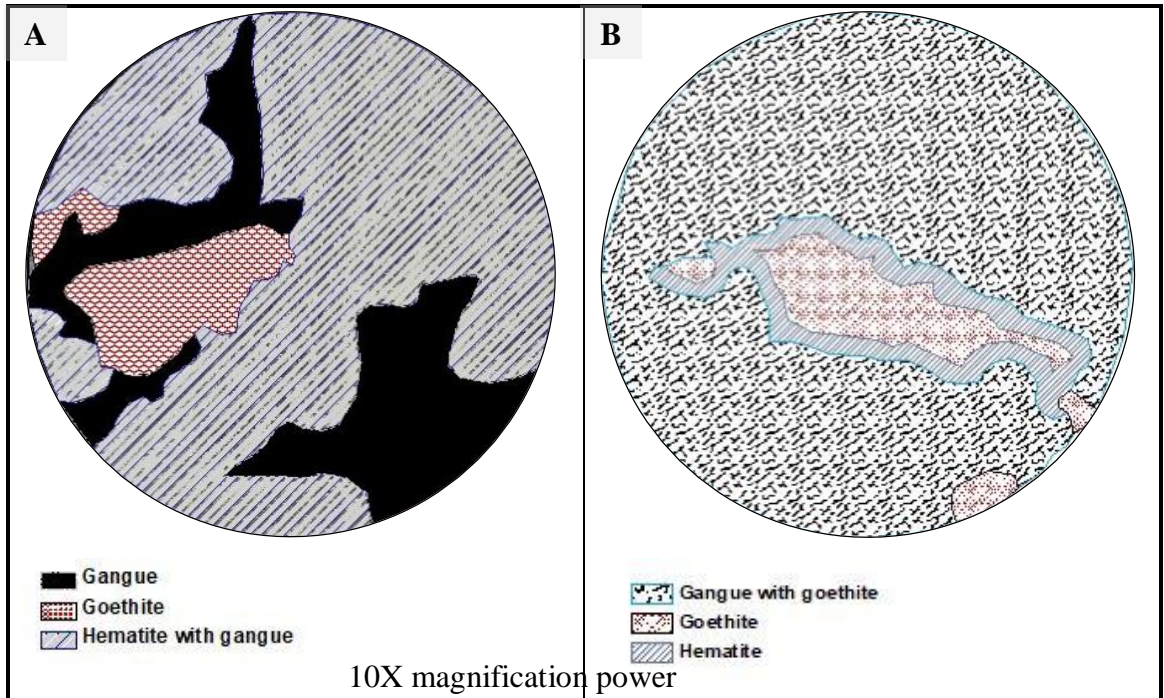


Figure 25. Sketched diagram of MSB13 (A) and MSB16 (B) showing mutual grain boundary and replacement relationship of goethite with hematite and the gangue.

Microphotographs of polished section iron ores are shown below for five selected samples.

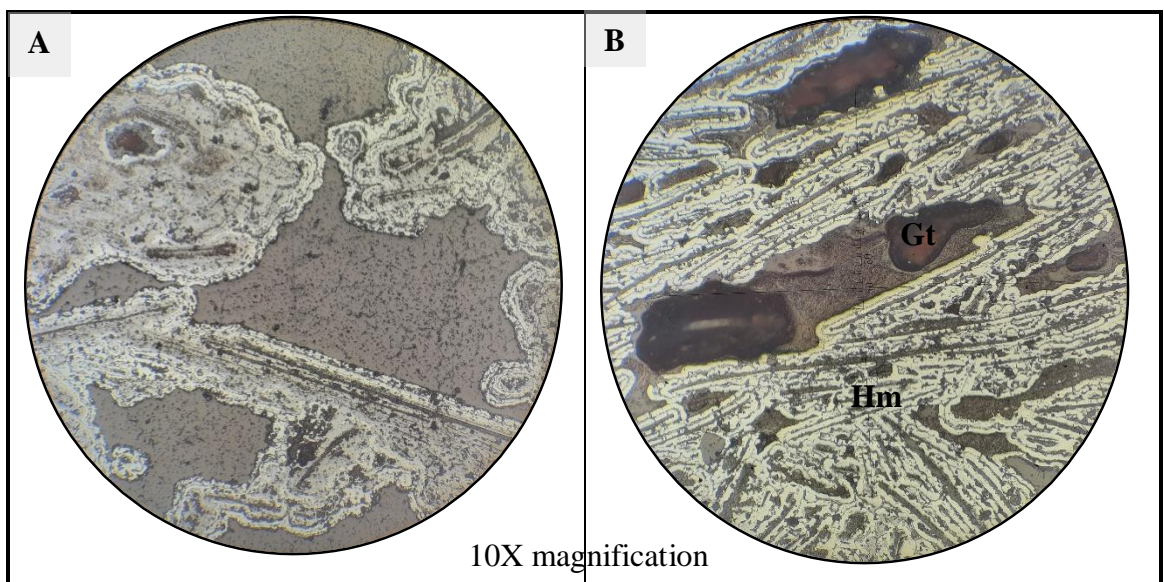


Figure 26. Photomicrographs of platy-hematite crystals MSB2 (A) and MSB13 (B) oolitic and botryoidal feature of Goethite and interlayered hematite ore.

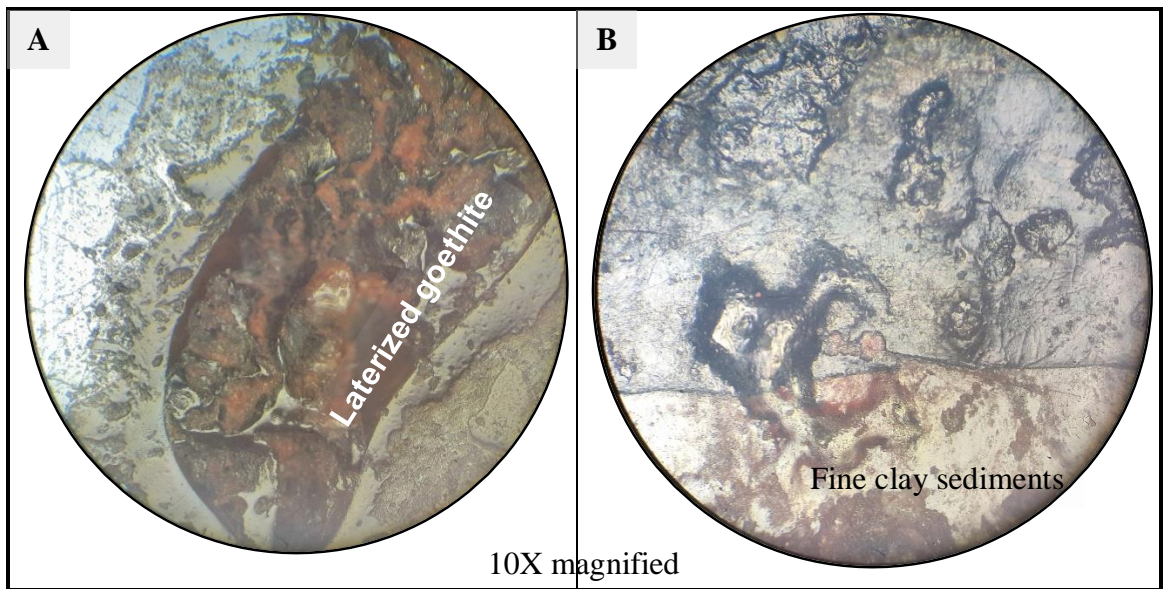


Figure 27.MSB8 (A) and MSB9 (B), Redish – grey brown weathered Goethite replacing the hematite and anhedral dumpy crystal developed in association to hematite.

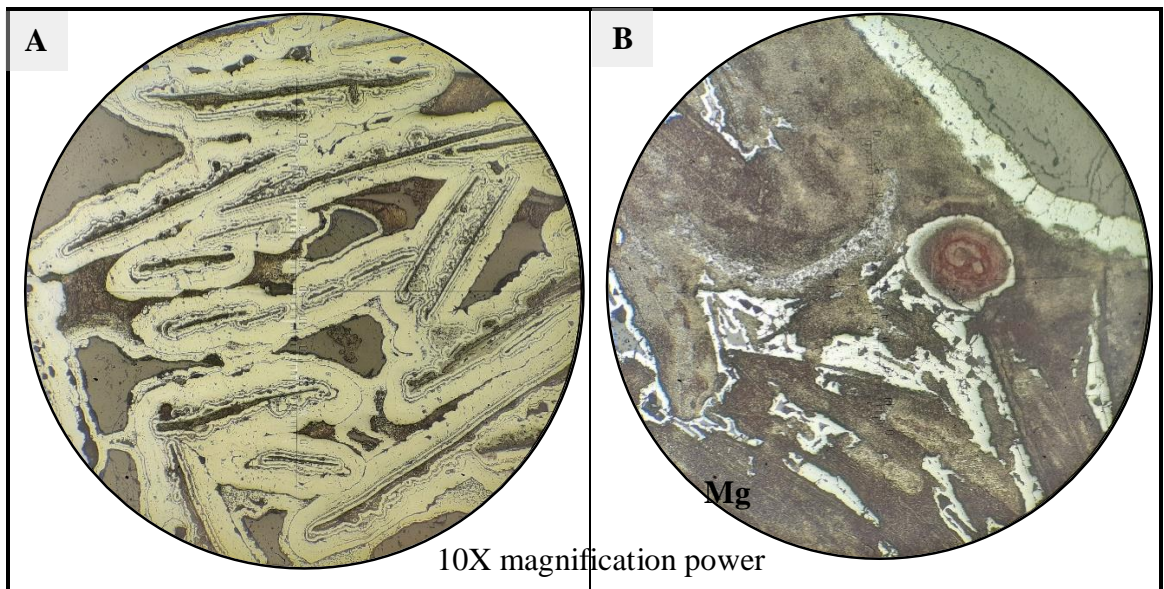


Figure 28.MSB13 (A) specularite - interlayered hematite (bright) and MSB14 (B) oolith – botrioidal of goethite red, brownish- grey with disseminated magnetite.

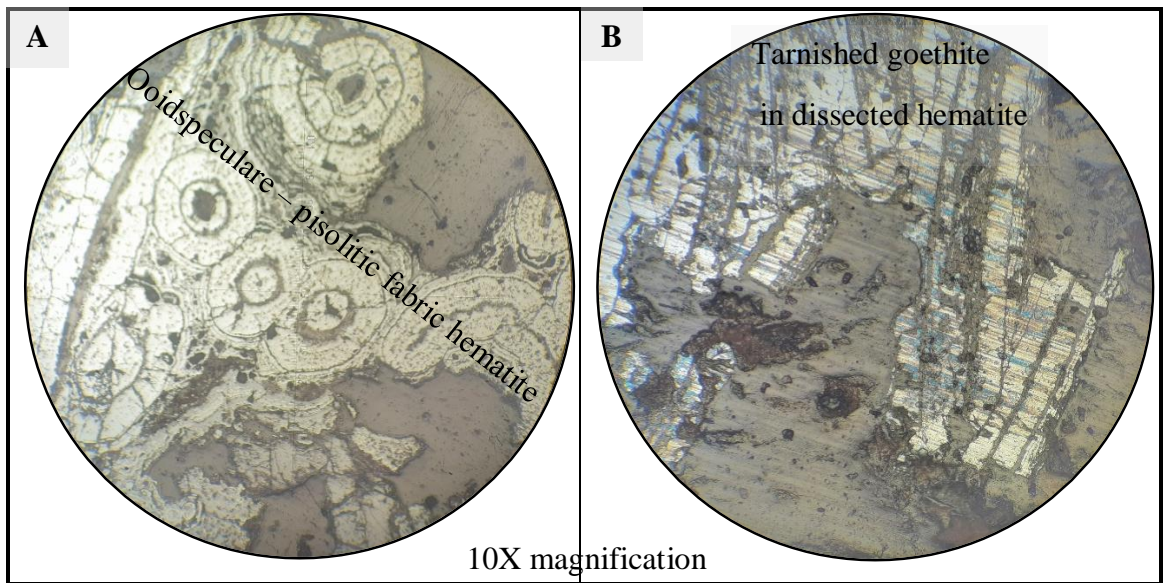
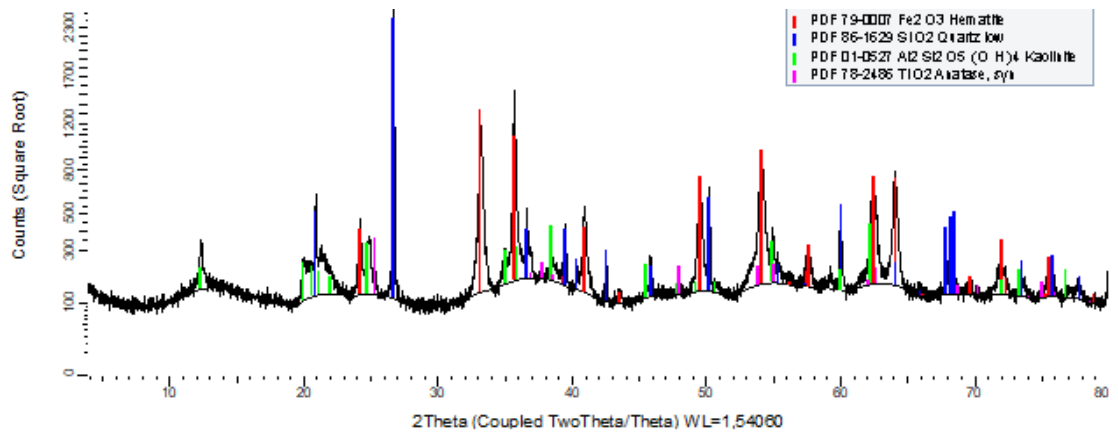


Figure 29. MSB16 Ooid specular-pisolitic fabric (A) and acicular or laths crystals fill voids or fractures regular reflections of hematite and bluish tint of Goethite iron oxides (B).

The semi quantitative analysis result is presented below (Table 7). The ore and gangue minerals identified include hematite, goethite, magnetite, kaolinite, quartz and anatase constituents. The XRD major picks occurs at maximum intensity of diffracted beam in root counts (Fig 30-34). The picks values are developed at specific crystallized mineral that corresponding the 2teta values. The pattern of the picks are determined by the intensity beams of hematite, goethite, kaolinite, quartz and anatase. The crystalline structures of ore minerals and gangues are identified from the diffracted beam energy. Hematite, goethite and kaolinite show the most reflection picks. These highest reflection beam tell us the most abundant ore minerals of the studied iron ore samples. The hematite and goethite dominant minerals observed from major pick of X-ray diffraction are confirmed in petrographic study of selected iron ore samples mentioned in the previous section.

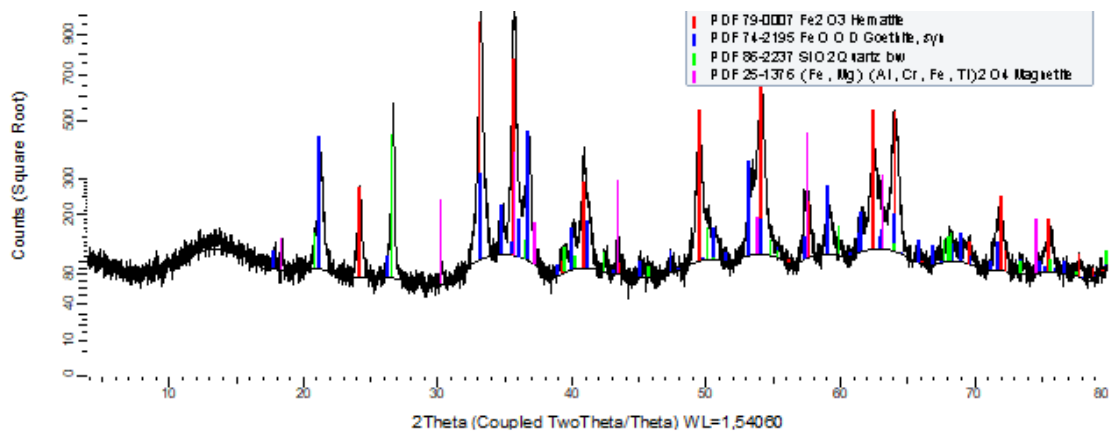
Five (MS-B1, MS-B5, MS-B10, MS-DB3 and MS-LW) iron ore with associate rocks are studied in XRD. The constituent mineral phases of these ore samples are hematite, goethite, kaolinite, quartz and anatase. Besides of this minerals MS-B5 and MS-DB3 iron ore samples collected from Millo and Dasue blocks show small magnetite crystalline reflection pick respectively (Fig.32&33). The highest reflection pick of radiation indicate hematite is the most crystalline ore mineral followed by goethite.

The massive and highly weathered samples of MS-B5 and MS-DB3 consists fractions of magnetite, which is probably the result of laterite weathering. The kaolinite is due to



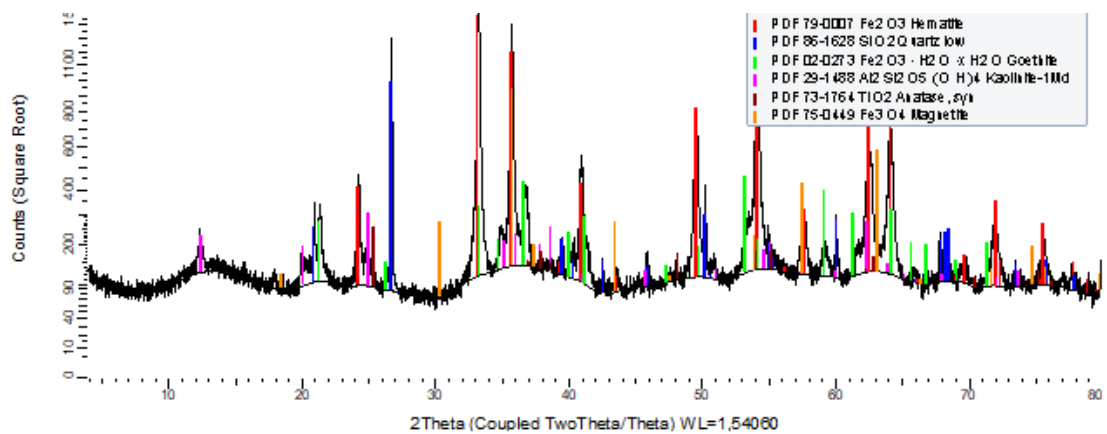
Obr 4. XRD difrakční záznam vzorku MS-B10 s vyznačenými piky od detekovaných fází.

Figure 31. XRD diffraction of sample MSB-10 iron ore strata bound with hosted sandstone.



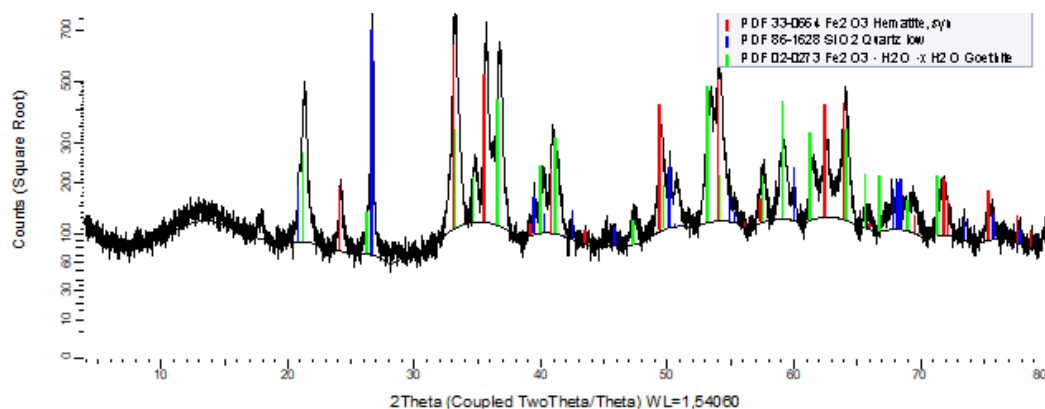
Obr 5. XRD difrakční záznam vzorku MS-B5 s vyznačenými piky od detekovaných fází.

Figure 32. XRD diffractions of sample MSB-5 interlayered needle silica with massive iron ore.



Obr 6. XRD difrakční záznam vzorku MS-DB3 s vyznačenými piky od detekovaných fází.

Figure 33. XRD diffraction value for the sample MS-DB3 weathered iron ore.



Obr 7. XRD difrakční záznam vzorku MS-LW s vyznačenými piky od detekovaných fází.

Figure 34. XRD diffraction value of the sample MS-LW massive - oolitic iron ore.

Table 2. XRD mineralogical analysis of iron ore samples.

Minerals wt%	MS-B1	MSB-10	MS-B5	MS-DB3	MS-LW
Quartz	1	21	12	12	13
Hematite	40	46.5	50	60	30
Goethite	59	8	32	16	57
Magnetite			3	0.5	
Kaolinite		23.5		11	
Rutile					
Anatas	1			1	
Poznámka	Ilmenite up to 1-2wt%	Ilmenite up to 1-2wt%	Ilmenite up to 1-2wt%	Ilmenite up to 1-2wt%	

Iron ore samples studied by XRD is also analyzed for some element chemistry. In addition to their mineralogical content the chemistry of iron samples show Fe content is considered as useful (Table 8). The concentrations of Al, Si, Fe and Zr show higher value whereas the alkali metal and alkali earth elements are show low range of value. This is consistent with the weathering of crust and enrichment in Fe, Al and Si. In other causes the surface weathering process increases the mobility and removal of Mg and K.

Table 3. Chemistry of iron ore samples analyzed for XRD study.

ppm	MS-DB3	MS-B1	MS-B10	MS-B5	MS-LW
Fe	373,736	537,803	249,863	484, 245	462,176
Al	65,073	16,681	91,304	17,140	15.203
Mg	27,793	33661	<LOD	36,217	30,598
Si	72,257	21,856	136,336	62,091	58,439
K	1, 476	1,566	1,308	1,687	1,794
Ca	<LOD	1,317	<LOD	1,109	1,861
Ti	7,975	503	8,420	552	<LOD
V	417	<LOD	114	<LOD	<LOD
Cr	195	205	148	7,487	221
Pb	367	758	175	572	569
Cl	27,166	28,051	19,793	19,065	22,673
Ga	70	175	31	116	128
As	39	<LOD	32	20	<LOD
Rb	8	28	5	19	19
Sr	22	33	24	54	28
Zr	338	128	458	127	106
Nb	55	68	190	97	77
Mo	55	98	24	77	70
Ag	<LOD	<LOD	<LOD	<LOD	9
Sn	49	68	35	61	48
Ba	76	194	49	307	157
Hg	<LOD	59	16	25	44
Bi	<LOD	17	<LOD	13	17

Lod = less than load of detection.

5.4 Geologic history

The Mekane Selam iron ore mineralization is situated in the Mesozoic-Tertiary sedimentary environment. Both sedimentary and volcanic associations are characterize the study. The geologic history of this environment is related with the early Precambrian to recent sedimentation and volcanisms. The basement rocks inferred as the Precambrian to the lower

formation of igneous and metamorphosed varieties. Those are completely covered by the Mesozoic carbonate and ferruginous clastics rocks. These sediments are resulted from transgression and regression processes of the sea. The transgression is deposits the oldest lower Adigrat sandstone. This formation is overlaid to the Precambrian basement which is not exposed in the study area. The regression process redeposit the meandering and breaded river sediments. Theses depositions are overlay to the early formation. It is the Debre Libanose Sandstone (DLS) ([Getaneh Assefa, 1991](#)). The current work shows this formation is the iron bearing rock. It is characterized by medium to fine grained with lenses of conglomerated sand and gravel size sediments. The sedimentation process is due to continuous weathering of crustal protolith. The weathering is assisted by transporting colloid iron in the sediment. The metal suspended to transporting and carrier media is reprecipitate in the depositional basin ([Worash and Solomon, 2015](#)). This iron ore deposition is enriched later as weathering process were enhancing gradually. Continuously weathered continental crust rocks deposit fine and thin layer sandstone overlaid to iron ore. This surface weathering of the iron bearing and early deposited rock enriches the concentration of Fe and mineralize it. Lastly the eruption of volcanisms linked with the Afar mantle plume deposits the volcanic lava flows (Fig.35). This volcanism produced the basaltic lava flows and pyroclastic tuff that overlay to the Mesozoic sediments.

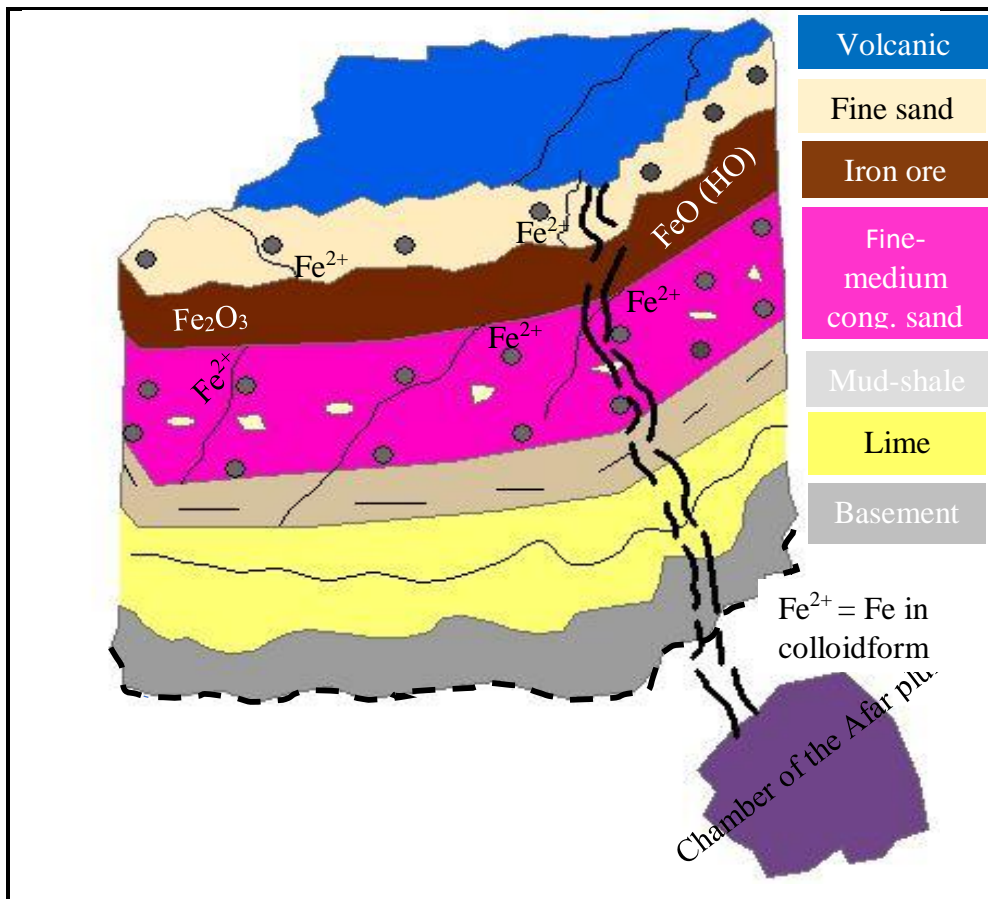


Figure 35. Hypothetically sketched for geologic history and model of the ore deposit.

Fe is supplied from the weathered continental crust and transported and deposited in the basin.

CHAPTER SIX

6 Geochemistry of the sedimentary rocks

Introductions

The chemical compositions of sediments are complex results of sequential processes acting on preexisting geologic materials. Geochemical behaviors of clastic sedimentary rocks are outcomes of parent rock composition: -weathering process, climatic condition during weathering, transportation mechanism and environment of depositional basin. These geologic processes leave significant geochemical signatures for the detritally derived siliclastic sediments. Shale is the most preservative sedimentary rocks of original mineral concentration and bulk chemistry of rocks (Pittijohn, 1975). It is used to normalizing other sediment concentrations. Geochemically analyzed silicate as main elements of oxides are useful information in sedimentary geochemistry. Sediment composition, genesis of

sedimentary rocks and the paleo - weathering of sedimentary rocks are inferred from the major and trace element analysis (Junji et al., 2016). The distribution of REE pattern is important indicative behavior with the genetic relationship of ores. Enrichment patterns of LREE is an indication of the sediments derived from the felsic upper continental crust source (Dupuis et al., 2006). Low content distributions of REE with considerable negative Ce anomaly is characterize ores originated from magmatic–low temperature hydrothermal conditions (Mokhtari et al., 2013, Hodkinson et al 1994). The different sedimentary processes have little effect on the fractionation of REEs Th, U, Sc and Rb (Meng et al., 2017). The negative Ce anomaly is related with recent weathering process of parent material. Generally the light REE concentration of silicic sediments show high enrichment and negative Eu anomaly. It behaves in similar manner with felsic igneous rock (Bekker et al., 2010). Iron in peat or bog and pond surface sea water is soluble in solutions as Fe^{2+} . The geochemistry of pelitic sediments and their response to weathering and metamorphism process shows a direct relations with protolith concentration. Physico - chemical processes and geological activities occurred in the earth's history are complex. These sequences of processes control the chemistry of sediments. The processes acting on past geologic materials produce the chemical composition of sediments and rocks exposed currently. The chemistry and type of sediment that host iron ore needs suitable environment for iron occurrence. The geochemistry and compositions of sedimentary rocks give a vital information to understand the host rocks of an ore deposit and genesis. The compositions of this sediment tell us the source area of sedimentary constitute, information on sedimentary environment and post sedimentary transformations of protolith. Sediments become enriched in metals (Zn, Mn Cu) and metalliferous minerals are as a result of exhalation processes at the base floor of seawater including Fe.

In general the geochemical compositions and mineralogical content of clastic sedimentary rocks are a results of: - the source rock compositions, influence of the atmospheric environment, rainfall, temperature conditions, chemistry and topography, durations of weathering, transportation mechanisms and post- depositional mechanisms or diagenesis, metamorphism and deformation (Hayashi et al., 1997).

6.1 Geochemistry of the host rock

The geochemical analysis of sandstone and associated rocks of the study area reveals that predominant constituent major elements are Fe_2O_3 , SiO_2 , Al_2O_3 , CaO , MgO , MnO , TiO_2 , Cr_2O_3 and P_2O_5 in various proportion. Ba, Ce and Eu concentrations show enrichment and

depletion in different samples. In addition, the Sr and Cr content of the analyzed samples were found to be high. The high concentrations ratio of Th and La is consistent with the characteristics of silicic rocks. However, the high content of Co, Cr and Sc are characteristics of basic Provenance. The REE distribution of the analyzed sedimentary rocks shows a pattern close to typical continental crust composition. The pattern of this REE in sediments are characterized by enrichment of LREE (La–Sm) and a smooth patterns of HREE (Gd–Lu) with pronounced depletion of Eu (see Fig. 36).

Major and trace element analysis of sandstone

Feldspar and quartz dominated arkose type sandstone with significant of clays shows wide variation in major and trace distributions. Major element content of the iron host rock is expressed in weight percentage in oxide forms while trace elements of iron and its hosts are expressed as ppm. This detrital sand is composed of SiO₂ (56.67-82.10wt %), Al₂O₃ (3.15-26.09wt %), CaO (0.08-4wt %), MgO (0.03-2wt %), Fe₂O₃ (0.62-21.1wt %) and a few content of K₂O and Na₂O (Table 9). It consists of elevated concentrations of SiO₂ with moderate Al₂O₃ percentage. Observed high content of Al₂O₃, Fe₂O₃ and SiO₂ from the major element analysis are due to laterite process. This chemical analysis of major element concentration of the analyzed sandstone shows moderately narrow range of variation. Major element composition of the samples show high concentrations of SiO₂ and Al₂O₃, moderate to high content of Fe₂O₃, low concentration of CaO, TiO₂, MnO and P₂O₅ and absence of Na₂O and K₂O. The sandstone of the area is the main lithology that hosts the iron ore body. The composition of the sandstone is evaluated from index of compositional variation (ICV) using the chemical analysis data. According to Cox et al (1995) $ICV = (Fe_2O_3 + K_2O + Na_2O + CaO + MgO + MnO + TiO_2) / TiO_2$. The ICV value of the sandstone varies from high to very high (9.85 - 42.66) with average value of 20.19. This ICV value of the sandstone indicates that it is composed of more quartz and feldspar with low proportion of clay content. Total alkali K₂O + Na₂O shows insignificant change for the ratio of K₂O / Na₂O. Based on Nesbitt and Young (1984) the constant value of alkalinity for the analyzed rock indicates that there is no total destruction of constituent feldspars from sandstone during surface weathering.

The whole rock trace element chemistry of the analyzed samples has a wide variation. The main trace element of the bulk chemistry consists Ba, Ce, Cr, Dy, Er, Eu, Gd, Hf, Ho, La, Lu, Nb, Nd, Pr, Rb, Sm, Sr, Ta, Tb, Th, Tm, U, Y, Yb, Zr, Cd, Co, Cu, Ni, Pb, Sc and Zn in ppm (Table.10). The chondrite normalized pattern trace element of clastic rocks are

enriched in Rb, Hf, Th, Nd, Ce and Sm and slightly depleted in Nb, Ta, Th, Sr and Zr (Fig 37). The trace element analysis of the sandstone samples shows high Zr concentration except sample MSd4. Alkaline felsic rocks and lower carbonates are the possible sources for the relatively high concentration of Zr, Nb and other REEs. The high content of light rare earth elements (La, Ba, Ce and Nd) than heavy rare earth elements is typical features of laterite iron crust ferruginous source. This is due to weathering process is insignificantly affect REEs.

Table 4. Major element chemistry of host and associated rock.

Comp.wt %	MSd1 Arenite	MSd2 Arenite	MSd3 Arenite	MSd4 Arenite	MSd8 Arenite	MSd1 1 Arenite	MSh 1 Wakes	MSh 2 Wakes	MSh 3 Wakes
SiO ₂	77.33	64.18	67.10	64.58	81.92	82.10	70.04	56.67	65.76
Al ₂ O ₃	7.64	19.26	20.07	8	3.15	5.17	14.75	26.09	20.82
Fe ₂ O ₃	0.62	5.30	1.79	21.1	0.21	0.65	2.27	3.51	1.69
CaO	0.29	0.17	0.09	4	0.08	0.28	0.34	0.16	0.16
MgO	0.21	0.17	0.08	2	0.03	0.11	0.16	0.07	0.16
Na ₂ O	0	0	0	0.12	0	0	0	0	0
K ₂ O	0	0	0	0.05	0	0	0	0	0
Cr ₂ O ₃	0.01	0.01	0	0	0.01	0.01	0.01	0.01	0.01
TiO ₂	0.21	1.16	1.56	0	0.35	0.70	1.12	1.40	0.84
MnO	0	0	0.02	0.01	0	0	0	0.01	0
P ₂ O ₅	0	0	0	1.26	0	0	0	0	0
LOI	5.38	8.03	7.53	0	1.55	3.62	7.72	10.26	8
Total	91.69	98.28	98.24	97.53	87.28	92.64	96.41	98.17	97.44

Table 5. Trace element chemistry of the host and surrounding rock.

Comp. ppm	MSd1	MSd2	MSd3	MSd4	MSd8	MSd1 1	MSh1	MSh2	MSh3
Ba	82.02	33.49	45.00	39.82	94.98	115.36	80.58	74.07	86.89
Ce	33.55	22.64	75.59	73.29	156.00	22.55	57.11	70.56	105.00

Cr	107.69	107	42.74	90.71	100.04	136.20	89.11	91.07	83.06
Dy	0.95	1.13	2.57	1.19	0.87	2.41	1.85	1.65	3.87
Er	0.38	1.00	2.00	0.89	0.50	2.04	1.44	1.34	2.78
Eu	2.28	0.20	0.59	0.29	0.81	0.25	0.57	0.49	0.72
Gd	4.00	1.03	2.55	1.17	2.03	1.64	2.11	1.76	2.90
Hf	2.86	11.71	50.74	15.00	6.22	20.27	13.09	24.83	8.89
Ho	0.13	0.25	0.57	0.28	0.16	0.66	4.00	0.35	0.91
La	20.62	13.19	53.75	40.17	70.73	13.04	41.51	52.22	60.10
Lu	0.06	0.21	0.58	0.21	0.10	0.45	0.28	0.38	0.61
Nb	0.60	18.92	16.39	19.00	3.83	10.32	16.70	20.10	21.13
Nd	27.65	6.00	21.60	18.40	80.03	6.36	19.86	25.00	21.45
Pr	4.50	2.34	6.47	7.02	21.06	2.10	5.85	6.85	8.30
Rb	0.84	0.60	1.43	0.28	0.68	2.30	2.83	2.91	6.65
Sm	14.05	0.89	3.43	1.87	7.17	1.12	3.09	3.26	3.26
Sr	101.51	20.30	39.00	54.35	136.35	48.01	88.32	44.10	67.27
Ta	0.20	1.30	1.22	1.34	0.31	0.88	1.21	1.41	1.40
Tb	0.05	0.16	0.37	0.19	0.18	0.34	0.28	0.25	0.49
Th	3.46	11.13	17.55	16.35	8.38	9.26	11.18	13.79	8.93
Tm	0.05	0.15	0.41	0.16	0.07	0.33	0.21	0.21	0.44
U	0.28	1.20	2.63	1.42	0.42	1.48	1.51	1.83	1.81
Y	2.83	6.86	15.52	7.60	3.60	18.88	9.93	9.29	21.52
Yb	0.31	1.36	3.38	1.35	0.52	2.68	1.72	1.99	3.72
Zr	106.58	433.19	1980.97	0.89	266.17	812.17	522.69	939.82	332.19
Cd	0.04	0.52	1.92	0.73	0.42	1.09	0.67	0.88	0.27
Co	1.78	3.41	1.44	1.81	0.90	1.34	2.70	2.55	3.29
Cu	1.15	12.82	0.66	6.14	0.49	7.35	6.58	4.47	3.11
Ni	44.02	17.83	4.49	12.66	4.21	6.43	10.26	6.88	8.90
Pb	6.36	7.13	14.60	12.49	19.77	5.01	15.69	15.37	7.28
Sc	9.00	17.19	24.44	16.72	5.39	10.54	12.50	15.39	19.89
Zn	<bdl	5.45	<bdl	9.78	<bdl	<bdl	<bdl	0.26	1.53
Total	576.29	760.6	2434.6	453.57	992.39	1262.86	1025.43	1435.33	898.56

The major and trace element content of mud–shale samples varies widely. Ba, Cr, Sr and Zr concentration is high in those fine sediments. The LREE/ HREE ratios of the fine sediment show high value (13.60- 28.22) and the low content of Eu. This is due to the felsic source rock.

One weathered sandstone sample (MSd1) show high concentration of LREE and highly depleted with HREE. The REE diagram shows general positive Ce and negative Eu anomaly (Fig. 36). Normalized cerium anomaly is typical of recent sediment because Ce behaves differently in oxidized condition and exists in Ce^{4+} , Ce^{3+} state which is absent in Archean sediments of reduced condition (Ridley,2013). Multi element plot of iron and host rock is given (in Fig.37). The diagram shows enrichment of Th and Pb for ‘iron ore samples and depletion of Ba, K and Zr for the host rock. Those enriched and depleted elements found in the host versus ore shows the iron is concentrated from felsic source rock. The enrichments of iron ore is due to lateritaization process. The relative concentration of Al_2O_3 and TiO_2 is the result of weathering. Those elements can be incorporated to the clay mineralogy and iron oxides while Zr is concentrated due to partitioning to coarse grained sandy quartz. Progressive weathering of parent rock resulted in depletions of soluble cation (Ca^{2+} , Mg^{2+} and Sr^{2+}) and enrichments of insoluble elements (Rb, Th, REE and Pb). The large pick of Th and Pb for the ore sample (Fig.36) is due to enrichment of large ion lithophile elements (LILE). The enrichment of those elements are mainly dependent on their mobility and enriched from supra subduction related melt that generates elevated Th, Pb and Ba (Breeding et al., 2004). The active continental margin setting of analyzed ore samples (Fig.41) of study area is subduction related setting. This setting is possibly concentrate those elements in the parent pock. Multi element pattern plot (Fig.37) indicates that the relative enrichment of Zr in iron ore sample and depleted within the host rock.

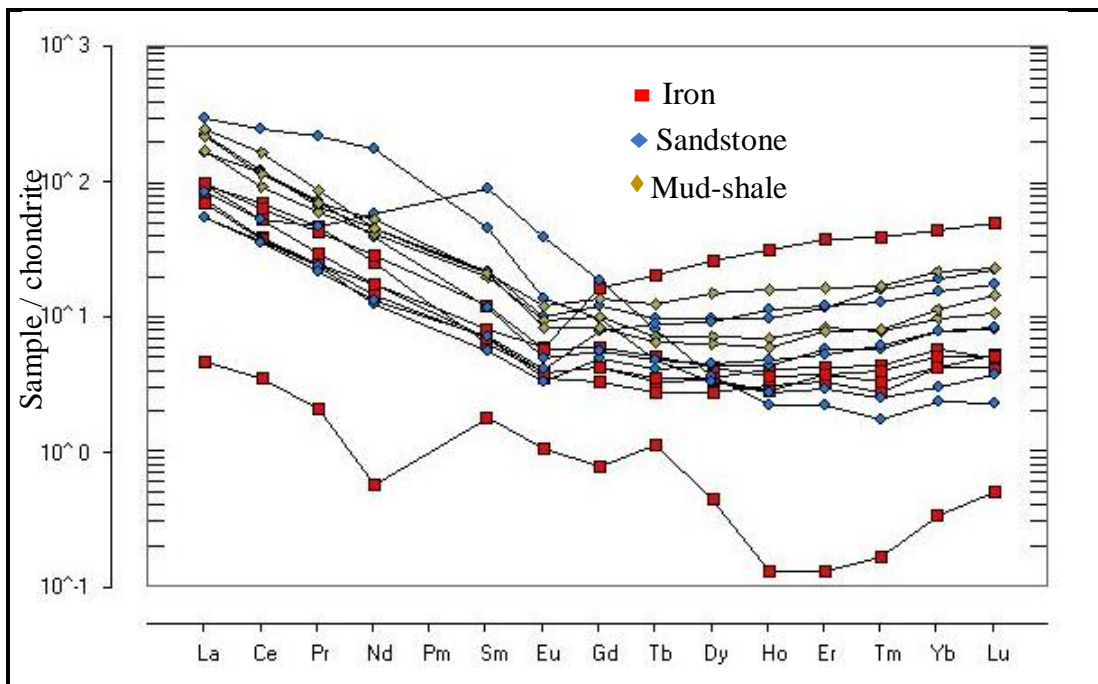


Figure 36. REE pattern for the iron ore, the host rock and surrounding fine sediments.

The high enrichment of LREE and slightly depleted with nearly flat pattern of HREE shows high degree fractionation between LREE/HREE ratios (La/Lu) in the host rock. Iron ore sample (MSB11) shows enrichment in HREE as compared with LREE. Sample (MSB15) is characterized by inconsistent distribution pattern (Fig 36). This is explained by probably the constituent REE in the ore samples are mobilized during weathering and re-precipitated out of the depositional environment as relatively compared with other ore samples. The sandstone sediment (MSd1) is enriched by LREE and highly depleted in HREE that is deviate the felsic source of sediments. This is due to fraction incorporation of overlaid volcanic basalt to the source sediments during weathering.

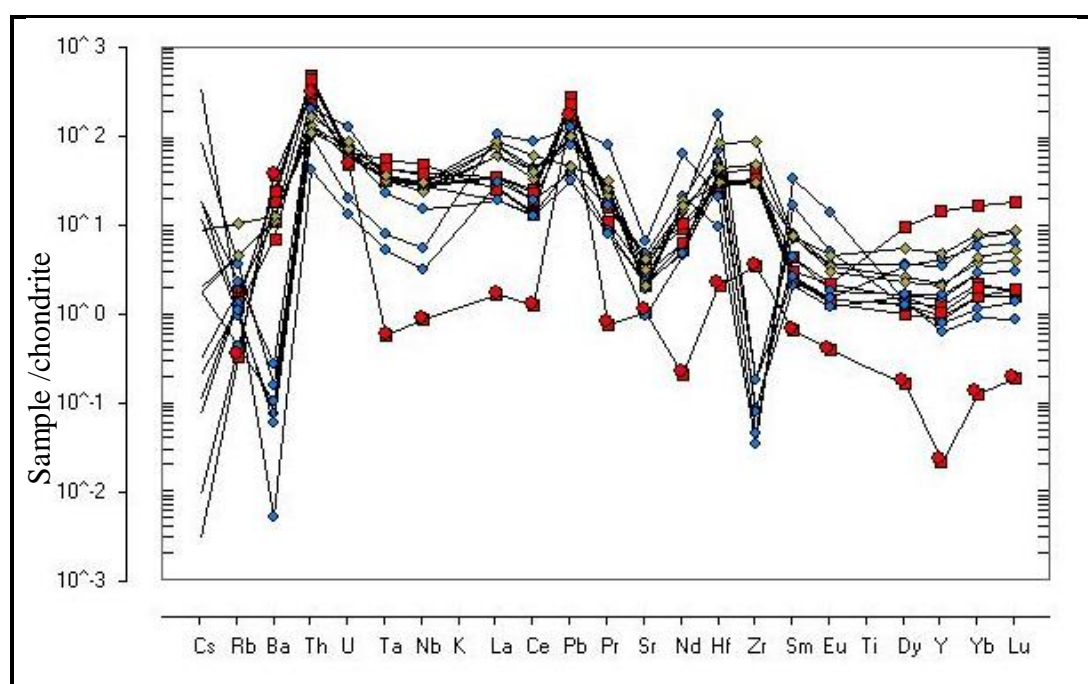


Figure 37. Multi element distribution for both iron ore and host rock samples.

Normalized multi element pattern shows the siliclastic sediments are significantly enriched in Rb, Th, U, La, Ce, Pb, Pr, Nd, Hf, Sm and slightly depleted in Ba, Sr, Nb, Zr in comparison to the iron ore (Fig. 37). High pick of Pb concentration is an indication of the iron ore sample is little affected by diagenesis. Because of easily soluble and mobile behavior of this element. Pb favors for lateritic enrichment. However, immobile Zr favors to the mechanically distributed heavy grains size minerals.

6.2 Geochemistry of the iron ore

Introduction

Sediments rich in iron are less sensible to solubility during weathering. In general iron is found in Fe^0 , Fe^{2+} and Fe^{3+} forms of highly reduced, reduced and oxidized states respectively. But, ferrous and ferric states of (Fe^{2+} and Fe^{3+}) are the most important once. The reduced and oxidized state of Fe^{2+} and Fe^{3+} determine the types iron ore mineral (Mansurova et al., 2006). The ferrous (Fe^{2+}) is changed to ferric (Fe^{3+}) as it is exposed in to the oxidized environment. In high temperature environment ferrous iron (Fe^{2+}) is substituted by Mn, Mg, Zn, Ni, Ti while ferric (Fe^{3+}) is by Al, V, Ti and Cr. The substitution of ferric (Fe^{3+}) iron in the tetrahedral lattices of alkali feldspar is the main reason for reddish alteration granites during weathering. In the oxygenated atmosphere and sea water environment iron is oxidized to ferric (Fe^{3+}) iron with providing low temperature. Solubility of ferric iron controls the concentration of Fe^{3+} . because it is complex and has insoluble behavior. However, Fe^{2+} is soluble and solutions having reducing character easily mobilize it. Large amount of iron is precipitated as ferrous iron when the environment is oxidized.

The Precambrian iron precipitation is characterized by typical depletion of LREE compared with HREE and negative Ce anomaly (Nsoh et al., 2014). However the rare earth element distribution pattern of the current iron ore shows the relative enrichment of REE and shows positive Ce anomaly. This results indicate that the iron deposit of the area is not BIF.

The chemical analysis of iron ore samples of Mekane Selam area shows low concentrations of major elements except SiO_2 and Fe_2O_3 . The aluminum content of the iron ore is variable from low (1.44 wt%) to moderate (19.23wt%) (Table 10). Hematite and silica concentration is high. Iron content of the study area ranges from low – very high percentage. The iron ore samples generally coupled with moderately low-highbeside those major oxides the loss on ignition (LOI) value of Mekane Selam iron ore samples are characterized by medium to high concentration.

Major element analysis of iron ore

Whole rock composition of Mekane Selam iron mineralization shows high concentration of Fe_2O_3 . It shows very low contents of MnO and P_2O_5 and alkali Earth metal oxides. The terrigenously introduced Al_2O_3 and SiO_2 major oxide and detrital traces of Zr and Nb show high concentration. ICP-AES analysis shows that iron occurrence chemically composed of the geochemical fraction of Fe_2O_3 , SiO_2 , CaO, Al_2O_3 , and P_2O_5 .

The content of major oxides varies from Fe₂O₃ (16.55% -77.93%), Al₂O₃, (1.44-19.22%), SiO₂ (8.60 - 59.02%), CaO (0.16-0.39%), MgO and P₂O₅ (0- 0.19% and 0-0.05%), Cr₂O₃, (0.03 - 0.11%) TiO₂ (0.02-1.48%). However, a few proportions of MnO, Na₂O and K₂O concentration is found in the analyzed ore samples. Analyzed major content of the ore samples indicate the quality of the iron with average (48.33wt %) of Fe₂O₃. The immobile elements (Al, Ti and Fe) especially during weathering, diagenesis and transportation of sedimentary process are form their relatively moderate-high concentration of oxides. The concentration those oxides are derived from felsic continent detritals. The total volatile content of the iron ore is determine from the temperature loss in ignition that show high – moderate range of values (Table, 11).

Table 6. Major element geochemistry of the iron ore sample.

Comp.in wt%	MSB3 Iron ore	MSB4 Iron ore	MSB6 Iron ore	MSB7 Iron ore	MSB11 Iron ore	MSB12 Iron ore	MSB15 Iron ore
SiO ₂	59.02	28.20	24.04	34.23	52.43	38.13	7.31
Al ₂ O ₃	1.61	17.38	3.83	4.29	19.23	9.66	1.44
Fe ₂ O ₃	34.31	43.38	68.23	54.86	16.55	43.10	77.93
CaO	0.21	0.25	0.23	0.22	0.16	0.39	0.16
MgO	0	0.02	0.01	0	0.06	0.20	0
K ₂ O	0	0	0	0	0	0	0
NaO	0	0	0	0	0	0	0
Cr ₂ O ₃	0.06	0.07	0.10	0.09	0.04	0.07	0.09
Ti ₂ O	0.46	1.17	0.90	1.48	1.06	1.22	0.02
MnO	0.01	0	0	0	0	0	0
P ₂ O ₅	0	0.01	0.02	0.02	0	0.05	0.03
LOI	3.84	9.37	3.80	4.53	9.22	6.65	7.31
Total	99.52	99.85	101.16	99.72	98.75	99.47	94.29

Trace element analysis of iron

The trace analysis of the ore and host rock samples were done using ICP- MS method to investigate the genesis and other characteristics of the ore. the trace element chemistry

analysis of iron ore show variable concentration of Ce (2.19 to 43.65ppm), Co (0.77 to 1.53ppm), Ni (7.90 to 20.24 ppm), Cu(5.07 to 74.87 ppm), Zn(<bld to 20.33 ppm) and Cr(83.34 to 234.44 ppm) content of minerals. Several trace elements (Zr, Cr, Ba, Ce, Sr, La, Th,Cu, Pb and Nb) are enriched in the ore samples of Mekane Selam. Trace element composition of iron in the study area shows high content of total Zr, Sr, Cr, Ce and Ba. The mobile (Ba and Sr) trace element content of iron ore varies from low- high proportions. Whereas immobile element Zr has high concentration. REE (La Ce Pr Nd Pm Sm Eu Gd Tb Dy Ho Er Tm Yb Lu) patterns normalized to chondurite are given in (Fig. 36). Eu and Ce show very low and high distribution respectively. The anomalous pattern of Ce is as a result of Ce³⁺ oxidized to Ce⁴⁺ to concentrate CeO₂ in oxidizing environment. The lack of negative Ce anomaly indicates absence of low surface temperature hydrothermal solution is contributed for iron mineralization. while the negative Eu anomaly is as a result of low temperature sedimentary environment due to increasing surface weathering. This shows absence of leaching for REEs by hydrothermal solution (Glusbey et al, 1997). It is also indicate that the absence of substituting Ca by Eu during hydrothermal. The negative Eu anomaly is also due to the effects of sediments are contaminated, mixed, dissolution and transportation of underlying carbonates during weathering.

Table 7. Trace element analysis of iron ore samples.

Comp.in ppm	MSB4 iron ore	MSB6 iron ore	MSB7 iron ore	MSB11 iron ore	MSB12 iron ore	MSB15 iron ore
Ba	76.24	150.75	125.27	47.47	167.77	265.23
Ce	24.13	43.65	23.34	33.07	39.64	2.19
Cr	220.12	206.89	234.44	190.09	188.59	83.34
Dy	0.72	0.90	0.92	6.75	1.12	0.12
Er	0.57	0.63	0.72	6.38	0.64	0.02
Eu	0.23	0.23	0.23	0.36	0.35	0.06
Gd	0.70	0.91	0.91	3.42	1.28	0.17
Hf	8.20	8.35	11.52	9.30	9.00	0.63
Ho	0.18	0.16	0.24	1.80	0.21	0.01
La	17.74	23.16	16.74	23.09	23.79	1.13
Lu	0.11	0.14	0.13	1.31	0.13	0.01
Nb	25.45	18.84	33.17	20.18	26.37	0.60

Nd	6.98	12.12	8.30	8.42	13.67	0.28
Pr	2.40	4.54	2.41	2.85	4.18	0.20
Rb	1.16	1.00	0.26	0.75	0.86	0.21
Sm	1.08	0.99	1.09	1.28	1.87	0.28
Sr	43.46	88.00	44.72	60.47	91.35	23.32
Ta	1.69	1.24	2.15	1.34	1.69	0.02
Tb	0.11	9.13	0.14	0.80	0.20	0.04
Th	31.50	35.25	40.61	20.52	36.45	25.13
Tm	0.07	0.09	0.12	1.03	0.10	0
U	1.49	1.37	1.40	1.23	1.20	1.03
Y	4.00	4.26	5.56	65.75	4.62	0.10
Yb	0.74	0.73	1.00	7.64	0.90	0.06
Zr	535.76	339.24	470.58	349.03	361.41	38.33
Cd	0.54	0.58	0.88	0.72	0.93	0.05
Co	1.20	1.04	0.77	1.38	1.53	1.06
Cu	9.55	12.19	9.80	5.07	16.29	74.87
Ni	20.24	13.18	15.23	7.90	16.39	15.08
Pb	39.23	41.16	43.37	23.09	36.65	26.91
Sc	12.85	8.93	10.57	10.41	10.81	9.57
Zn	20.33	<bdl	<bdl	<bdl	2.04	5.66

bdl = below detection limit of the instrument used for analysis.

CHAPTER SEVENE

7 Discussions

Field investigation of the study area gives clues about the ore formation mechanism and mineralization nature and type of ore deposit. The field observation reveals that the various developments of erosional unconformity through the vertical section of iron hosting rock. The ore deposit is in the sedimentary terrain. The iron ore body of the area is varies from stratified bed and residual fragmentations of iron clasts and gravel size host. These observation of depositional gaps, geologic terrain and ore type are indications of lateritic weathering of ferruginous sandstone for the mineralization in the area.

The thin section description of rocks are used to determine the degree of weathering and transportation mechanism. It is also important to identify the constituent minerals within the rock and for classification. The thin section analysis of sandstone shows the quartz and altered feldspar. From the results of petrographic description and study the rock is classified as arkose type sandstone (Table 1). Through progressive enhancing of weathering the quartz is immobile compared with fine clays and silts. Weathering live surface alteration and secondary pore space filling to the remnants of arkosic feldspar while quartz grain is not yet. The quality of sediments are increased by removing fragile and fine sediments through gradual weathering and transportation. The angular and sub angular grains of the sandstone constituent minerals under petrographic description were related with significant transportation of weathered regolith. The petrographic description of iron host rock is characterized by relative low proportion of matrix and presence altered feldspar and quartz. Texturally it shows moderate – less sorting of angular and sub angular quartz and feldspars. Those characteristics of the host rock is results of mineralogical and textural immaturity due to residual deposition of sediments.

The mineralogical study under ore petrography is important to discriminate the iron ore minerals, textural characterization and mineral paragenesis of the ore. The polished section description shows the iron ore samples have dominantly hematite, goethite ore mineralogy and other gangue phase. The non-fragile magnetite due to weathering is fragmented and dispersed through hematite boundary and gangues in rare concentration under petrography. An interlayered hematite observed under petrographic description (Fig.28, 29) are due to weathering and sedimentation of iron ore. Surface blue wish tarnishing and laterized goethite in dissected hematite is the manifestations of laterite weathering. The goethite is concentrated due to recrystallization through replacement of micro platy hematite during the laterite iron formation (Kumar et al., 2010; Boudeulle and Muller, 1988). Ore microscopic study of texture and paragenesis characterization of the ores show variable morphological habit for goethite and hematite is transformed to secondary goethite. Boudelle and Muller (1988) and Devkota and Paudle (2012) described that these mineralogical constituent and behavioral characteristic is an indication of laterite iron mineralization. The hematite occurs as stratified as well as cementing the goethite and gangues. Hematite and goethite documented from XRD analysis paragenetically characterized under ore petrography by gradual replacement of goethite for hematite (Fig 25 and 26 B). Based on Sahoo et al (2018), this is due to sedimentary replacement of hematite through fractures or cleavage surface of minerals by goethite. However, the

fragmented rare distribution of magnetite observed in ore petrography is an input due to detrital derivation.

Mineralogical study of iron ores comprise kaolinite, magnetite, hematite, goethite and anatase (Fig 30-34). Kaolinite is typical clay mineral that formed by the surface weathering (supergene) process. The presence of this clay mineralogy in X- ray diffraction analysis interpreted as the Mekane Selam iron formation is due to laterite process. Anatase is the titanium polymorph mineral that can be stable for the low surface energy condition. Anatase is documented from XRD mineralogical study. The presence of this mineral in the ore sample is an indication of iron mineralization of the study area is due to surface lateritization. Those mineralogical constituents analyzed quantitatively by XRD from iron ore samples are characteristics of iron formed from weathering process or laterite (Boudulle and Muler, 1988).

In addition to this the weathering activity is possibly inferred from the secondary, heavy immobile and resistant minerals. Elements (Fe, Al and Si) are analyzed from the same iron ore samples of XRD (Table 3). Those elements are enriched in the ore samples. These elements are continuously concentrated near to the weathering profile. Because those elements are immobile and possibly form their corresponding oxides during laterite process. The surface weathering and subsequent removal of weathering susceptible constituents of the iron ore show depletion in those easily removable elements (Sc, Rb and Ba, Mg, K).

Major element analysis of the Mekane Selam iron occurrence show very high quantity of Fe_2O_3 , SiO_2 and moderate to high Al_2O_3 content (Table 4). The high concentration of those major oxides are as a result of laterite process. Because their constituent individual elements are relatively immobile during weathering. The abundant geochemical signatures of those oxides are typical characteristics of laterite iron formation (Irabor and Okolo, 2010). The surface chemical weathering (alteration) index / alteration (CIA) is determined from the chemical analysis data according to Nesbitt and Young (1982) using formula of $\text{CIA} = \{ \text{Al}_2\text{O}_3 / (\text{Al}_2\text{O}_3 + \text{CaO} + \text{Na}_2\text{O} + \text{K}_2\text{O}) * 100 \}$.

CIA of iron ore $\{ 19.22 / (19.22 + 0.16 + 0 + 0) \} * 100 = 99.17\%$ and $\{ 1.61 / (1.61 + 0.21 + 0 + 0) \} * 100 = 88.46\%$, for maximum and minimum chemical value respectively.

CIA of host rock $\{ 21.14 / (21.14 + 0.12 + 0 + 0) \} * 100 = 99.44\%$ and $\{ 3.14 / (3.14 + 0.08 + 0 + 0) \} * 100 = 97.52\%$, for maximum and minimum chemical value respectively. The

value of both iron ore and host rock samples of chemically analyzed result have very high weathering index value. This CIA value show that iron ore and the host rock samples are subjected to intensive weathering process. The result indicate that the Mekane Selam iron mineralization is deposited due to the surface laterite through weathering of iron bearing continental crust rocks.

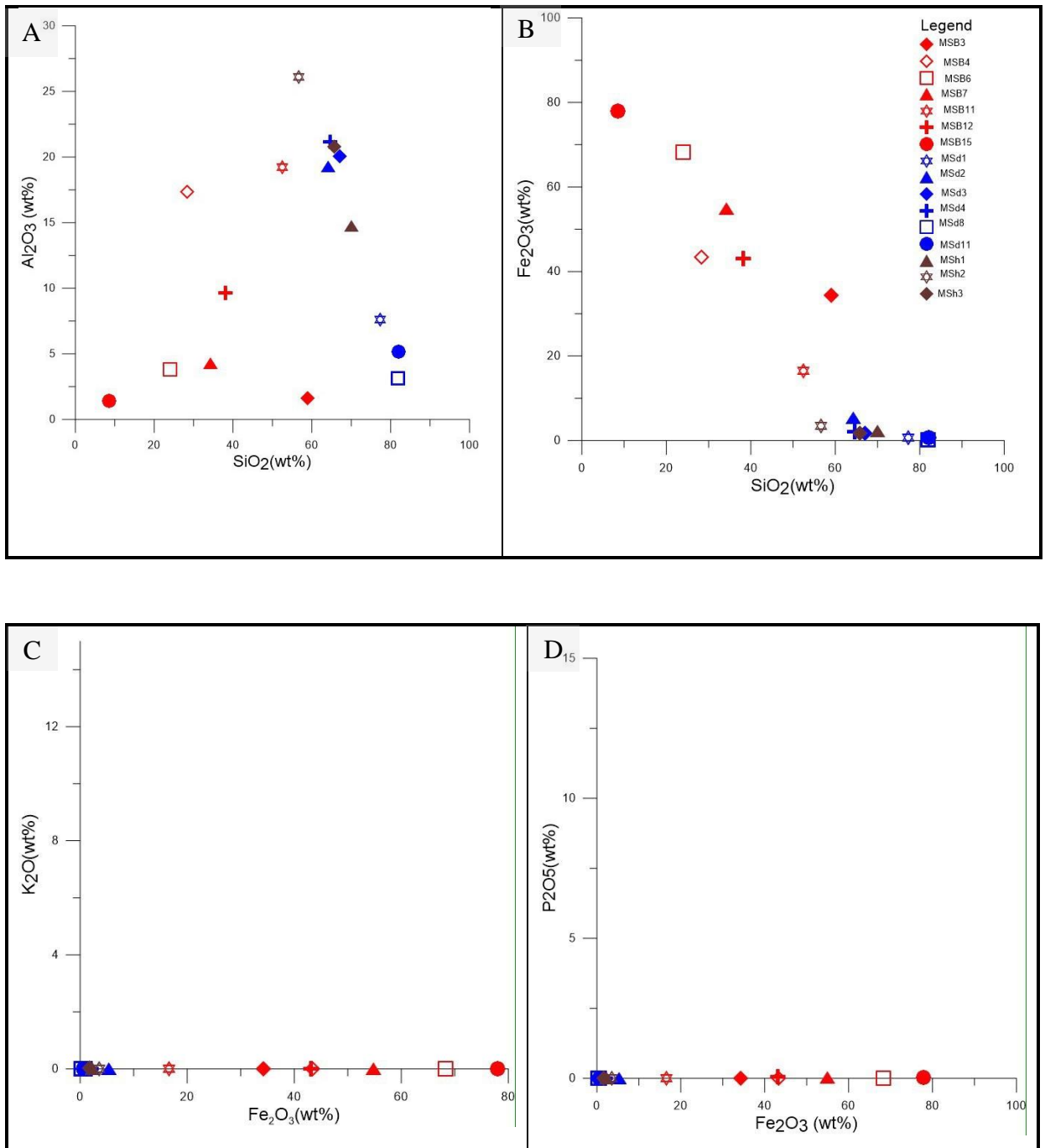


Figure 38. *Liner plots of geochemical data for major oxides of both iron ore and host rock.*

The Al₂O₃ vs SiO₂ liner plot (Fig.38 A and B) of the host rock samples show enriched in both silica and aluminum oxide but, sample (MSd8 and MSd11 are depleted in Al₂O₃).

However, the ore samples are enriched in aluminum oxide and silica except samples (MSB3 and MSB15) depleted in silica and both Al_2O_3 and SiO_2 respectively (A). The ore samples are highly enriched in Fe_2O_3 and SiO_2 except sample (MSB15) is depleted in SiO_2 while the host rock is depleted by Fe_2O_3 (B). In laterite weathering process the concentration of Al_2O_3 , Fe_2O_3 and SiO_2 is increased and positively correlated. Plot Fe_2O_3 vs SiO_2 shows host depletion in Fe_2O_3 . This indicates that the iron ore is separately deposited and confirm the bedding of field observation to the host. Plot K_2O and P_2O_5 vs Fe_2O_3 (Fig.38 C and D) shows iron ore samples have very low concentration in both K_2O and P_2O_5 . However, increasingly enrichment in Fe_2O_3 for both plot. The depletion in alkali metal oxides are consistent with easily removal of K during weathering. Depleted P_2O_5 is due to little concentration of apatite in iron. Because P is behaved as incompatibly in the protolith and the absence of phosphate in the iron ore is increase the iron quality and requires less processing technology.

The very high alteration index value and the relationship behavior of major oxides indicate that the Mekane Selam iron mineralization is results of surface weathering process. This shows the study area iron mineralization would have been enriched by surficial supergene lateriaization through gradual removals of mobile alkali metals and leaching of quartz and aluminum to high concentration.

Geochemically analyzed ore and host rock samples of the Mekane Selam area is plotted on the ternary diagram of Al_2O_3 - SiO_2 - Fe_2O_3 (Fig. 39). This plot is used to understand the degree of laterization. For this major oxide ternary plot the host rock samples are plotted in the region of kaolinization. This shows the host rock of the area is subjected to high degree of kaolinization to give the kaolinite clay mineral that documented from XRD analysis (see Fig. 30-34). The ore samples are plotted in the region of weak – strong laterization. This show that iron ore samples are affected by weak and strong degree of laterization. The ore samples degree of laterization indicate that Fe mineralization of the area is due to laterite process. However, the host rock is subjected to high degree of kaolinization in order to concentrate kaolinite clay minerals. The hematite (Fe_2O_3) content from the chemistry analysis (16.55 - 77.93) is concentrated due to gradual increasing of residual laterization. The high content of SiO_2 varies from (56.76-82.10) Table 4 in the sandstone is results of leached silica during laterization. This high silica concentration in the samples are due to strong weathering of the host rock subjected to kaolinization process. The ternary plot

shows that the residually concentrated iron is increases through the progressive lateritization.

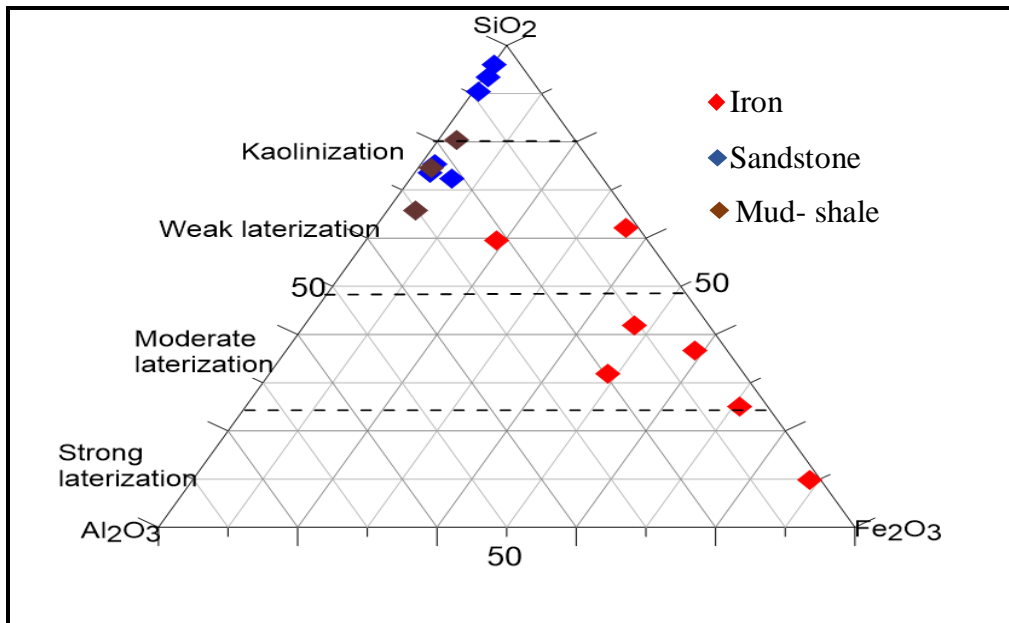


Figure 39. Ternary Al_2O_3 - SiO_2 - Fe_2O_3 plot showing different degree of lateritization for iron bearing rock after (Shellmann, 1986).

Chemistry of whole rock analysis show the high concentration of Zr, Nb and Al (Table 4). Zircon is the heavy mineral that is highly resistant to weathering. Al and Nb are detritally derived elements. The high concentration of those elements were an indication of laterite weathering. The abundance of heavy, accessory and immobile element within the host and ore shows parent materials subjected to weathering of surface lateritization (Kelepertsis, 2002).

Masidul and Marinal (2020) describe the weathering indices of Al_2O_3 / Fe_2O_3 , SiO_2 / Fe_2O_3 , SiO_2 / Al_2O_3 and K_2O / Al_2O_3 in relation to compositional variability (ICV) of the source. The geochemical analysis data of the samples give low and high value. This range of values indicate the compositional variability. ICV of the rock is due to intensive weathering of parent rocks. The analyzed samples show decreasing in CaO, Na₂O, K₂O and enhancing in Al₂O₃ and SiO₂ concentration. Because the laterite process removes those alkali and alkali earth metal oxides and make enrichments of Al₂O₃ and SiO₂ (Junjie et al., 2016). The content of these major oxides determine the characteristic of increasing the degree of weathering (Meng et al., 2017). The concentration of SiO₂, Al₂O₃, Fe₂O₃ and

TiO₂ ranges from high to moderate. The contents of analyzed samples are closely comparable with the average composition of Upper continental crust (UCC). This indicates that UCC is the typical source of host rock. However, the concentrations of CaO, MgO and Na₂O – K₂O are low. This is less comparable with that of UCC. Because those constituent elements of the oxide are soluble and mobile during laterization. The contents of TiO₂ and P₂O₅ of analyzed samples are very low. This depleted concentration of basic TiO₂ oxides is due to the source protolith is highly evolved felsic rock. The P₂O₅ depletion is indication of less accessory phase of apatite.

REE plot shows LREE enrichment and HREE relative smooth pattern with negative Eu and positive Ce anomaly (Fig. 36). This enriched LREE and depleted HREE is due to the source sediment is crust materials. The negative Eu anomaly shows that the iron mineralization is a result of oxidizing of iron during laterite formation. It is due to no leaching of Ca and substitution of Eu because of non-hydrothermal overprinting for mineralization. The high concentration of Ce observed in the analyzed iron and host rock samples are due to relatively larger mobility of cerium element in the laterized condition. This anomalous concentration of cerium because of different behavioral response of Ce to surface environment to concentrate CeO₂ in redox condition.

7.1 Geologic setting

The iron occurrence of Mekane Selam area is mainly associated with the volcano-sedimentary geologic setup. The area is located in the upper Blue Nile Basin. It comprises of limestone, intercalated muddy to shale, sandstone and volcanic lava flows with associated pyroclastic. The upper sub basin of Blue Nile is occupied by the Debre Libanose sandstone and Mughher mudstone formation. It consists of lower and upper section of sandstone varieties. The lower sandstone section comprises an alternation of sand lamination and thin mud–shale. However, the upper formation is alternating to the laterized iron and weathered detritals of thin sand sediment. The geology and mineralization with relative volcano-sedimentary distribution of the area is shown in (Fig. 10). While the stratigraphic section is presented in (Fig. 22). Massive, weathered – lenticularly stratified conglomerated sedimentary succession and volcanic pyroclastic are the main characteristics of the setting. Specifically the sedimentary terrain of the study area is dominated by sandstone succession. The mineralized zone is suitably associated within this quartz-feldspar abundant ferruginous sediment. Whereas the volcanic cover is known by basaltic–ash deposits. The

arkosic sandstone is host iron. It is underlayed by the bottom limestone and overlain by top basalt and pyroclastic. The lithological constituents of the area indicate the setting is continental crust. The iron mineralization of the area is due to weathering of this setting. The geologic setting of the study area is determined from the whole rock geochemistry.

The ratios of $\text{Al}_2\text{O}_3/\text{TiO}_2$ major oxide shows variable values ranging from 7.37-36.38 with average (16.5). This variation indicates that weathered continental crust is the main supply of deposited sediment (Fyffe and Pikerill, 1993). Trace and rare earth element stability during diagenesis and weathering are described by Bhatia and Taylor (1981). This study helps to infer the geologic setting of depositional area for the target area. Enriched pattern of LREE and relatively flat distribution of HREE with negative Eu anomaly (see Fig. 36) is compositional characteristic of upper continental crust (Oni et al., 2014). This shows that the geochemically analyzed rock samples of the study area confirms the continental crust is the possible source setting. Concentration of trace elements like Zr, Cr, Co, Sc, Hf, Th and Y are unaltered in concentration at the time of mobilization and deposition (Emannuel et al., 2017). The chemistry of analyzed samples show relative high concentration of those traces. This indicates the host rock has felsic source supplied from upper continental crust. Th/U ratio vs Th is plotted to understand the probable source area of the sediments (Fig. 40). All analyzed sandstone, mud-shale and iron ore samples are plotted in the upper crust region. Systematic weathering trend helps to infer the protholith. No any host rock and ore samples fall in the field of mafic source. The plot indicates there is no mafic source to supply sediment and metal during laterite deposition. The weathering trend represented by the trace diagram shows extensively weathered upper continental crust is the main sediment source and concentrated Fe of the Mekane Selam area. Iron is weathered from the upper crust with corresponding transportation and deposition. This iron is concentrated as hematite and goethite in the basin. Therefore, Th / U vs Th trace element diagram shows the earth's crust is source of Fe and sedimentary basin is suitable depositional site. According to Devkota and Paudel (2012) rounded to sub rounded textures of oolite (weathering result) iron characterize deltaic source. The same result observed under ore petrography of analyzed ore samples from the study area indicate probably weathered deltaic and continental clastic are input sources.

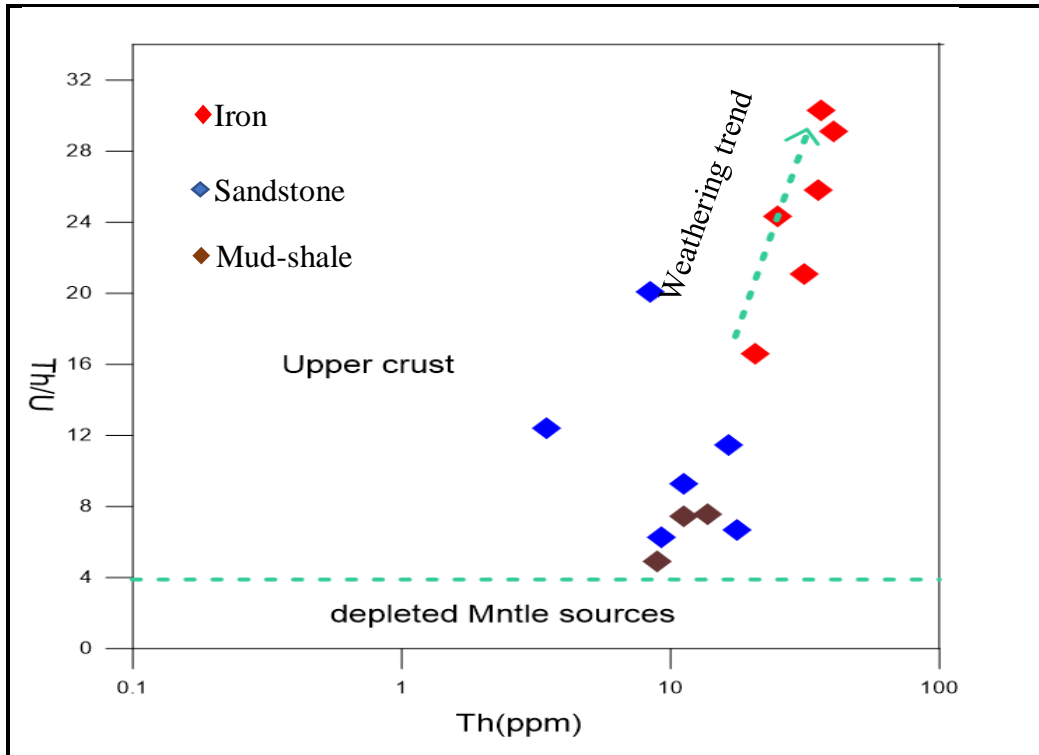


Figure 40. Plot of Th vs U to show the source of sediments after (McLennan et al., 1993).

Based on Adiotomer et al (2017) the Al_2O_3 / TiO_2 , La / Co, Cr / Th ratios with respective values of (7.39-24.78), (9.73-78.55), (2.43-31.12) are low – high. This content is positively correlated with felsic protoliths of upper continental crust composition. It is the sources of concentrated Fe and deposited sediment. In contrast the Ni / Cr ratio of (0.04-0.41) is very low. This shows that the mafic rock composition has insignificant contribution for the source of Fe and sediment supply.

7.2 Interpretation

The presence of quartz and Zircon minerals in the analyzed rock samples are an indications of the Mekane Selam iron formation is due to weathering of iron bearing parent rock. The angular to sub angular textural grain of iron clasts and host rock are deposited as a result of residual weathering process. The goethite, hematite, kaolinite, magnetite and rutile minerals of quantitatively XRD analyzed are interpreted as the iron occurrence of study area is due to surface laterite. The REE plot suggests that magmatic differentiation process of the basaltic lava flows fractionates and incorporate some mafic sediments to the felsic protolith source. Very rare distributions of magnetite found in the iron ore sample is probably indication of concentration occurring due to wind and water actions to weathered

heavy sediments. The secondary iron ore minerals of goethite and hematite reported from ore petrography are due to Fe enrichment from source rock weathering and corresponding transportation with deposition in the basin. The high content of Zr and low Eu from chemical analysis are interpreted as the iron mineralization is originated from residual weathering. The large concentration of Ce in the studied samples are as a result of surface supergene leaching of REE at the time of lateritization process. The negative and positive anomalies of Eu and Ce in normalized plot indicate the absence of hydrothermal input of Fe but, precipitation of iron from oxidation-reduction activity. Felsic composition protholith is source rock for deposited sediment were interpreted from the high value of LREE / HREE ratio and characteristics of enriched pattern of LREE with slightly negative Eu anomaly and smooth pattern of HREE.

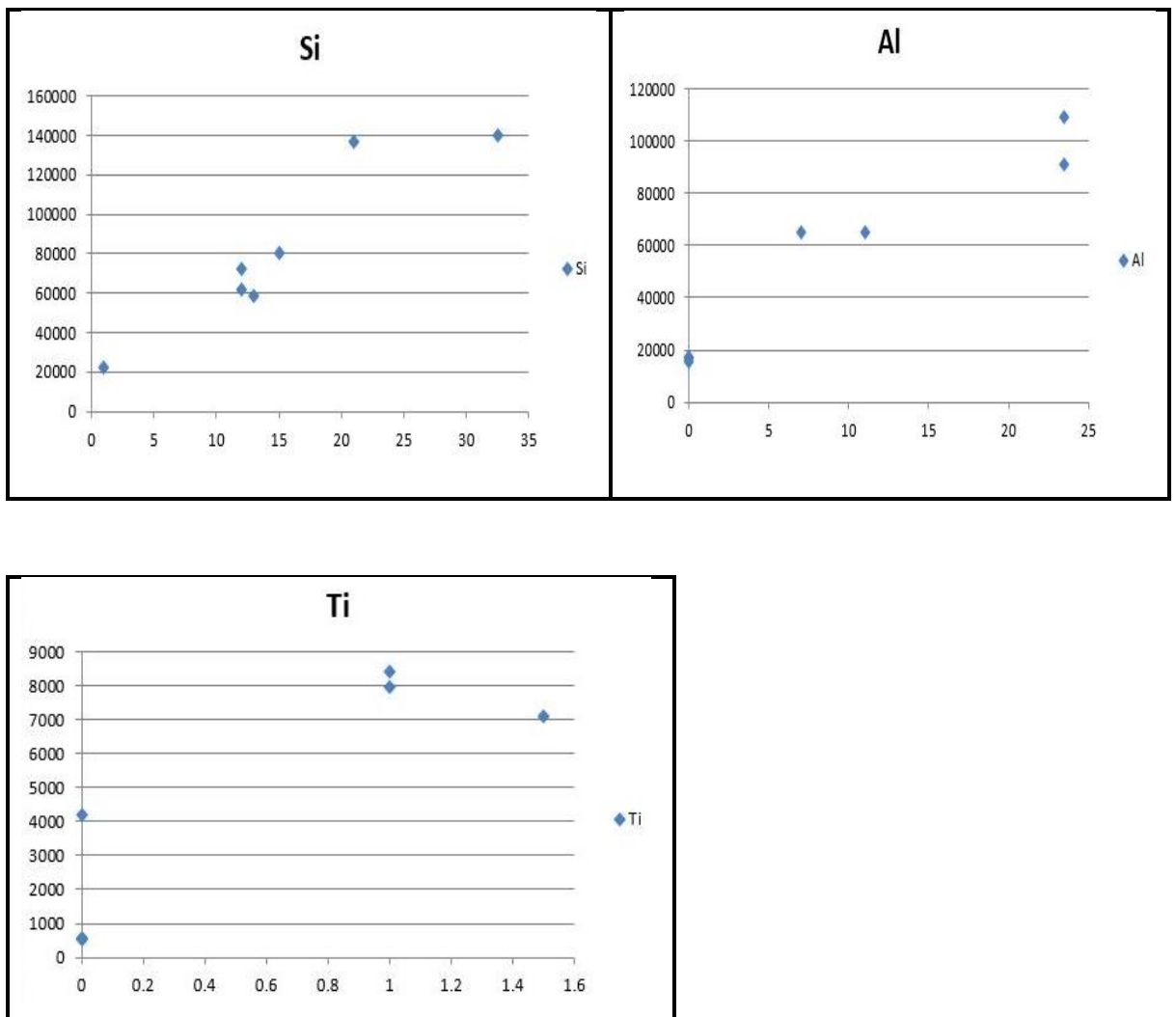


Figure 41. Correlated plot for Si- Qtz and Al- Kaolinite.

Relatively good correlation is shown between methods for Si–Qtz and Al– Kaolinite. The plot of iron ore samples shows the distribution of enriched silica and aluminum with fractionated immobile titanium concentration during surface weathering process. Positively correlated plot of Si-Al suggested that the clay mineral (kaolinite) identified in XRD analysis has been enrichment from silica dominated intensive weathering. The linear diagrammatic pattern of Ti is negatively correlated with the Si and Al. The relationship is interpreted as lateritic weathering of crust has insignificant role for Ti enrichment and low mafic source contribution.

7.3 Genesis of iron

The Davidson et al (2018) discussions indicates that magmatic-sedimentary depositions are common genetic mechanism for iron mineralization. Sedimentary ore forming process is responsible for the Mekane Selam iron occurrence. The iron ore formation of the area passes through basic sedimentary ore forming mechanisms. The deltaic and terrestrial continent are sources of iron due to weathering. The surface runoff and wind actions are the possible transporting media. The valleys of highland and gully erosional surfaces are used as path ways for iron. The sedimentary basin is depositional site and preservative for the bedded iron ore. The possible origin of Mekane Selam iron mineralization is understood from field observations, systematic analysis and interpretations of petrographic–geochemical data. The iron ore occurrence of the area is hosted in the sandstone. The field investigation indicate that the possible origin of iron mineralization for in the area is laterite. Because no mineralization in the volcanic yet. Field investigation of the study reveals that iron ore body is bounded by two texturally distinct sandstones. The fine-medium grain sandstone with lenses of conglomerate alternation is underlain to the iron ore body. The iron ore is overlaid by fine weathered sandstone. This sediment stratigraphic succession and host rock association is the fact that its origin is sedimentary due to laterite weathering.

The hematite but, replaced by goethite mineralogical content reported from XRD and characterized using ore petrography for iron ore samples confirm sedimentary origin (genesis) of iron as a result of laterization (Dvison et al., 2018). Goethite is paragenetically replacing hematite along the grain boundary of the ore minerals under petrography. This kind of secondary goethite recrystallization is indication of laterite origin (Sahoo et al., 2018). The Mekane Selam iron ore petrographic study shows dominant mineralogy of hematite, goethite and few magnetite fragmentation and other gangue phases. This iron ore

minerals show the mineralization mechanism is surface laterite process. Because those mineral phases are characterized by surface weathering. Iron is concentrated and reprecipitate in the site of weathering residually. This deposition is occurring within current continental environment of the sandstone. This concentrated iron sourced from weathered continent (Worash Getaneh and Solomon Tadesse, 2015) for enrichment as well as modified by diagenetic processes. Large percentage of hematite mineral documented from XRD and ore petrographic characterization indications of this modification.

Negative anomaly of Eu (see Fig.36) is due to sedimentary and diagenesis enrichment of iron which is not hydrothermal precipitation (Bekker, 2010). High concentration of Cr and Pb are results of diagenetically enriched iron (Novoselov et al., 2018). The high concentration of Al_2O_3 and Fe_2O_3 observed from geochemical results show immobile enrichment during weathering and diagenesis. This is the typical indication of laterite iron deposition. The hematite and goethite secondary transformed minerals those documented from XRD and ore microscope are due to weathering of preexisting iron bearing rock (Bourman, 1988). Iron originated from laterite minerlogically consists of hematite, goethite and kaolinite (Boudulle and Muller, 1988; Kumar et al., 2010). The analyzed iron ore samples using petrography and XRD show those mineralogy. This confirms the genesis is lateritic.

Normalized chondurite plot of iron and host rock shows high concentration of Ce (Cerium) (Fig.36). This anomalous value of Ce is consistent with oxidized zone of laterite process (Devez et al., 2017). Iron ore samples (MSB11) shows enrichment distribution of HREE (Fig. 36). This is because of the laterite process applied for the Mekane Selam iron leaches REE and precipitate them in the same depositional basin. Strong enrichment of HREE observed in iron ore is due to laterite origin or genesis (Beukes et al., 2003). High CIA values of the host rock (mentioned in previous section) is due to intensive surface weathering. This weathering of iron bearing sources rock increases iron concentration (mineralization) of the area.

The major oxides of iron ore and host rock of the study area is plotted on the ternary diagram of $SiO_2 - Al_2O_3 - Fe_2O_3$ (Fig.43). The plot of the ore samples geochemical result on this ternary diagram is used to understand the possible genesis of iron mineralization of the study area. Most of the iron ore samples are plotted within the region of laterite except sample (MSB3). This sample is due to less affected by laterization. However, all other ore samples are subjected to high degree of laterization to concentrate hematite (Fe_2O_3). This

plot shows the iron ore samples are enriched due to intensive surface laterite process. The plot of ore samples show favoring the hematite formation by increasing of laterization while the host rock is more favoring to kaolinite formation rather than bauxite.

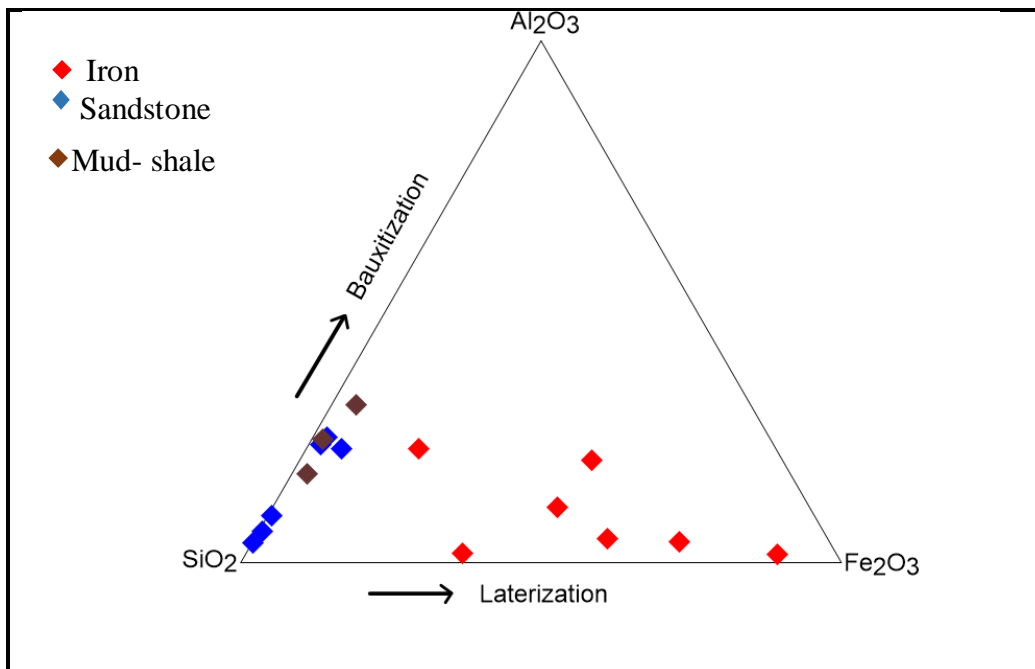


Figure 42. Ternary plot of SiO_2 - Al_2O_3 - Fe_2O_3 showing iron enrichment by laterite after (Gardner and Walsh, 1996).

Major oxide geochemical data of iron ore and host rock samples of Mekane Selam are plotting on SiO_2 - Al_2O_3 - Fe_2O_3 triangular diagram (Fig. 44). This plot is for genetic relationship between laterite types that concentrates the iron occurrence of the study area. The plot shows two iron ore samples are plotted in the region of ferricretes. Those samples are subjected to residual deposit of ferruginous where the upper zone of ore body is altered to ferricretes laterite type in which more than 20% Fe_2O_3 is concentrated. In this ternary plot much of the ore samples lay in the Fe - Laterite. The trend of plotted ore samples show the highest concentration of iron is to award Fe-Laterite. This Fe-Laterite is the laterite type in which the ore is subjected to large degree of laterization and concentrate abundant hematite ore mineral. The diagram conclude that the genesis of iron in the study area is due to laterite mineralization. The iron bearing source rock is concentrated as hematite iron oxide while the quartz-feldspar dominated host rocks were deposited as silica or kaolinite.

Therefore, the Mekane Selam iron occurrence genesis is laterite and ferricretes and Fe-Laterite are the contributing laterite type for mineralization process.

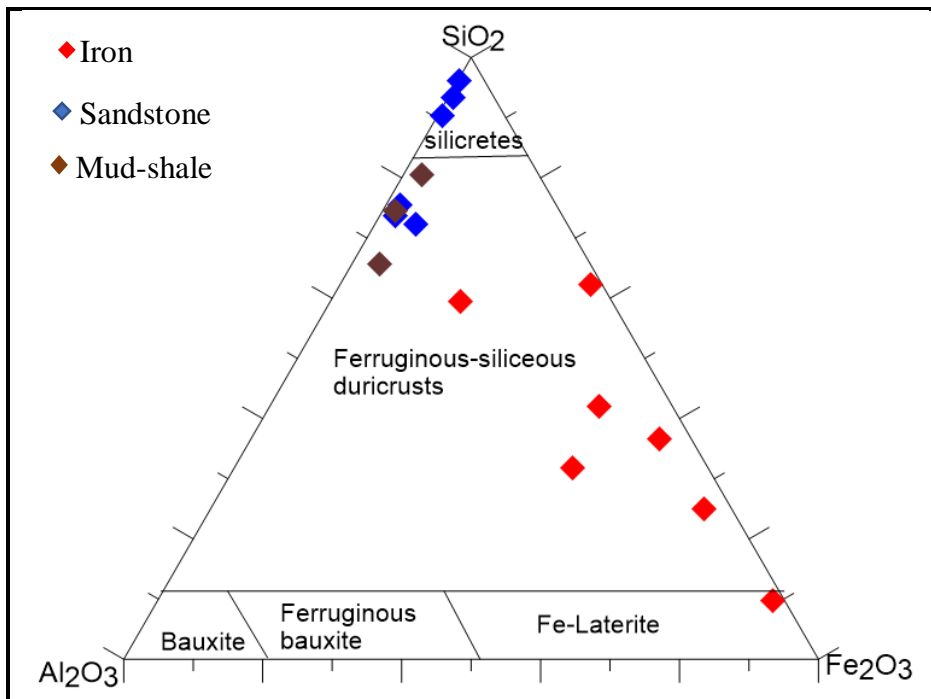


Figure 43. Ternary diagram of $\text{SiO}_2\text{-Al}_2\text{O}_3\text{-Fe}_2\text{O}_3$ showing the genetic relationship after (Dury, 1969; Bassam and Tamar, 1998).

Therefore, the genesis of Mekane Selam iron mineralization is mainly due to sedimentary ore forming process. The geochemical and mineralogical studies show that laterite surface weathering is the main genesis. However, the iron deposited by laterite is continuously modified its concentration and texture by other sedimentary processes.

7.4 Resource of the area

The iron resource of Mekane Selam area has been estimated from the geochemically analyzed information and field investigation activities. Seven iron ore samples were analyzed for the Fe content determination. With this information and from the field data the total iron ore resource of the study area is estimated using the formula of resource = $A * T * \rho$ where A= the area calculated from different blocks, T is the average thickness and ρ is the bulk density with the pore volume. XRD study of the iron ore samples show hematite, goethite and magnetite are the dominant identified mineralogical phases. According to the data assessed on 7/16/2020 <http://webmineral.com> the dominant constituent minerals hematite and goethite bulk density are 5.04g/cm^3 and 4.13g/cm^3 respectively. The average bulk density (4.6g/cm^3) of the mineralogical compositions used to estimate the resource of the area.

Table 8. Estimated resource of Mekane Selam iron occurrence.

Blocks		A(m ²)	Th (m)	V(m ³)	BD	T	Fe ₂ O ₃ %	Av. gr	T-Total	Total tang of the area	Total reserve of each block	Total reserve of the area
Millo	M ₁	98437.65	4	393750.24	4.6g m/cm ³	1.81M ton	68.23	0.3	8.8M ton	20.88 Mton	2.64 M ton	4.95 M ton
	M ₂	186632.11	3.75	699870.41	4.6g m/cm ³	3.21M ton						
	M ₃	83047.82	4.2	348800.84	4.6g m/cm ³	1.60M ton	77.93					
	M ₄	64565.71	5.5	355111.4	4.6g m/cm ³	1.63M ton						
	M ₅	20028.25	6	120169.5	4.6g m/cm ³	0.55M ton	34.31					
Agia gora	A ₁	101300.87	2.5	253252.18	4.6g m/c M3	1.16	43.38	0.27	2.67M ton	0.72Mton		
	A ₂	61867.12	4	247469.48	4.6g m/cm ³	1.13						
	A ₃	23929.4	3.5	83752.9	4.6g m/cm ³	0.38	54.86					
Dasu e	D1	65453.31	2.5	163633.28	4.6g m/cm ³	0.75M ton	43.1	0.2	1.64Mt on	0.33 Mton		
	D2	130348.28	1.5	195522.42	4.6g mcm ³	0.89M ton						
Lege work e	L	450352.51	3.75	1688821.91	4.6g m/cm ³	7.77M ton	16.55	0.16	7.77Mt on	1.2Mton		

A = Area, Th =Thickness BD= Bulk density T= Tang T-Total= total tang of the blokes
Av. gr.= average grade

The average grade concentrated hematite is under estimate the individual tang of the block because due to the fact that from all ore body iron ore samples were not analyzed.

As indicated in the previous section the thickness of ore is non-uniform through vertical and horizontal laterite. Having this variations in to consideration the resource estimation of iron occurrence for the study area average thickness is taken for the calculation. The average grade is calculated by weighting to the variation in volume. The average thickness of iron is taken from the measurement of well exposed ore and simple manual trenches with various vertical thickness and horizontal length for different blocks during field observation. The less adequately spaced number of field data, limitation on the manual trenching, difficulty to take hand digging pit and non-incorporated drilling works are determine the level of geologic knowledge and economic profitability of the study area. The shape of ore body, dimension are measured from the outcrop and possible trenches. However, the quantity and quality of iron is determined from results of selected representative samples. Therefore, based on the field investigation and analyzed samples for mineralogical content and geochemical information the iron mineralization of Mekane Selam area could be classified as an indicated resource.

If the geologic knowledge increasing confidentially through the detail sampling closely spaced drilling and borehole the estimated resource of the area is probably translated to reserve level.

CHAPTER EIGHT

8 Conclusion and recommendation

8.1 Conclusion

The Mekane Selam iron mineralization is considered as the ore deposit resource that is formed by sedimentary accumulation and laterite concentration mechanism. This is understood from the field investigation conducted and other mineralogical and geochemical analysis in the study area. The petrographic basis show that sandstone of study area is classified as arkose type consisting 12.83% - 49% detrital quartz grain, (36% - 79.5%) altered feldspars and 0.33% - 14.16% matrix (ground mass). It is the most possible host rock for iron mineralization of the area.

Hematite (30-60%), goethite (8-59%), magnetite (0.5-3%), kaolinite (11-23.5%), quartz (1-21%) and anatase (1%) are the mineralogical composition of ore and gangues of the iron ore of the area studied using XRD and Ore petrography. Those mineralogy and gangue of the ore body and associated rocks are interpreted as concentration of iron is due to

secondary surface weathering process. Hematite and goethite are the ore minerals that occupy the large portions of the ore body and associated rock. The diagenesis and sediment recrystallization are a significant Fe ore concentration and modification mechanisms during mineralization processes. The petrographic study and X-ray diffraction analysis of iron ore and field observation suggests that the Mekane Selam iron mineralization is enrichment due to laterite origin (genesis).

The geochemical analysis of high concentration in SiO_2 , Fe_2O_3 and Al_2O_3 and very low contents of alkali and alkali earth metals (K_2O , Na_2O , and MgO) with high CIA value are indicate the major ore forming process is lateritic weathering. Low content of P_2O_5 and TiO_2 major oxides of chemically analyzed ore and host rock shows the quality of iron and depleted mantle is not source of deposited sediment. SiO_2 - Fe_2O_3 - Al_2O_3 ternary diagram of major oxide plot indicate the iron ore body of the study area is subjected to low and strong degree of lateritization. However, the host rock of iron ore is subjected to high degree of kaolinization process. The degree of lateritization and kaolinization concentrate residual iron and kaolinite (clay mineral) through progressive weathering process respectively.

The geochemical characteristic of host rocks and ore body of study area suggests that felsic continental crust is the source of clastic rock while passive and active continental margins are the tectonic setting of depositional basin. Felsic composition protolith and insignificant role of mafic rock composition is interpreted from the ratios of selected trace element. Very high to moderate LREE/HREE ratios of whole rock chemistry is interpreted as a result of strong degree of fractionation through deposition between enriched and depleted REE content after weathering. Normalized – chondurite enrichment in LREE with negative Eu and positive Ce anomaly of iron ore and host rocks are consistent with felsic UCC protholith source and Fe mineralization in oxidized basin. Anomalous concentration of cerium is as a result of surface supergene oxidation and leaching of REEs are due to diagenetic alteration and modification during sedimentation.

The geochemical result of low content in MgO and absence of sulfur suggest that the environment of iron deposition is occurs within non-marine to shallow but, not fully marine. The REE pattern of the whole rock chemistry shows enrichment in LREE and relatively smooth distribution of HREE with negative Eu anomaly suggests that the iron mineralization process of Mekane Selam area is free hydrothermal fluid inputs.

The mineralogical content and geochemical data analysis and synthesis are conclude that the Mekane Selam iron occurrence is genetically laterite and modified by other sedimentary digenetic process. The chemistry analysis of iron ore body samples indicate the quality of iron is high contains 16-77wt% Fe₂O₃ composition and very low proportion of phosphates (P₂O₅). Degree of lateritization increase the quality of iron through Fe₂O₃ oxidation. The geochemistry, mineralogical study and field observation suggests that iron mineralization of the study area is classified as an indicated resource. For Mekane selam iron ore deposit due to continuous erosion, early mining and for its profitability other detail works are recommended.

8.2 Recommendation

The Mekane Selam iron mineralization is exposed due to continuous erosion and washed away hence, to save the resource early mining is recommended. A thin overburden thickness to the ore body makes the mineralization of the area is economically profitable. This study is to understand the origin of mineralization and preliminary investigation of the extent However, further drilling, surface excavation and other geological works will needed to know detail about the resource. The geochemical analysis of ore samples has 48% average Fe₂O₃ content this result show that the Mekane Selam iron is useful quality. Although, the non-geologic aspect (economic condition) and resource estimation requires detail analysis and study. The good access for ores except some blocks and relatively near to Addis is important for the economical profitability of iron resource of the area. Finally further exploration and detail delineation to increase metallic resource of the area is required within Blue Nile and upper sub Basin.

References

- Abbate, E., Bruni, P., Peter, M., Delme, C., Laurenzi, M., Miruts Hagos, Bedri, O., Rook, L., Sagri, M., Libsekal, Y. (2014). The East Africa Oligocene intertrappean beds: Regional distribution, depositional environments and Afro/Arabian mammal dispersals.
- Abebe T., Maetti P., Bonini M., Corti G., Innocenti F., Mazzarini F. and Pecksay (2005). Geological map of the northern Main Ethiopian Rift and its implication for the volcano – tectonic evolution of the rift. *Geological Society of America, Map and Chart Series MCH094* 1:200, 000: **20**.
- Abiy Ayalew, Dejene H/ Mariam, Fekadu Hailu, Ferede Chumburo, Mulugeta H/ Mariam and Temesgen Alemayehu (2015). Geology of Debre Markose map sheet, ministry of mines, Geological Survey of Ethiopia.
- Adewole, A. and Emmanuel, T. (2017). Mineralogical and geochemical trends in the residual soils above basement rocks in ore area, southwestern Nigeria. **9** (3).
- Adiotomer, E., Innocent, E., and Adaikpoh, E. (2017) Geochemistry of fluvial sediments from Geregue, Southwest Nigeria. *Delta state University*.
- Afify, A., Sanz-montero, M. and Calvo, J. (2018). Differentiation of ironstone type by using rare Earth elements and yttrium geochemistry - a case study from the Bahariya region Egypt. *Elsevier Ore geology review*. **96**:247-261
- Albarède, F. (2009). Geochemistry an introduction. Cambridge University Press.
- Aleva, G. (1994). Laterites concept, Geology, Morphology and Chemistry. International soil reference and information center (ISRIC), Wageningen, Netherlands, 169.
- Armstrong-Altrin, J. S., Lee, Y. I., Kasper-Zubillaga, J. J., & Trejo-Ramírez, E. (2017). Mineralogy and geochemistry of sands along the Manzanillo and El Carrizal beach areas, southern Mexico: implications for palaeoweathering, provenance and tectonic setting. *Geological Journal*. **52**(4), 559-582.
- Asuke, F., Bello, K.A., Muzzammil, M.A., D.G. Thomas, D.G., Auwal, K. and Yaro, S. A. (2019). Chemical and mineralogical characterization of Gidan Jaja iron ore, Zamfara state, Nigeria. *Nigerian Journal of Technology*. **38** : (1) 93-98.
- Aubry, A. (1986). Observations géologiques sur les pays Danakils, Somalis, le royaume de choa et les pays Gallas – Bull, Soc. Geol.Fr. **14**:201-222; Paris.
- Bassam, K. and Tamar, M. (1998). Genesis of the Hussainiyat ironstone deposit, western desert, Iraq. *Mineralium deposita* **33**: 266-282.

- Bekker, A., Slack, J. F., Planavsky, N., Krapez, B., Hofmann, A., Konhauser, K. O., & Rouxel, O. J. (2010). Iron formation: the sedimentary product of a complex interplay among mantle, tectonic, oceanic, and biospheric processes. *Society of Economic Geology*, **105**: 467-508.
- Bethy. (1973). Correlation of Mesozoic sediments I Northern Yemen and Tigray Northern Ethiopia. *American Association of Petroleum Geologist Bulletin*.57: 2440-2446.
- Beukes, N., Gutzmer, J. and J. Mukhopadhyay (2003). The geology and genesis of high grade hematite iron ore deposit. *Applied Earth Sciences*. **112**. Provinces) Geological and geophysical prospecting Ljublijana, Yugoslavia, 66p.
- Beyth, M. (1972). Paleozoic sedimentary basin of Mekele Outlier, Northern Ethiopia. *American Association of Petroleum Geologist Bulletin*. **12**:2426-2439.
- Bhatia M R and Taylor S R (1981). Trace element geochemistry and sedimentary province. A study from the Tasman Geosyncline. *Chem.Geol.* 33(115-125).
- Bhatia, M. and Crook K. (1986) Trace element characteristics of graywackes and tectonic setting discrimination of sedimentary basins. *Contrib. Petrol.* **92**(2) 181-193.
- Bhattacharya, H.N. and Ghosh, K.K. (2012). Field and petrographic aspect of the iron ore mineralization of Gandhamaradn hill, keonjhor, Orissa, and their genetic significance. *Jornal Geological Society of India*. **79**: 497-504.
- Binks RM, Fairhead JD. (1992). A plate tectonic setting of Mesozoic rifts of West and central Africa. *Tectonophysics*. **213**:141-151.
- Bosellini A. (1989). The continental margins of Somalia: their structural evolution and sequence stratigraphy. *Memorie di Scienze Geologiche, Padova* **41**: 378-458.
- Boudulle, M. and Muller, J.P. (1988). Structural characteristics of hematite and Goethite and their relationship with kaolinite in laterite from Cameroon. A TAM study. *Bull. Mineral.* 111:149-166.
- Breeding, C, Ague, J. and Brocker, M. (2004). Fluid metasedimentary rock interactions in subduction one melange implication for the chemical composition of arc magmas. *Geology*, **32**: 11041-1044.
- Bruno, K., Nicholas, A., Henriette, L., Florence, B., Arnaud, P., Yirgu, G., Ayalew, D. Dominique, W., Jerram A., Francine, K., and Claudine, M. (2004). Flood and shield basalts from Ethiopia magmas from the African Super swell. *Journal of petrology*. **45** (4):793-834.

- Bussert, R. Schrank, E. (2007). Palynological evidence for a latest Carboniferous –Early Permian glaciation in Northern Ethiopia. *Journal of African Earth Science*. **49**: 201-210.
- Cannon, R., Simiyu-Sianbu, W. M. N. and Karanja, F. M. (1981). The Prot-India Ocean and a probable Paleozoic/Mesozoic triradial rift system in East Africa. *Earth planet. Sci. Letts*. **52**:419-426.
- Chukhrov, F.V. Moscow and USSR (1973). On the genesis problem of thermal sedimentary iron ore deposits. *Mineral deposita*. **8**: 138-147.
- Conliffe, J. (2015). Geological Setting and Genesis of High-Grade Iron Ore Deposits in the Eastern Labrador trough, Newfoundland and Labrador.
- Conliffe, J. (2016). Geology and geochemistry of high grade iron ore deposit in the Kivivic timmins and ruth lake areas, western Labrador. *New found land and Labrador department of natural science. Report of Geological Survey*. 1-16.
- Conliffe, J., Kerr, A. and Hanchar, D. (2012). Mineral commodity of Newfoundland and laborador, Iron ore Geological Survey Mineral commodities series, Canada. (7): 110.
- Cox, R., Lowe, D. and Cullers, R. (1995). The influence of sediment recycling and basement composition on evolution of mud rock chemistry in the southwestern. *United states. Geochim Cosmochim Acta*. **59**:2919-2940.
- Dainelli. G. (1943). Geologia dell's Africa oriental. **4**: Rent Acc. Ital., Centro Studi Africa Orint. Ital.; Roma.
- Daniel Meshesha and Ryuichi Shino (2007). Crystal contamination and diversity of magma sources in the northwestern Ethiopian volcanic provinces. *Mineralogical and Petrological Sciences*. **102**:272-290.
- Devis, P., Bonhoure, J. and Pourret, O. (2017) Rare Earth element geochemistry in an iron rich nickel laterite from new Calidonia.
- Devkota, S. and Paudel, L.P. (2012). Petrology and genesis of the Bhainskati iron ore deposit of Palapa district, western Nepal. *Bulletin of the departments of Geology*. **15**: 63-68.
- Dupuis, C., He bert, R., Dubois- cote, V., Guilmette, C. and Wang, Z. (2006). Geochemistry of sedimentary rocks from mélangé and flysch unit south of the yarlung Zangbo suture zone southern Tibet. *Journal of Asian Earth Science*. **26**: 489-508.
- Dury.G. (1969). Perspectives on geomorphic processes. **56**. Washington. Association of American Geographers.

- Davidson, E., Egirani, Mohd T., Latif, Nanfe R., Poyi, Napoleon Wesley and Shukla, Acharjee (2018). Genesis use and environment implication of Iron Oxides and ores. <http://dx.doi.org/10.5772/intechopen.57776>.
- Ethiopian institute of Geological Survey (EIGS) (1990). Geological and Geophysical exploration report on Kunnti, Dedro and Galleti (Werfedo) areas Harerge. Ministry of Mines and Energy, Ethiopian Institute of Geological Survey, Unpublished technical report.
- Ethiopian institute of Geological Survey (EIGS) Ethiopian institute of Geological Survey (1986). Report on the Geology and Iron occurrences within the explored Guba project area. Technical report, GSE, Addis Ababa, Ethiopia.
- Emmanuel, A., Innocent, E. and Edwin, A. (2017). Geochemistry of fluvial sediments from Geregu southwest Nigeria. *De Gruyter Open*.
- Ethio -Korean Iron Exploration Project (1990). Geological and geophysical Exploration work on the iron ore of Melka Arba (Bale). EIGS (Ethiopian institute of Geological Survey), Unpublished. Report, 79p.
- Eugene, F. Nsoh, Ako, Thomas Agbor, Jacques Etame and Emmanuel C.Suh (2014). Ore texture and Geochemistry of the Nkout iron deposit, South East Cameroon. *Science, Technologies et Development*. **15**:43-52.
- Fairhead JD. (1988). Mesozoic plate tectonic reconstructions of the central South Atlantic Ocean. The role of west and central African rift system. *Tectonophysics* **155**: 181-181.
- Fatuque, H. and Bubul, B. (2019). Whole rock geochemistry of tertiary sediments of Mizoram foreland basin NE India implications for source composition tectonic setting and sedimentary processes. *Acta Geochim.* **38**(6):897-914.
- Flores, G., (1973). The Cretaceous and Tertiary sedimentary basin of Mozambique and Zululand. In: Blant, G (ed.). *Sedimentary Basins of South and Eastern Africa Coasts, part 2. Paris Association African Geological Surveys*, 81-111.
- Gani ND. Abdelsalam MG, Mazzarini F., Abebe T., Pecskey Z. and Gani MR. (2007). Blue Nile incision on the Ethiopian plateau: Pulsed plateau growth, Pliocene uplift and hominid evolution. *GSA Today*. **17**: 4-11.
- Gani ND. Abdelsalam MG. (2006). Remote sensing analysis of the Gorge of the Nile, Ethiopia with spatial emphasis on Dejen- Gohtsion region. *Journal of African Earth Sciences*. **44**: 135-150.

- Gani, N. D., Abdelsalam, M. G., Gera, S., & Gani, M. R. (2009). Stratigraphic and structural evolution of the Blue Nile Basin, northwestern Ethiopian plateau. *Geological Journal*. **44**(1), 30-56.
- Gani, N. D., Abdelsalam, M.G., Gera, S. and Gani, .M.R. (2008). Stratigraphy and structural evolution of the Blue Nile Basin, Northern Ethiopian Plateau. *Geological Journal*. Online Publication. DOI: 10.1002/gj.11127.
- Gardner, R. and Walsh, N. (1996). Chemical weathering of metamorphic rocks from low elevations in southern, Himalaya. *Chemical Geology*. **127**:161-176.
- Geharing, A. (1990) Diagenesis of ferriferous phases in the northampton ironstone in the Cowthick quarry near Corby England. *Geol. mag.* **127**(2)169-176.
- Geological Survey of Ethiopia (GSE) (2007). Geology of Debre Markose Map sheet Northwestern Ethiopia. Unpublished technical report GSE, Addis Ababa, Ethiopia 87pp.
- Getaneh Asefa and Saxena, G. N., (1984). Review of Ethiopian lignite Occurrence prospects and possibilities. *Energy. Explor, Exploit.* **3**: 35-42.
- Getaneh, A., (1991). Lithostratigraphy and environment of deposition of the Late Jurassic – Early Cretaceous sequence of the central part of Northwestern Plateau, Ethiopia. *N. Jb. Geol. Paläont.Abh.* **182** (3): 255-284.
- Glasby, G., Stuben, D., Jeschke, G. and Garbe-Schonberg, C. (1997). A model for the formation of hydrothermal manganese crusts from the pitcairn Island hotspot, *Geochim. Cosmochim. Acta.* **61**:4583-4597.
- Gouin, P. and Mohr, P., (1964). Gravity traverse in Ethiopia (interim report), *Bull. Geophy. Obs.* Addis Ababa, (7): 185-239.
- Gross, G. (1996). Stratiform iron in Geology of Canada mineral deposit type. *Geological Survey of Canada*. **8**: 41-54.
- GSE (2018). Preliminary report on iron occurrence of Mekane Selam. Technical report GSE (Geological Survey of Ethiopia) (1975). Iron at Dim, Arbaminch Gamo, Gofa. Technical report, GSE Addis Ababa, Ethiopia.
- Gutzmer, J., Chisonga, B.C., Beukes, N.J. and Mukhopadhyay, J. (2008). The geochemistry of banded iron formation-hosted high-grade hematite-martite ores *Economic Geology (SEG Reviews)*. **15**: 157-183.
- Hadi, O. (2018). Island arc and active continental margin Adakites from the sabzevar zone Iran. *Petrology*, **26**(1) :69-113.

- Hamrla M. (1966). The iron and manganese ore deposits in Ethiopia reprinted from *Geologia -Razparave*, in proccla-9.Kntiga, Ljubljana, Yugoslavia, 439-
- Hayashi, K., Fujisawa, H. Holla, H. and Ohmoto, H. (1997). Geochemistry of approximately 1.9 Ga sedimentary rock from northeastern Labrador, Canada. *Geochim Cosmochim Acta*, **61**(19):4115-37.
- Herron, M. (1988). Geochemical classification of terrigenous sands and shales from core or log data. *J. Sed. Petrol.* **58**:820-829.
- Hodkinson, R., Stoffers, P., Scholten, P., Cronan, D., Jeschke, G. and Rogers, T. (1994). Geochemistry of hydrothermal manganese deposits from the pitcairn island hotspot, southeastern Pacific. *Geochim Cosmochim Acta.* **58**(22):5011-5029.
- Hofmann C., Courtillot V., Feraud G., Rochette P., Yirgu G. Ketefo E. and Pik R. (1997). Timing of the Ethiopian flood basalt event and implications of Plume birth and global change. *Nature.* **389**: 838-841.
- <http://ispatguru.com/beneficiation-of-iron-ores/> (from April 6, 2016 on March 16, 2020).
- <http://webmineral.com/data/Goethite, hematite and magnetite.>
- <https://www.steel.org/~media/Files/AISI/Making%20Steel/Article%20Files/ironore.PDF> (March 16, 2020).
- <https://www.ispatguru.com/geology-prospecting-and-exploration-for-iron-ore-deposits/> (March 15, 2020).
- <https://www.ispatguru.com/mining-of-iron-ores/> (march 16, 2020).
- Hunegnaw, A., Sage, L. Gonnard, R. (1998). Hydrocarbon potential of the intracratonic Ogaden Basin, SE Ethiopia. *Journal of Petroleum Geology.* **21**: 401-425.
- Irabor, E. and Okolo, P. (2010). Chemical and mineralogical characteristics of lateritic iron ore deposit at Iyuku Etsako west local Government area of Edo state, Nigeria. *Global Journals of pure and applied Science.* **16** (2):309-312.
- James, H.L. (1966). Chemistry of the iron-rich sedimentary rocks. *U.S. Geol. Survey.* 6th edition, 440pp.
- Jayawardand, D., Balasooriya, N. and Weer Acoon, W. (2014). Geochemical characteristics of hydrated iron- ore deposit in Dela, Sri Lanka. **16**: 43-52.
- Jepson D.H and Athearn, M.J., (1961). General Geological Map of Blue Nile River Basin of Ethiopia. 1:1000000 Scale.
- John, U. Solomon iokoso, A. and Idrisisa, F. (2019). Mineralogical and geochemical study of ironstones around Koton Karfi part of southern bida basin, north central Nigeria. *JETIR.* **6**(12).

- Jonsson, E., Troll, V., Hogdahl, K., Harris, C., Weis, F., Nilsson, K. and Skelton, A. (2013). Magmatic origin of giant Kiruna- type apatite iron- oxide ores in central Sweden. *Scientific report. Journal of African Earth Sciences*. **99**:463-489.
- Jpsen, D.H., Athearn, M. J. (1964). Land and Water Resource of the Blue Nile Basin. Ethiopia's Water Resource Department. Addis Ababa, Ethiopia 221.
- Junjie, H., Qi, L., Juan, L., Jing, H. and Dongsheng, G. (2016). Geochemical characteristics and depositional environment of the middle Permian mudstone from central Qiangtang basin, northern Tibet. *Geological Journal*. **51**:560-571.
- Kamen-Kaye, M. (1978). Permian to Tertiary fauna and paleogeography Somalia, Kenya, Tanzania, Mozambique, South Africa. *Jour. Petrol. Geol.* **1**:81-110.
- Kamen-Kaye, M., (1978). Permian to Tertiary fauna and paleogeography of Somalia, Kenya, Tanzania, Mozambique, South Africa. *Jour. Petrol. Geol.* **1**: 81-110.
- Karsten Knorr and Marck Bornefeld (2012). Analysis of iron ore – A combined XRD, XRF and MLA study. Conference paper. DOI:10.1314/2.1.1576.5445.
- Kazmin, V., (1975). Explanations of the Geology map of Ethiopia. *Ethiopian Geological Surveu, Bulltein*. **1**: 1-15.
- Kazmin (1979a.) Stratigraphy and correlation of volcanic rocks in Ethiopia. I.E.G.S. Unpublished report, Addis Ababa Ethiopia.
- Kelepertsis, A. (2002). Mineralogy and geochemistry of the Pliocene iron- rich laterite in the Vatera area, Lesvos Island, Greece and its Genesis. *Journal of geochemistry*. **21**(3).
- Kevin G. Taylor and Joe H. S. Macquaker (2011). Iron minerals in marine sediments record chemical environments. **7**:113-118.
- Kieffer, B., Arndt, N., Lapierre, H., Bastien, F., Bosch, D., Pecher, A., Yirgu, G., Ayalew, D., Weis, D., Jerram, D., Keller, F. and Meugniot, C. (2004). Flood and shield basalt from Ethiopia: magmas from African super swell. *Journal of petrology*. **44**:793-834.
- Krenkel E. (1992). Abessomalien (Absessinien und Somalien). Hand book of Regional Geology, *Heidelberg*. **7**: 8.
- Kumar, C. (2003). Chemical metallurgy principles and practice. Bhabha Atomic Research Center, India.
- Kumar, R., Akella Satya Venkatesh, U. and Roy, S. (2010). Mineralogical characteristics of iron ore in Jada and Khondobond area in Eastern India with implications on beneficiations. *Resource Geology*. **60** (2): 203-2

- Lakshmiddevamma, B., Reddy, V., & Gope Naik, V. (2017). Iron Ore Mineralization of Ramagiri Greenstone Belt, Anantapur District, Andhra Pradesh, India. *International Journal*. **6** (1):577-586.
- Lentz, D. R. (2003). Geochemistry of sediments and sedimentary rocks historical to research perspectives. Inorganic geochemistry of sediments and sedimentary rocks: evolutionary considerations to mineral deposit-forming environments. Edited by DR Lentz. *Geological Association of Canada*. 4, 1-6.
- Lewis, D. M. (1976). Geochemistry of manganese, iron, uranium, lead-210 and major ion in the Susquehanna River. Department of Geology and Geophysics.
- Luigi Beccualuva, Gianluca Bianchini, Claudio Natali and Franca Siena (2009). Continental flood basalt and mantle plume a cause study of the Northern Ethiopian plateau. *Journals of petrology*. **50** (7):1377-1403.
- M.M.E (Ministry of Mines and Energy) (1999). The Geology of Muger cement factory area Abay Basin, North Showa. Unpublished report, M.M. E, Addis Ababa, Ethiopia, 25pp.
- M.M.E. (Ministry of Mines and Energy) (1995). The Geology of Jema river valley Abay Basin, North Showa. Unpublished report, Addis Ababa Ethiopia.
- Mahmoud, M. H., Hatem, M. El., Salem, M., Adel, A. and Omar, A. (2018) Genesis of iron deposit in Bir UM Hibal area, Southeast Aswan Egypt, Remote- sensing- structural – lithological – ore mineralogical contributions. *Middle East Journal of applied science*. **8** (1): 19-36.
- Mansurova, N., Malysheva, T., Korovushkin, V., Gibadulin, M., Legin, V. and Gostenin, V. (2006). Comparative analysis of the mineralogical composition and metallurgical properties of the sinters obtained from iron ore bearing charges of different origin. *Metalluregist*. **50**: 9-10.
- Masidual, H. and Mrinal, K. (2020). Sandstone – shale geochemistry of Miocene Surma group in Bandarban anticline, SE Bangladish implications for province, weathering and tectonic setting. *Earth Science*. **9**(1): 38-51.
- Masresha G/ Selase and Wolf uwe reimold (2000). A review of metallic mineral potential of Ethiopia. *Inventaire des ressources en minerais metalliques de l' Ethiopie*.
- Masresha Gebreselasse (2002). Review of Melka Arba iron ore resource. Unpublished report Geological Survey of Ethiopia, 31p.

- McHargue T., Heidrick T. and Livingstone J. (1992). Tectonostratigraphic development of the interior Sudan rift, Central Africa. In *Geodynamics of Rifting. 2 cause history Studies on Rift: North and South America and Africa*, Ziegler PA (ed). *Tectonophysics*. **213**: 187-202.
- McLennan, S., Hemming, S., McDaniel, D. and Hanson, G. (1993). Geochemical approaches to sedimentation province and tectonic. *GSA Spec. Publ.* 284:21-40.
- Meng, Q., Sachsenhofer, R., Pingchang, Z., Renjiezhou, F. and Wang, K. (2017). Mineralogy and geochemistry of fine grained clastic rock in the Eocen Huadian basin NE China implication for sediment provenance pale climate and depositional environment. *Australian Journal of Earth Sciences*. **110**. Vienna.
- Mengesha Tefera, Tadiwos Chernet and Workineh Haro (1996). Explanation of Geological Map of Ethiopia. Ethiopian institute of Geological Survey, Addis Ababa Ethiopia, 80pp.
- Merla, G. Abbate, E., Azzaaroi, A., Bruni, P., Fazzuoli, M., Sagri, M. and Tacconi, P. (1979). Explanation of the Geological map of Ethiopia and Somalia with map of Major land forms. Consiglio Nazionale dell Ricerche Italy, 95pp. Firenze.
- Merla, G., Abbate, E., Canuti, P., Sagri, M. and Tacconi, P. (1973). Geological map of Ethiopia and Somalia. Consiglio Nazionale delle Ricerche, Firenze.
- Mir Ali Asghar Mokhtari, Ghader Hossein Zadeh and Mohamad Hashem Emami (2013) Genesis of iron – apatite ores in Posht -e- Badam Block (central Iran) using REE geochemistry. *Journal of Earth syst. Sci. India*. **122** (3):795-807.
- Mohr, (1962). The Geology of Ethiopia Addis Ababa University Press. 269p.
- Mojtaba, H., Momeni, A.A., Behrouz, R. and Saeed K. (2013). Relationship Between petrographic characteristics and engineering properties of Jurassic sandstone Hamedan, Iran. *Articles in rock mechanics and rock engineering*. MOM, GSE, Addis Ababa, Ethiopia, 57pp.
- Moreno, M. M. T., da Rocha, R. R., & Godoy, L. H. (2014). Major elements geochemistry of sedimentary rocks from Corumbataí Formation, Santa Gertrudes Ceramic Pole, São Paulo, Brazil. *Geomaterials*. **4**(1):11.
- Muwanguzi, A. Karasev, A., Byaruhanga, G. J. and Jonsson, P. (2012). Characterization of physical and metallurgical properties of Natural iron ore for iron production. *International scholarly research Network*.
- Nesbitt, H.W. and Young, G.M. (1982). Early Proterozoic climates and plate motions inferred from major element chemistry of lutites. *Nature* **299**: 715-717.

- Nomura, T., Yamamoto, N., Fulii, T. and Takiguchi, Y. (2015). Beneficiation plants and pelletizing plants for utilizing low grade iron ore. *Kobleco technology review*. (33).
- Novoselov, K., Belogub, E., Kotlyarov, V., Filippova, K. and Sadykov, S. (2018). Mineralogical and geochemical features of oolitic ironstones from the Sinara–Techa deposit, Kurjan district Russia. *Geology of ore deposit*, **60** (3) 265-276.
- Oni, A., Olatunji, S. and Ehinola, A. (2014). Determination of provenance and tectonic setting of Niger delta clastic facies using well- Y Onshore delta state, Nigeria. *Journal of geochemistry*.
- Oyelowo Bayowa, Gbenga Ogungdesan, Razak Majolagbe and Simeon Oyeleke. (2016). Geophysical prospecting for iron ore deposit around Tajimi village, Ilokoja, North-central Nigeria.
- Paul, Ramdotr (1980). *The ore minerals and their inter growth*. Second edition. Oxford.
- Pettijohn FJ, Potter PE, Sieer R (1987). *Sand and sandstone*. Springer, Berlin. 306
- Peuker, U., Kwade, A., Teipel, U., Jackel, H. and Mutze, T. (2012). Mineral renewable and secondary raw materials processing-current engineering challenges.
- Planavsky, N., Rouxel, O., Bekker, A. and Lyons, T.W. (2008). Rare Earth element evidence for redox structure evolution abs. *Goldschmit 2008 conference, Vancouver B. C. Canada*. **72** (1) 753.
- Ridely, J. (2013). *Ore deposit geology*. Cambridge University press. New York.
- Robb.L. (2005) *Introduction to ore forming processes*. Black well, United states of America.
- Rodolfo, Christiansen, Jose, Kostadioff, Julia, Bouhier and Patrica, Martinez (2018). Exploration of iron ore deposit in Patagonia. Insights from gravity, magnetic and SP modeling. *Geophysical prospecting*. **66**: 1751-1763.
- Rotter, M., Tegel, M., & Johrendt, D. (2008). Superconductivity at 38 K in the iron arsenide (Ba_{1-x}K_x)Fe₂As₂. *Physical Review Letters*. **101**(10), 107006.
- Roy, S, and Venkatesh, A.S. (2009). Mineralogy and geochemistry of banded iron formation and iron ores from eastern India with implications on their genesis. *Journal of Earth System Science*. **118**:619-641.
- Russo A., Assefa G. and Atnafu B. (1994). Sedimentary evolution of the Abay River (Blue Nile Basin, Ethiopia. *Neues Jahrbuch für Geologie und Palaeontologie Monatshefte*. **5**: 291-308.
- Sahoo, L. Ratha, BK and Nayak, BK (2018). Mineralogical and Geochemical characterization of iron ore deposit of Koira region of Sundargarh district of Odisha.

- International Journals of multidisciplinary research and development*. **5**: (4) 194-199.
- Schwertmann, U. (1969). Die- bildung von eisenoxidmineralen. *Fortschr. Miner.* 46:274-285.
- Senbeto Chewaka, (1981), Evaporite deposit in the northeastern Ethiopian Rift Vally.in plate tectonics and metallogenesis Ethiopian Institute of Geological Survey, Ministry of Mines and Energy. (2): 44-47. Addis Ababa Ethiopia.
- Serawit Amene, Tamrat Mojo (1999). The geology of mugher cement factory area abay basin north showa, ministry of mines.
- Shellmann, W. (1986). A new definition of laterite. *Mem. Geol. Surv. India*. **120**:1-7.
- Sherif, Farouk, Mohamoud, El. Rhamany, Hatem- El Desoky, Ahmed Khalil and Wael, Fahmy (2015). Geochemical characterstics of goethite bearing deposits in the Dakhla Kharga oases, western desert, Egypt. *International Journal of Scientific Engineering and Applied Science*. **1**: (8).
- Shunbro, M. (1968). The Ambaradom formation (formerly the Upper Sandstone). Unpublished report, Geological Survey of Ethiopia, Addis Ababa 26
- Silva, R.C.F., Lobato, C. A. R. and Hagemann, S. (2011). Petrographic and geochemical study at giant serra, Nort iron ore deposit in the carajas mineral province Para, state, Brasil. *Geomomos*. **19**(2) 189-223.
- Solomon Tadesse (2009). Mineral Resources Potential of Ethiopia. Addis Ababa university press.
- Spoerl, J. (2016) A brief history of iron and steel production.
- Stefanni, G. (1933). Saggio di una carta geologica dell's Ertreia, della Somalia e dell's Ethiopia, 1:2000000. Note illustrative. I.G.M. 195pp. Firenze.
- Subrata Roy and A.S. Venkatesh (2009). Mineralogy and geochemistry of banded iron formation and iron ores from eastern India with implications on their genesis. *Earth Syst. Sci*. **118** (6): 619-641.
- Sujan, Devkota, Lalu Prasad Paudel (2012). Petrology and genesis of the Bhainskati iron ore deposit of Palpa District, western Nepal. *Bulleein of the department of Geology*. **15**:63-68.
- Tadesse Alemu (2012). Geology of Ethiopia. Geological Survey of Ethiopia (GSE), unpublished technical report, Addis Ababa Ethiopia.
- Taylor, S. and McLennan, S. (1985). The continental crust: its composition and evolution. *Blackwell Oxfor*.

- Teklewold, A. and Moore, J. M (1989). Final report on Gore- Gambela geo traverse Western Ethiopia. A report on the international development research and on cooperative project between Addis Ababa University and Ethiopian Institute of Geological Survey and the Ottawa-Carleton Geoscience center Canada.
- Torsten Schwarz (1996). Laterites concepts, Geology, morphology and chemistry. *Article in clay mineralogy*.
- Upadhyay, R., Roy, S., Venkatesh, A., Rao, M. and Banerjee, P. (2009). Relevance of geological aspects and ore mineralogy in selecting beneficiation methods for processing of Eastern Indian iron ore. *Mineral processing and extractive metallurgy*. **118**(1).
- Villiers, J.P.R.de and Lu, L. (2015). XRD analysis and evaluation of iron ores and sinters. Iron ore. <http://dx.doi.org/10.1016/B978-1-78242-156-6.00003-4>.
- Welela Ahemed Mohamed (2002). Hydrocarbon potential of the Blue Nile basin central Ethiopia. Ministry of mines.
- Welela, (2009). Sedimentation and depositional environments of the barremian – senomanian Debre Libanose Sandstone, Blue Nile (Abay) Basin, Ethiopia. *Cretaceous research*. **30**:1133-1145.
- Wolela, A. M., (2002). Hydrocarbon Potential of the Blue Nile Basin, Central Ethiopia. Draft report, Ministry of Mines, Addis Ababa, Ethiopia.
- Worash Getaneh and Solomon Tadesse (2015). Text book of Economic Geology. Addis Ababa University Press.
- Worku. T. (1988). Sedimentology, diagenesis and hydrocarbon potential of the Karro sediments (Late Paleozoic to Early Jurassic), Ogaden Basin, Ethiopia. M. Phil. Dissertation, University of Reading, 222pp.
- Yao, M., Deshun, Z. and Minglong, L. (2017). Geochemistry evidence for depositional settings and province of Jurassic argillaceous rocks of Jiyuan basin North China. *J. Earth Syst. Sci.* **126**(14).
- Yilma, A. D., and Awulachew, S. B. (2009). Characterization and Atlas of the Blue Nile Basin and its Sub basins.

Appendix I

Field observation data of ore bodies

Easting	Northing	Blocks	
448795	1182345	Agiagra	
448637	1182356		
448638	1182252		
448635	1182145		
448983	1181730	Legeworke	
440112	1181742		
449149	11811711		
449210	1181500		
449276	1181048		
449518	1180963		
449946	1181273		
450216	1181370		
450338	1181715		
450523	1181550		
450356	1183447		
450379	1183380		
450305	1183582		
450055	11833887		
450052	1183336		
449902	1182860		
450059	1182602		
449829	1182785		
449928	1182802	Millo	
447946	1182723		
449655	1182847		
449708	1182862		
449760	1182719		
451058	1185977	Dasue	
451119	1185559		
451160	1185608		

451215	1185694	
451304	1185799	
449060	1185123	
449054	1185137	
448822	1185161	
448758	1185190	

Appendix II

Geochemistry

Major oxide analysis of host rock

Comp.wt %	MSd1 Arenite	MSd2 Arenite	MSd3 Arenite	MSd4 Arenite	MSd8 Arenite	MSd1 1 Arenite	MSh 1 Wakes	MSh 2 Wakes	MSh 3 Wakes
SiO ₂	77.33	64.18	67.10	64.58	81.92	82.10	70.04	56.67	65.76
Al ₂ O ₃	7.64	19.26	20.07	8	3.15	5.17	14.75	26.09	20.82
Fe ₂ O ₃	0.62	5.30	1.79	21.1	0.21	0.65	2.27	3.51	1.69
CaO	0.29	0.17	0.09	4	0.08	0.28	0.34	0.16	0.16
MgO	0.21	0.17	0.08	2	0.03	0.11	0.16	0.07	0.16
Na ₂ O	0	0	0	0.12	0	0	0	0	0
K ₂ O	0	0	0	0.05	0	0	0	0	0
Cr ₂ O ₃	0.01	0.01	0	0	0.01	0.01	0.01	0.01	0.01
TiO ₂	0.21	1.16	1.56	0	0.35	0.70	1.12	1.40	0.84
MnO	0	0	0.02	0.01	0	0	0	0.01	0
P ₂ O ₅	0	0	0	1.26	0	0	0	0	0
LOI	5.38	8.03	7.53	0	1.55	3.62	7.72	10.26	8
Total	91.69	98.28	98.24	97.53	87.28	92.64	96.41	98.17	97.44

Major oxide analysis of iron ore

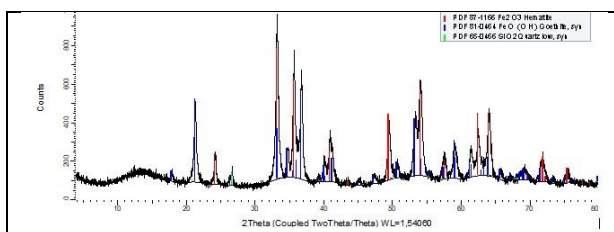
Comp.in wt%	MSB3 Iron ore	MSB4 Iron ore	MSB6 Iron ore	MSB7 Iron ore	MSB11 Iron ore	MSB12 Iron ore	MSB15 Iron ore
SiO ₂	59.02	28.20	24.04	34.23	52.43	38.13	7.31
Al ₂ O ₃	1.61	17.38	3.83	4.29	19.23	9.66	1.44

Fe ₂ O ₃	34.31	43.38	68.23	54.86	16.55	43.10	77.93
CaO	0.21	0.25	0.23	0.22	0.16	0.39	0.16
MgO	0	0.02	0.01	0	0.06	0.20	0
K ₂ O	0	0	0	0	0	0	0
NaO	0	0	0	0	0	0	0
Cr ₂ O ₃	0.06	0.07	0.10	0.09	0.04	0.07	0.09
Ti ₂ O	0.46	1.17	0.90	1.48	1.06	1.22	0.02
MnO	0.01	0	0	0	0	0	0
P ₂ O ₅	0	0.01	0.02	0.02	0	0.05	0.03
LOI	3.84	9.37	3.80	4.53	9.22	6.65	7.31
Total	99.52	99.85	101.16	99.72	98.75	99.47	94.29

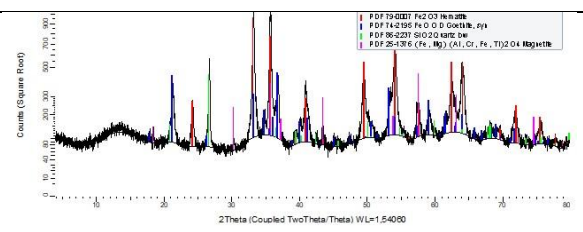
Appendix III

Mineralogical study

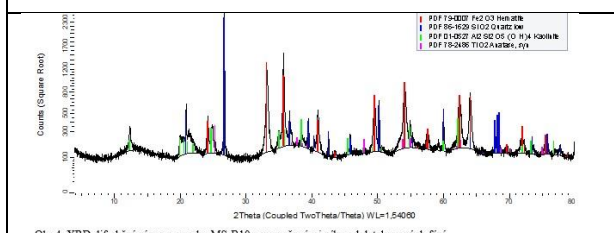
A) XRD



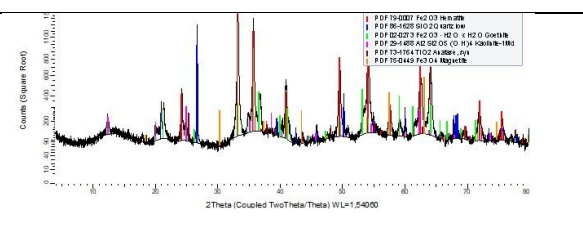
Obr 3. XRD difrakční záznam vzorku MS-B1 s vyznačenými píky od detekovaných fází.



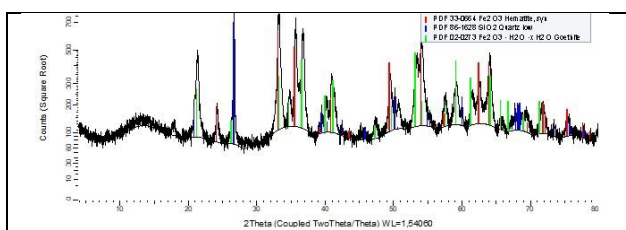
Obr 5. XRD difrakční záznam vzorku MS-B5 s vyznačenými píky od detekovaných fází.



Obr 4. XRD difrakční záznam vzorku MS-B10 s vyznačenými píky od detekovaných fází.



Obr 6. XRD difrakční záznam vzorku MS-DB3 s vyznačenými píky od detekovaných fází.



Obr 7. XRD difrakční záznam vzorku MS-LW s vyznačenými píky od detekovaných fází.

B) Polished section

